

Morphing planar triangulations

by

Fidel Barrera-Cruz

A thesis
presented to the University of Waterloo
in fulfillment of the
thesis requirement for the degree of
Doctor of Philosophy
in
Combinatorics and Optimization

Waterloo, Ontario, Canada, 2014

© Fidel Barrera-Cruz 2014

Author's Declaration

I hereby declare that I am the sole author of this thesis. This is a true copy of the thesis, including any required final revisions, as accepted by my examiners.

I understand that my thesis may be made electronically available to the public.

Abstract

A *morph* between two drawings of the same graph can be thought of as a continuous deformation between the two given drawings. A morph is *linear* if every vertex moves along a straight line segment from its initial position to its final position. In this thesis we study algorithms for morphing, in which the morphs are given by sequences of linear morphing steps.

In 1944, Cairns proved that it is possible to morph between any two planar drawings of a planar triangulation while preserving planarity during the morph [22]. However this morph may require exponentially many steps. It was not until 2013 that Alamdari et al. proved that the morphing problem for planar triangulations can be solved using polynomially many steps [2].

In 1990 it was shown by Schnyder [50, 51] that using special drawings that we call *Schnyder drawings* it is possible to draw a planar graph on a $O(n) \times O(n)$ grid, and moreover such drawings can be found in $O(n)$ time (here n denotes the number of vertices of the graph). It still remains unknown whether there is an efficient algorithm for morphing in which all drawings are on a polynomially sized grid.

In this thesis we give two different new solutions to the morphing problem for planar triangulations. Our first solution gives a strengthening of the result of Alamdari et al. where each step is a *unidirectional* morph. This also leads to a simpler proof of their result.

Our second morphing algorithm finds a planar morph consisting of $O(n^2)$ steps between any two Schnyder drawings while remaining in an $O(n) \times O(n)$ grid. However, there are drawings of planar triangulations which are not Schnyder drawings, and for these drawings we show that a unidirectional morph consisting of $O(n)$ steps that ends at a Schnyder drawing can be found. We conclude this work by showing that the basic steps from our morphs can be implemented using a Schnyder wood and weight shifts on the set of interior faces.

Acknowledgements

My eternal gratitude to my supervisor Professor Penny Haxell. I am very grateful to her for her excellent guidance, constant encouragement and for introducing me to the wonderful subject of Schnyder woods. I am also very grateful to Professor Anna Lubiw for her great advice and for introducing me to the beautiful subject of morphs. Thank you both for sharing your knowledge and for helping me learn more about research.

Big thanks to my committee, this includes Professors Joseph Cheriyan, Chris Godsil and William Trotter. This work greatly benefited from their feedback.

To the Professors at the Faculty of Mathematics who shared their knowledge with me, be it inside or outside a classroom, thank you. There were many others who made my stay at Waterloo a very pleasant experience. I am grateful to them, particularly to my friends and to the staff members of the Department of Combinatorics and Optimization.

Mainly two triangles have shaped the path I have followed along my life. I have tried, as much as possible, to stay at the barycenter of such triangles. Thank you Fernando, José Manuel and Rubén for giving me an example to follow. My gratitude to Fer, Lorena and Saula for their endless patience and for the lessons they have taught me about the many things that one does not usually learn in a classroom.

I am thankful for the financial support provided by Mexico's Conacyt.

Dedication

To the memory of my dear Mother

Table of Contents

List of Figures	xiii
1 Introduction	1
1.1 Planar graph drawings	2
1.1.1 Tutte’s algorithm	2
1.1.2 Schnyder’s algorithm	2
1.2 Morphs	3
1.2.1 Floater and Gotsman’s algorithm	5
1.3 Outline of this work	5
2 Background on Schnyder woods	9
2.1 Schnyder woods	9
2.2 Existence of Schnyder woods	10
2.3 Properties of Schnyder woods	14
2.4 Planar drawings from Schnyder woods	18
2.5 Face weights	21
2.6 Flipping triangles	24
2.7 Flip distance between Schnyder woods	26

3	Morphing planar graph drawings with unidirectional moves	29
3.1	Overview of Cairns' algorithm	29
3.2	The technique used by Alamdari et al.	32
3.3	A pseudo morph with unidirectional morphing steps	33
3.4	Avoiding coincident vertices	36
4	Morphing from one Schnyder drawing to another	47
4.1	Planar morphs from weight distributions	49
4.2	Flips on faces define morphs	50
4.3	Morphs from flips in separating triangles	58
4.4	Traversing the Schnyder lattice	68
5	Morphing from a planar drawing to a Schnyder drawing	73
5.1	Existence of a contractible edge	74
5.2	Extending the Schnyder wood	75
5.3	Finding the weight distribution	78
5.4	Handling the exceptional case with $\deg(u) = 5$	87
5.5	Towards a morph using unidirectional morphs	94
5.6	Morphing to a Schnyder drawing using unidirectional morphs	99
5.7	Morphing planar triangulations using Schnyder drawings	100
6	Simulating morphing steps via weight shifts	103
6.1	Simulating flips by weight shifts	103
7	Future work	107
	References	109

List of Figures

1.1	A sequence of triangle flips, counterclockwise along the top row and clockwise along the bottom row. In each drawing the triangle to be flipped is darkly shaded, and the one most recently flipped is lightly shaded. The linear morph from each drawing to the next one is planar. Bottom right illustrates the trajectories followed by vertices during the sequence of flips.	6
2.1	Conditions (D1) and (D2) from the definition of a Schnyder wood. In our figures we use red, green and blue to denote 1, 2 and 3 respectively	11
2.2	A Schnyder wood of the icosahedron.	12
2.3	Consider the 2-connected outerplanar subgraphs of G , G_1 and G_2 , and use the induction hypothesis.	12
2.4	The base case, a Schnyder wood for K_4	13
2.5	From left to right, the Schnyder woods S' and S	14
2.6	Possible types of interior faces in a Schnyder wood.	15
2.7	It is not possible for C to enclose vertices or to contain chords, otherwise, irrespective of the orientation of C , we can obtain a cycle enclosing fewer faces.	16
2.8	Paths and regions for vertex v defined by a Schnyder wood of a planar triangulation.	18
2.9	Three possible ways of having vertices x and y , in each case we have $R_i(u) \subseteq R_i(v)$	19
3.1	Some polygons with shaded regions representing their kernels.	30
3.2	A 4-gon $abcd$	33

3.3	A boundary vertex of degree 3.	35
3.4	All three boundary vertices of degree 4.	36
3.5	A disk D centered at a whose intersection with the kernel of P (the lightly shaded polygonal region) is a non-zero-area sector S (darkly shaded). (a) Vertex a is convex and S is a positive sector. (b) Vertex a is reflex and S is a negative sector.	38
3.6	The one-sided case where S_i lies to one side of L_i , illustrated for a positive sector S_i . (a) An L_i -directional morph to S_{i+1} . (b) p remains inside the sector if and only if it remains inside D and between the two lines ba and ea	39
3.7	The two-sided case where S_i contains points on both sides of L_i . (a) An L_i -directional morph from the positive sector S_i bounded by $b_i a e_i$ to the negative sector S_{i+1} bounded by $e'_{i+1} a b'_{i+1}$. (b) p remains inside the sector if and only if it remains inside D and on the same side of the lines bb' and ee'	40
3.8	Points x and y move from x_0 to x_1 and from y_0 to y_1 respectively.	40
3.9	N_i (lightly shaded) is an L_i -truncation of S_i in the one-sided case. N_{i+1} is darkly shaded. L_i and L'_i are the slab boundaries for N_i	42
3.10	N_i (lightly shaded) is an L_i -truncation of S_i in the two-sided case. N_{i+1} is darkly shaded. L'_i and L''_i are the slab boundaries for N_i	43
4.1	A sequence of triangle flips. In each drawing the triangle to be flipped is darkly shaded, and the one most recently flipped is lightly shaded. The linear morph from each drawing to the next one is planar. At the bottom we illustrate the piecewise linear trajectories followed by vertices during the sequence of flips.	48
4.2	A flip of a counterclockwise oriented face triangle xyz showing changes to the regions. Observe that $\Delta_1(yz) \cup \{f\}$ leaves $R_2(v)$ and joins $R'_3(v)$ for any $v \in D_1(x)$	52
4.3	Region in which x and its descendants move.	57
4.4	The linear morph defined by a flip of a separating triangle might not be planar if weights are not distributed appropriately. Here we illustrate the flip of the separating triangle in thick edges. Snapshots at $t = 0$, and $t = 1$ are the top. The bottom drawing corresponds to $t = 0.7$, note the edge crossings.	59

4.5	(a): Positions given by the Schnyder wood of the whole graph, the barycentric grid is also shown. (b): Black vertices assigned coordinates with respect to the Schnyder wood of the separating triangle, the local barycentric grid is displayed too. (c): Same position assignment for black vertices as in (b) with grid from (a). (d): Simultaneous drawing of (a) and (b).	60
4.6	A flip of a counter-clockwise oriented separating triangle xyz	62
4.7	The morph resulting from flipping a separating triangle.	68
5.1	The case where $\deg(u) = 3$, and $(y, x) \in S'$ has colour 1.	76
5.2	The case where $\deg(u) = 4$, and $(x, z) \in S'$ has colour 1.	77
5.3	Arcs $(v, x), (z, x) \in S'$ have colour 1.	78
5.4	Arcs $(x, v), (z, x) \in S'$ have colours 3 and 1 respectively.	79
5.5	3-gon	80
5.6	4-gon	80
5.7	5-gon case 1. The weights a, b and c assigned by \mathbf{w}' on the left, and the weights p, q, r, s and t assigned by \mathbf{w} on the right.	82
5.8	5-gon case 2	85
5.9	No vertex mapped to the shaded triangle	89
5.10	5-gon case 3	92
6.1	The face f and its three neighbours.	104

Chapter 1

Introduction

A morph can be thought of as a continuous deformation between two given structures. At a high level, we can say a morph is an animation whose initial frame is the first structure, and as time goes by the shape of the first structure changes smoothly until the second structure is obtained as the final frame of the animation. Thus we can state in very broad terms that the morphing problem consists of determining a continuous deformation between two given structures, where the deformation has to satisfy some given constraints. Morphing can arise in the study of computer graphics [38] and can be used for producing visual effects for movies [4]. Morphing graphs can be of use in medical imaging and geographical information systems [7, 8], where the problem consists of reconstructing a surface given a sequence of parallel slices. In this thesis we treat the problem of morphing straightline drawings of planar triangulations. In this problem we are given a planar triangulation T together with two planar drawings of it and we should produce a morph between the two drawings with the restriction that each frame of the resulting animation is a planar drawing of T . In this work we provide two different solutions to the morphing problem. Our main tool for the solution given in Chapter 3 is the notion of *unidirectional morphs*, which we introduce here. Our second solution, presented in Chapters 4 and 5, makes use of Schnyder woods, an important concept due to Schnyder [50, 51] that has had many significant generalizations and applications in graph theory, partially ordered sets, and computer science (see e.g. [1, 3, 9, 12, 13, 15, 16, 18, 20, 21, 23, 25, 28–33, 39–42, 47, 49, 56, 57].)

In this introductory chapter we begin by mentioning some relevant results regarding straightline drawings of planar graphs in Section 1.1. Then we formally introduce concepts related to morphs in Section 1.2. In Section 1.2 we also comment on previous work on morphing and related problems. Finally, in Section 1.3 we provide an outline of this thesis.

1.1 Planar graph drawings

In 1948, Fáry [27] showed that every planar graph admits a straightline drawing in which no two edges cross. Later, in 1963, Tutte [55] presented an algorithm which yields planar drawings of 3-connected planar graphs. However, this algorithm often does not yield good vertex resolution and for each $n \geq 2$ there is a graph with n vertices whose drawing requires exponential area [26, 53]. It was not until 1990 that de Fraysseix, Pach and Pollack [24] and Schnyder [50] independently provided linear time algorithms that produce straightline drawings of a given planar graph on n vertices in an $O(n) \times O(n)$ grid.

Throughout this thesis we mainly discuss straightline drawings of planar graph so, unless stated otherwise, whenever we write drawing we mean straightline drawing. When thinking about straightline drawings we can see that they uniquely determined by the positions of the vertices, since the edges will be represented by the line segments joining the images of their endpoints. We now provide some more details on the algorithms of Tutte and Schnyder.

1.1.1 Tutte's algorithm

Tutte's algorithm for drawing 3-connected planar graphs ([55]) works as follows. Given a 3-connected planar graph G a face $f = v_1 \dots v_k$ of G is chosen and its vertices are placed so that the polygon delimited by f is convex. The positions assigned to vertices of f is then fixed and the positions of the remaining vertices is determined by solving a system of linear equations involving the Laplacian matrix of the graph [37]. Another approach for obtaining the coordinates of vertices not incident to f is by proceeding iteratively in the following way. For each $v \in V \setminus \{v_1, \dots, v_k\}$ we assigning it to the point

$$(x_v, y_v) := \frac{1}{\deg(v)} \sum_{u \in N(v)} (x_u, y_u),$$

until (x_v, y_v) converges [11]. In the following section we will mention a morphing algorithm which is based on Tutte's graph drawing algorithm.

1.1.2 Schnyder's algorithm

Here we provide an overview of Schnyder's method for producing straightline drawings of planar triangulations, which will form the basis of our work in Chapters 4 and 5. We

treat this method in detail in Chapter 2. A Schnyder wood is a special type of orientation and partition, or assignment of colours, of the edges of a planar triangulation into three edge disjoint trees, which was first introduced in [51]. There it is shown that every planar triangulation admits a Schnyder wood, and Schnyder woods are used to provide a characterization of planar graphs in terms of the dimension of their incidence poset.

In [50, 51] it is shown that Schnyder woods can be used to obtain planar straightline drawings of planar triangulations. These drawings are realized in an $O(n) \times O(n)$ grid. The way such drawings are obtained is by counting the number of faces in certain regions that are given by the Schnyder wood. In a paper by Dhandapani [25], where he proves that given a planar triangulation there exists a greedy drawing of it, it is noted that for a given Schnyder wood one can obtain a whole class of planar straightline drawings for the corresponding triangulation. This class of drawings arises from assigning positive weights to the interior faces and then adding the weights of the faces in the regions. In later chapters we will see how these weight assignments can be used to produce morphs.

1.2 Morphs

The results on planar straightline drawings of graphs began with proving existence and then showing a method to obtain planar drawings on a grid, possibly of exponential size. This was followed by efficient algorithms that obtain drawings of planar graphs on a grid of size $O(n) \times O(n)$. As we will see below, there has been a similar development in results for planar morphs.

Consider two drawings Γ and Γ' of a graph G . A *morph* between Γ and Γ' is a continuous family of drawings of G , $\{\Gamma^t\}_{t \in [0,1]}$, such that $\Gamma^0 = \Gamma$ and $\Gamma^1 = \Gamma'$. When considering a planar triangulation, we say a face xyz *collapses* during the morph $\{\Gamma^t\}_{t \in [0,1]}$ if there is $t \in (0, 1)$ such x, y and z are collinear in Γ^t . We call a morph between Γ and Γ' *planar* if Γ^t is a planar drawing of T for all $t \in [0, 1]$. A morph is said to be *linear* if each vertex moves from its position in Γ^0 to its position in Γ^1 along a line segment and at constant speed. We will denote such linear morph by $\langle \Gamma^0, \Gamma^1 \rangle$. We extend the previous notation in the following way. If $\Gamma_1, \dots, \Gamma_k$ are straightline planar drawings of a graph, then $\langle \Gamma_1, \dots, \Gamma_k \rangle$ denotes the morph that consists of the $k - 1$ linear morphs from Γ_i to Γ_{i+1} for $i = 1, \dots, k - 1$.

In 1944, Cairns proved that it is possible to morph between any two drawings of a planar triangulation [22]. An algorithm that morphs between drawings of a fixed planar triangulation can be derived from Cairns' proof, and such algorithm requires exponentially many steps. We provide an overview of this algorithm in Chapter 3. Then, in 1982,

Thomassen ([54]) provided a generalization of the result of Cairns to 2-connected planar graphs. The algorithm from Thomassen’s result provides a planar morph between any two convex drawings of a fixed 2-connected planar graph such that at each point in time during the morph the current drawing is convex. Thomassen’s approach consists of augmenting the given graph to a *compatible triangulation* [54] (later rediscovered independently by Aronov et al. [6]) and then using Cairns’ procedure to morph between the drawings, thus also requiring exponentially many steps.

In 1999, Floater and Gotsman provided a polynomial time algorithm to morph between any two drawings of 3-connected planar graphs [36]. A property of this algorithm is that the trajectories followed by the vertices may be complex. By using *compatible triangulations*, Gotsman and Surazhsky [52] provided a morph based on that of Floater and Gotsman in which the vertices follow linear trajectories if possible or trajectories that are close to linear. The last two algorithms are based on the drawing algorithm of Tutte. Note that for these algorithms, as for Tutte’s drawing algorithm, it is possible to have drawings that require exponential area.

In 2006 Lubiw, Petrick and Spriggs showed that it is possible to morph between two planar orthogonal graph drawings while preserving planarity [45]. See also the journal version of Biedl et al. [14]. Their morph uses polynomially many steps, where each step is either a linear morph or an operation that introduces bends in the edges incident to a vertex. Their morph also provides a lower bound for the distance between any two vertices. In 2011 Lubiw and Petrick provided a planar morph between any two planar drawings of a graph that allows edges to bend and consists of polynomially many linear morphing steps [44].

More recently, Alamdari et al. [2] proposed a polynomial time algorithm, based on Cairns’ approach, that provides a morph between any two drawings of a planar triangulation using $O(n^2)$ linear morphs, where n is the number of vertices of the planar triangulation. Very recently it was announced by Angelini et al. [5] that they obtained a morphing algorithm using only $O(n)$ linear morphing steps. Our Algorithm 1 from Chapter 3 [10] is used as an essential subroutine in their algorithm. However, the development of the theory of planar morphs is still missing the final step, namely, an algorithm that keeps all drawings on a polynomial-sized grid. This remains an important open problem [43]. As we will mention again in Chapter 7, we have some hope that our work in Chapters 4 and 5 could help make this final step feasible.

1.2.1 Floater and Gotsman's algorithm

Here we provide an outline of Floater and Gotsman's algorithm. It is based on Tutte's algorithm for drawing graphs.

We are given as input two convex drawings Γ_0 and Γ_1 of a planar 3-connected graph, where the corresponding exterior faces coincide. Since the exterior faces coincide, the exterior vertices v_1, \dots, v_k remain fixed during the morph. Then, we express each interior vertex as a convex combination of its neighbours in each drawing, that is for each interior vertex v we write

$$(x_{i,v}, y_{i,v}) = \sum_{u \in N(v)} \lambda_{i,u}(x_{i,u}, y_{i,u}), \quad (1.1)$$

$i \in \{0, 1\}$, with $\lambda_{i,u} > 0$ for each $u \in N(v)$ and $\sum_{u \in N(v)} \lambda_{i,u} = 1$, $i \in \{0, 1\}$. The existence of the coefficients, $\lambda_{i,v}$ for each $u \in N(v)$ and $v \in V \setminus \{v_1, \dots, v_k\}$, is a consequence of the convexity of each of the drawings. It was shown by Floater and Gotsman in [34, 35], by generalizing a result from [55], that a solution to the system (1.1) yields a convex drawing.

The morph proposed in [36] consists of varying the coefficients of the barycentric coordinates in a linear fashion, that is,

$$\lambda_{t,u} = (1 - t)\lambda_{0,u} + t\lambda_{1,u},$$

for each $u \in N(v)$ and $v \in V \setminus \{v_1, \dots, v_k\}$. Finally, for each $t \in [0, 1]$ we are left to deduce $(x_{t,v}, y_{t,v})$, and this can be done by solving the following system of linear equations

$$(x_{t,v}, y_{t,v}) = \sum_{u \in N(v)} \lambda_{t,u}(x_{t,u}, y_{t,u}).$$

Thus, by Floater and Gotsman's result, which generalizes Tutte's drawing algorithm, we get a planar drawing for each $t \in [0, 1]$ and thus a morph from Γ_0 to Γ_1 .

1.3 Outline of this work

In this work we are only concerned with morphing drawings of planar triangulations. This thesis is structured as follows. In Chapter 2 we begin by introducing some preliminaries on Schnyder woods. We introduce the concept of Schnyder wood and then we show that any planar triangulation admits a Schnyder wood. We then move on to show how to obtain a planar drawing from a Schnyder wood and an assignment of positive weights on

the interior faces. All this discussion is based on the original papers of Schnyder [50, 51]. Then we show that any planar drawing of a planar triangulation may be obtained from a Schnyder wood together with some assignment of weights on the interior faces. In general planar triangulations may admit more than one Schnyder wood. It is known that the set of Schnyder woods of a planar triangulation defines a distributive lattice [19, 30, 48]. We conclude Chapter 2 by presenting the basic operation that is used to traverse the lattice and by providing a bound on the distance in the lattice between any two Schnyder woods of a fixed planar triangulation. This latter material is based on the works of Brehm [19], Felsner [30] and Ossona De Mendez [48].

The new contributions of this thesis are given in Chapters 3 to 6. A substantial part of this material represents joint work with P. Haxell and A. Lubiw. In Chapter 3 we present an improvement on the result of Alamdari et al. [2], where instead of using linear morphs the morphs are restricted further so that at each step every vertex moves along a fixed direction. This is done without increasing the number of steps required. We use the term *unidirectional* to describe this type of morph. This restriction has the advantage of making the resulting morph simpler and also simplifying the proof of the result.

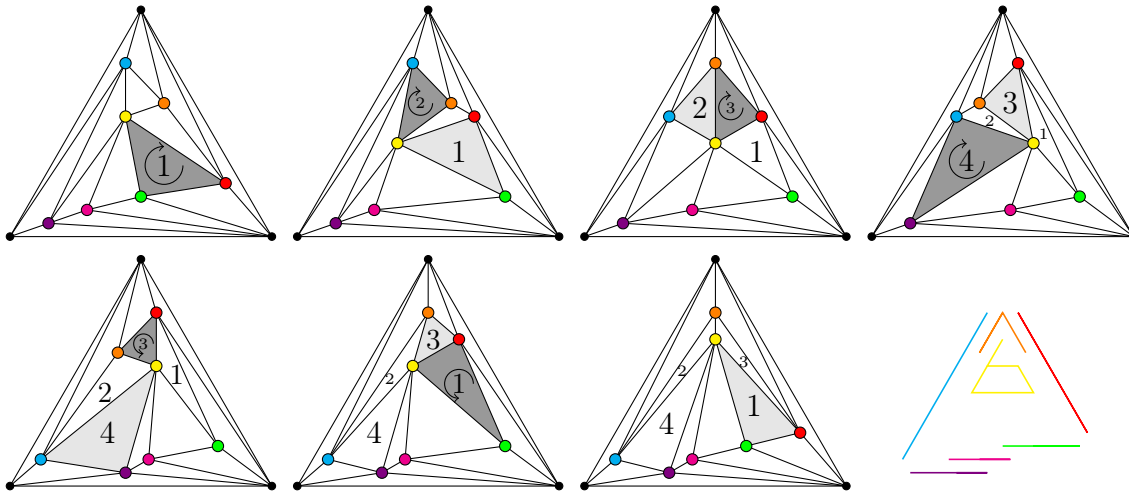


Figure 1.1: A sequence of triangle flips, counterclockwise along the top row and clockwise along the bottom row. In each drawing the triangle to be flipped is darkly shaded, and the one most recently flipped is lightly shaded. The linear morph from each drawing to the next one is planar. Bottom right illustrates the trajectories followed by vertices during the sequence of flips.

So far, of the morphs we have described, none of them have the property that the drawings at each intermediate step can be realized in a grid of polynomial size. In Chapter 4

we present a planar morph between any two *Schnyder drawings* consisting of $O(n^2)$ steps, where each of the intermediate drawings can be realized in an $O(n) \times O(n)$ grid. In Figure 1.1 we show the intermediate drawings from the morph resulting from performing some *facial flips*. One class of drawings for which the result of Chapter 4 does not apply is the set of drawings which arise from allowing negative weights on the interior faces. However, it can be shown that it takes $O(n)$ *unidirectional* morphing steps to morph from an arbitrary drawing of a planar triangulation to a *Schnyder drawing*. This is shown in Chapter 5. The previous result together with our result from Chapter 4 imply that it is possible to morph between any two drawings of a planar triangulation in $O(n^2)$ steps, where only $O(n)$ drawings are drawings that may not be realizable in an $O(n) \times O(n)$ grid.

Chapter 6 is devoted to showing how it is possible to simulate the basic morphing steps from our results on morphing Schnyder drawings by using weight shifts. Finally, in Chapter 7 we provide some possible lines of research for our future work.

Chapter 2

Background on Schnyder woods

In this chapter we introduce some common background and useful tools for future chapters. Our main aim is to provide an introduction to the theory of Schnyder woods for the case of planar triangulations.

We start the chapter by defining Schnyder woods. In Section 2.2 we provide a proof of existence of Schnyder woods. Section 2.3 develops the theory of Schnyder woods by presenting some of their basic properties. We then move on to Section 2.4 where we show how Schnyder woods can be used to obtain planar drawings of triangulations. All of the material in Sections 2.1–2.4 is based on the original papers of Schnyder [50, 51]. We continue exploring the relations between planar drawings of triangulations and Schnyder woods in Section 2.5 and show that any planar drawing can be “obtained” from a Schnyder wood by assigning (not necessarily positive) weights to the interior faces of the triangulation, this was already observed in [25]. In general a planar triangulation may admit more than one Schnyder wood, in fact there can be exponentially many for a fixed planar triangulation [32]. Some aspects regarding the set of Schnyder woods for a fixed triangulation are explored in Section 2.6. It is known that the set of Schnyder woods is well structured, it defines a distributive lattice, as shown in [19, 30, 48]. In Section 2.7 we provide a bound for the distance between any two Schnyder woods in the lattice. We obtain this bound based on work of Brehm [19] and an observation of Miracle et al. [46].

2.1 Schnyder woods

This section is devoted to introducing Schnyder woods. For a graph G and $v \in V(G)$ we use $N_G(v)$ to denote the set of neighbours of v in G .

Given a planar triangulation T , we will distinguish one of its faces and we will call it the *exterior face*. We will use a_1, a_2 and a_3 to denote the vertices incident to the exterior face and they will be referred to as *exterior vertices*. To picture this geometrically, we can think of an embedding of T in the plane with $a_1a_2a_3$ being the unbounded face. The vertices in $V \setminus \{a_1, a_2, a_3\}$ will be called *interior vertices*. The three edges incident with $a_1a_2a_3$ will be called *exterior edges* and edges not incident with the exterior face will be referred to as *interior edges*. Faces of T different from $a_1a_2a_3$ will be called *interior faces*, we denote by $\mathcal{F}(T)$ the set of interior faces of T . If C is a cycle in a planar triangulation T so that $T - C$ is disconnected, then we define

$$T \setminus C = T - \{v \in V(T) : v \text{ is a vertex in the interior of the region bounded by } C\}$$

and

$$T|_C = T - \{v \in V(T) : v \text{ is a vertex in the interior of the unbounded region defined by } C\}.$$

When C is a triangle whose removal disconnects the graph, we call C a *separating triangle*. In this case, we can observe that $T \setminus C$ and $T|_C$ are planar triangulations. When considering $T|_C$, with C a triangle, we will let the vertices of C be the exterior vertices of $T|_C$. Given $S \subseteq V(T)$ we denote the graph induced by vertices of S by $T[S]$. Finally, for $v \in V(T)$, we use $N(v)$ to denote the set of neighbours of v .

A *Schnyder wood* S of a planar triangulation T with respect to a face $f = a_1a_2a_3$ is an assignment of directions and colours 1, 2 and 3 to the interior edges of T such that the following two conditions hold, see Figure 2.1.

- (D1) Each interior vertex v has outdegree 1 in colour i , $i = 1, 2, 3$. At v , the outgoing edge in colour $i - 1$, e_{i-1} , appears after the outgoing edge in colour $i + 1$, e_{i+1} , in clockwise order. All incoming edges in colour i appear in the clockwise sector between the edges e_{i+1} and e_{i-1} .
- (D2) At the exterior vertex a_i , all the interior edges are incoming and of colour i .

We call conditions (D1) and (D2) the *interior vertex property* and *exterior vertex property* respectively. We present an example of a Schnyder wood of the icosahedron in Figure 2.2.

2.2 Existence of Schnyder woods

In this section we show that every planar triangulation admits a Schnyder wood. Before stating the result, let us introduce some notation and prove a couple of useful lemmas.

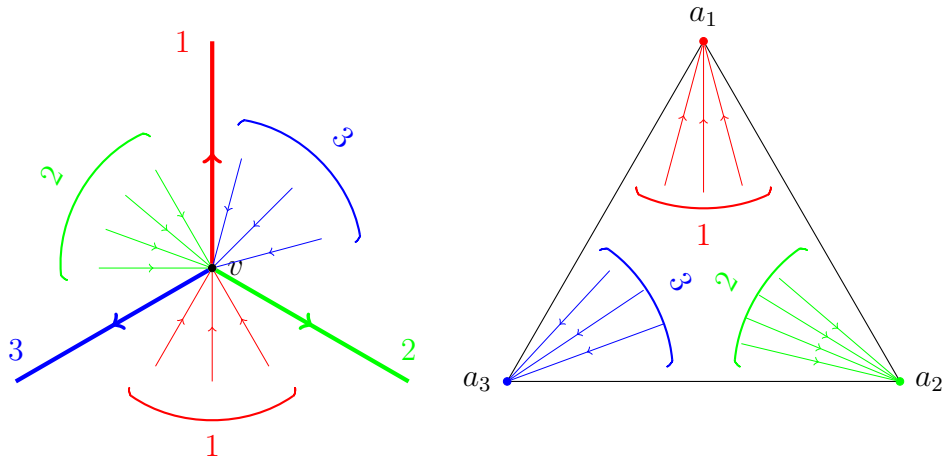


Figure 2.1: Conditions (D1) and (D2) from the definition of a Schnyder wood. In our figures we use red, green and blue to denote 1, 2 and 3 respectively

Given a planar triangulation $T = (V, E)$ and $u \in V$ with $uv \in E$ we denote by $T_{u,v}$ the graph obtained by deleting the vertex u in T and adding edges between the neighbours of u in T and v . This can be thought as contracting uv and disregarding any resulting multiple edges and loops, and renaming the image of the contracted edge to one of its endpoints, namely v . We abuse notation and will refer to this operation as an edge contraction.

Lemma 2.2.1. *Let $T = (V, E)$ be a planar triangulation on n vertices and let $uv \in E$. If u and v share exactly two neighbours, then $T_{u,v}$ is a planar triangulation on $n - 1$ vertices.*

Proof. It should be clear that $T_{u,v}$ is planar. Now, since u and v share exactly two neighbours, it follows that the number of edges of $T_{u,v}$ is 3 fewer than those in T . Therefore $T_{u,v}$ is planar, has $n - 1$ vertices and $3n - 6 - 3 = 3(n - 1) - 6$ edges. Thus the claim follows. \square

Let us prove one more lemma about 2-connected outerplanar graphs before stating the main theorem of this section.

Lemma 2.2.2. *A 2-connected outerplanar graph with at least 4 vertices contains at least two non adjacent vertices of degree 2.*

Proof. We proceed by induction on the number of vertices n . For $n = 4$ the statement is clearly true as the 4-cycle and the complete graph on 4 vertices minus an edge, the only 2-connected outerplanar graphs on 4 vertices, satisfy the required property.

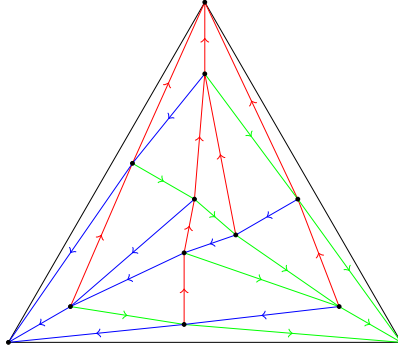


Figure 2.2: A Schnyder wood of the icosahedron.

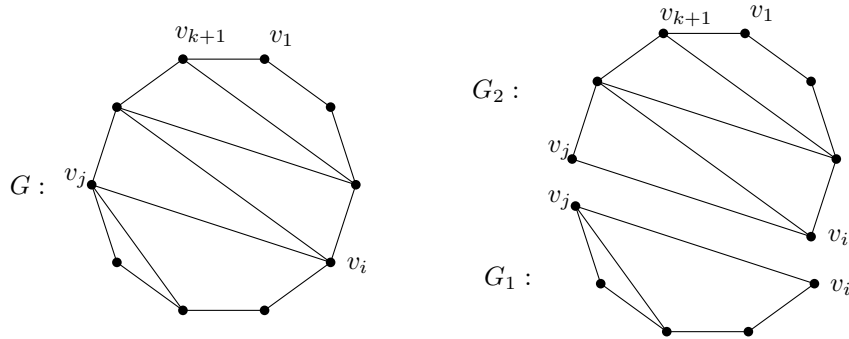


Figure 2.3: Consider the 2-connected outerplanar subgraphs of G , G_1 and G_2 , and use the induction hypothesis.

Now assume the result holds for 2-connected outerplanar graphs with $n \leq k$ vertices. Let G be a 2-connected outerplanar graph with $k + 1$ vertices, say v_1, \dots, v_{k+1} , and let C denote the exterior cycle of G . Without loss of generality we may assume that $C = v_1 v_2 \dots v_{k+1}$. If G is isomorphic to the cycle on k vertices then the result clearly holds. So suppose there is an edge $v_i v_j$ of G that is a chord of C . Let $S_1 = \{v_i v_{i+1} \dots v_j\}$ and $S_2 = \{v_j v_{j+1} \dots v_i\}$ and define $G_l := G[S_l]$, $l \in \{1, 2\}$ (see Figure 2.3). Clearly each G_l , $l \in \{1, 2\}$, is a 2-connected outerplanar graph with at least one fewer vertex than G and by the induction hypothesis it contains at least two non adjacent vertices of degree 2. Since $v_i v_j$ is an edge in G_l , then at least one of the vertices of degree 2 is different from v_i and v_j in each G_l . Thus these are two non adjacent vertices of degree 2 in G . \square

We now offer a proof of existence of Schnyder woods.

Theorem 2.2.3 (Schnyder [50, 51]). *Let T be a planar triangulation. If f is a face of T*

then there exists a Schnyder wood with respect to f .

Proof. Let us proceed by induction on the number of vertices. We may assume without loss of generality that a_1 , a_2 and a_3 , the vertices incident to f , appear in clockwise order in the embedding of T .

The result is clearly true when T has 4 vertices. In this case the three interior edges are oriented away from the unique interior vertex b . We assign colour i to edge ba_i , see Figure 2.4.

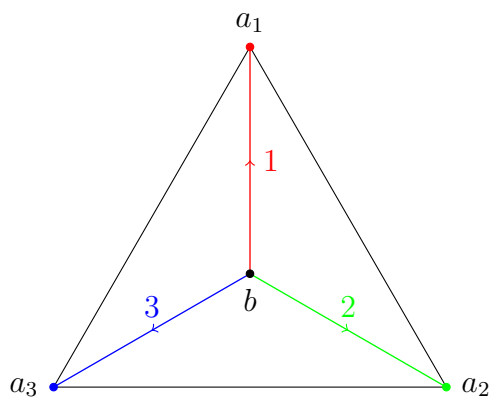


Figure 2.4: The base case, a Schnyder wood for K_4 .

Now, suppose every planar triangulation on at most k vertices admits a Schnyder wood with respect to any face. Let T be a planar triangulation on $k + 1$ vertices. Let $H := T[N_T(a_1)]$. Clearly H is a 2-connected outerplanar graph, so by Lemma 2.2.2 it has at least two non adjacent vertices of degree 2. We now have that at least one of these two vertices, call it b , is different from a_2 and a_3 , since a_2 and a_3 are adjacent in H . Since $\deg_H(b) = 2$ then $|N_T(a_1) \cap N_T(b)| = 2$. It now follows from Lemma 2.2.1 that $T' := T_{b,a_1}$ is a planar triangulation on k vertices. Thus by the induction hypothesis T' admits a Schnyder wood S' with respect to $a_1a_2a_3$.

We now show how to obtain a Schnyder wood for T from that of T' . We may assume without loss of generality that all edges incoming to a_1 in S' are of colour 1, otherwise cyclically rotating colours yields a Schnyder wood satisfying this requirement. Let c_1, \dots, c_l be the neighbours of b different from a_1 and not in $N_T(a_1)$, see Figure 2.5. Without loss of generality $a_1, b', c_1, \dots, c_l, b''$ is the clockwise order of the neighbours around b in T , where $\{b', b''\} = N_T(b) \cap N_T(a_1)$. Note that in S' the edges $c_i a_1$ are all of colour 1 and incoming to a_1 , $1 \leq i \leq l$. We now define S as follows. For an edge $uv \in E(T)$, with

$u, v \notin \{b\}$, we orient and assign colour to uv as in S' . We let $(b, a_1), (b, b')$ and (b, b'') be of colours 1, 2 and 3 respectively. Finally, each (c_i, b) will be of colour 1, $1 \leq i \leq l$, see Figure 2.5. Let us show that S as defined above is a Schnyder wood of T . Clearly the vertex property, either interior or exterior (see properties (D1) and (D2)), holds for any vertex not in $N_T(b) \cup \{b\}$, since the arcs in S coincide with those from S' . The only possible obstruction for the interior vertex property (D1) to hold at c_i is the arc (c_i, b) . Recall that (c_i, a_1) was replaced with (c_i, b) , both having colour 1 and oriented away from c_i . So the interior vertex property holds at each c_i , $1 \leq i \leq l$. Now, it can be seen that the interior vertex property holds for b' , since (b, b') has colour 2 and is incoming to b' between the outgoing arcs of colours 1 and 3. A similar argument shows that the interior vertex property holds at b'' . Finally, we can note that the interior vertex property holds at b by construction. The fact that all arcs in S are of colour 1 and incoming to a_1 implies that the exterior vertex property holds at a_1 , thus concluding the proof. \square

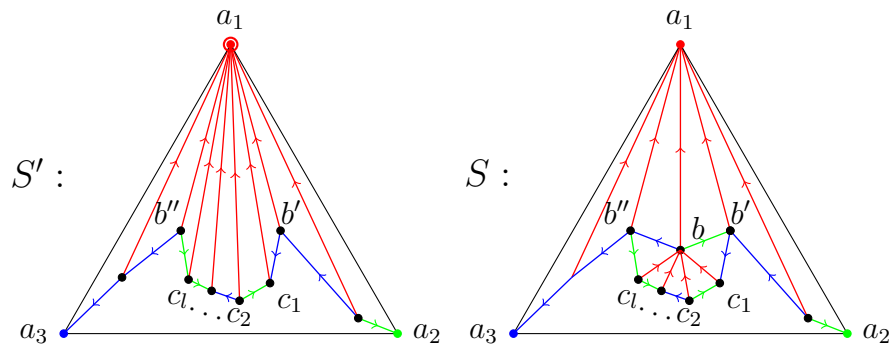


Figure 2.5: From left to right, the Schnyder woods S' and S .

In [50] it is proved that given a planar triangulation T and an exterior face, a Schnyder wood can be obtained in $O(n)$ time, here n is the number of vertices of the planar triangulation.

2.3 Properties of Schnyder woods

In this section we present some basic properties of Schnyder woods which we will find useful to derive further results in the following sections.

As we will see, one of the relevant properties is that Schnyder woods define a partition of the interior edges into three edge disjoint trees, each tree defined by each of the colour classes. We begin by proving the following lemma.

Lemma 2.3.1. *Let S be a Schnyder wood and let f be a face incident to three interior vertices. Then, up to rotation of colours, f is of one of the four types illustrated in Figure 2.6.*

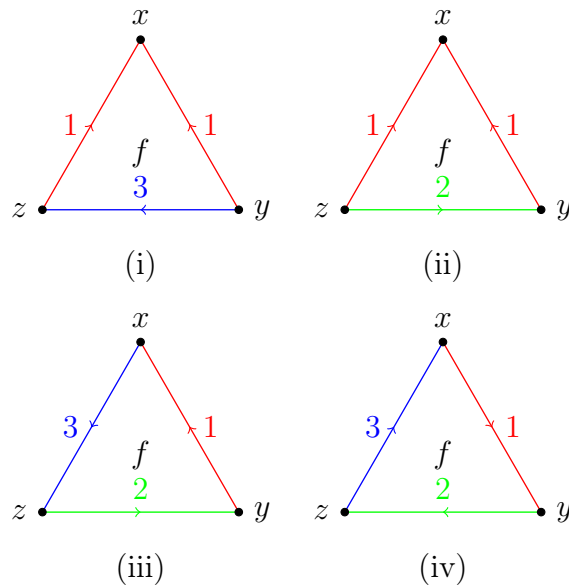


Figure 2.6: Possible types of interior faces in a Schnyder wood.

Proof. Let x , y and z be the vertices incident to f in clockwise order. First note that it cannot occur that (y, x) and (x, z) are in S and have the same colour as this contradicts the interior vertex property (D1) at x . It now follows that f cannot be bounded by arcs of the same colour, that is, at most two arcs of f have the same colour.

We proceed by considering two possible cases, depending on the number of arcs bounding f that have the same colour. If exactly two arcs incident to f have the same colour, say i , then they must both be incoming to the same vertex, say x , from what we argued above. By using the interior vertex property (D1) at y we have that either (y, z) has colour $i - 1$ in S or (z, y) has colour $i - 1$ in S .

Finally, let us consider the case where no two arcs incident to f have the same colour. Therefore all three arcs have different colours. Suppose that (y, x) is an arc in S . Without

loss of generality we may assume (y, x) has colour i . By the interior vertex property (D1) at x have that (x, z) must be of colour $i - 1$, or else (z, x) would have been of colour i . Similarly, using the interior vertex property (D1) at z implies that (z, y) must be of colour $i + 1$. An analogous argument can be used to show that if (x, y) is an arc in S of, say colour i , then (y, z) has colour $i + 1$ and (z, x) has colour $i - 1$ in S . This concludes the proof. \square

For a Schnyder wood S , we define T_i to be the set of arcs of colour i and $T_i^- = \{(u, v) | (v, u) \in T_i\}$, that is, T_i^- is the set of arcs in T_i reversed. Let x be an interior vertex. Observe that by following the outgoing edges of colour i starting at x we eventually reach a_i , the uniqueness of this directed path follows from the fact that at each vertex there is a unique outgoing edge of colour i . Denote by $P_i(x)$ the directed path in colour i from x to a_i . Our aim is to prove that each T_i defines an acyclic digraph. This is a straightforward consequence of the following lemma.

Lemma 2.3.2. *Let T be a planar triangulation. If S is a Schnyder wood of T , then the digraph defined by $T_{i-1}^- \cup T_i \cup T_{i+1}^-$ is acyclic.*

Proof. Let us proceed by contradiction. Suppose C is a directed cycle in $T_{i-1}^- \cup T_i \cup T_{i+1}^-$ which encloses as few faces as possible. We show that C cannot enclose more than 1 face, and thus the result follows from Lemma 2.3.1.

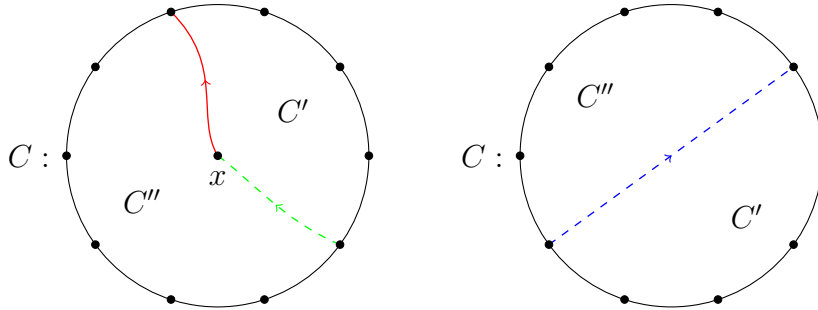


Figure 2.7: It is not possible for C to enclose vertices or to contain chords, otherwise, irrespective of the orientation of C , we can obtain a cycle enclosing fewer faces.

Suppose there is a vertex x inside the region enclosed by the cycle C . Consider the subpaths P_i and P_{i+1} of the paths $P_i(x)$ and $P_{i+1}(x)$ respectively that start at x and end at the first vertex they reach that is on C . Note that P_i and P_{i+1} do not have any vertices in common inside C , or else this would contradict the minimality of C since $P_i \cup P_{i+1}^-$

would contain a cycle enclosing fewer faces than C . We have arrived to a contradiction, since $P_i \cup P_{i+1}^{-1} \cup C$ contains a directed cycle containing fewer faces than C .

Now, assume C encloses more than one face and no vertices. Then C contains a chord. Irrespective of the colour and orientation of this chord, we see that there is a cycle enclosing fewer faces than C , a contradiction. The result now follows from Lemma 2.3.1 by observing that each possible face type is acyclic in $T_{i-1}^- \cup T_i \cup T_{i+1}^-$. \square

From the previous result, together with the fact that at each vertex there is a unique outgoing edge in each colour, we can see that a Schnyder wood defines a partition of the interior edges of a planar triangulation into three edge disjoint trees, T_1 , T_2 and T_3 , where the edges in T_i are those in S having colour i . Each of these trees can be thought of as being rooted at an exterior vertex, that is, T_i is rooted at a_i . One more consequence of Lemma 2.3.2 is that for a given vertex v , the three outgoing paths, $P_i(v)$, $P_{i+1}(v)$ and $P_{i-1}(v)$ are vertex disjoint. These properties will be of relevance in a later chapter, so we summarize them now.

- (P1) The digraph defined by $T_{i-1}^- \cup T_i \cup T_{i+1}^-$ contains no directed cycle. In particular, any two outgoing paths at a vertex v have no vertex in common, except for v , that is, $P_i(v) \cap P_j(v) = \{v\}$ for $i \neq j$.
- (P2) The outgoing path of colour i leaving v ends at a_i .

We say vertex v is a *descendant* of vertex u in T_i if u is a vertex of $P_i(v)$. For a vertex u , we define the set of descendants of u in T_i as

$$D_i(u) := \{v \in V(T) : v \text{ is a descendant of } u \text{ in } T_i\}.$$

By observing the outgoing paths at a given interior vertex v , we can see that for each v we obtain a partition of the set of interior faces of the planar triangulation into three sets. The i -th region, $R_i(v)$, is defined to be the region bounded by $P_{i+1}(v)$, $P_{i-1}(v)$ and $a_{i+1}a_{i-1}$, see Figure 2.8. We will also use $R_i(v)$ to denote the set of vertices or edges incident to some face in the region. Note that the sets $R_1(v)$, $R_2(v)$, $R_3(v)$ do not define a partition on the set of vertices or edges, as any vertex or edge of $P_i(v)$ belongs to $R_{i-1}(v)$ and $R_{i+1}(v)$.

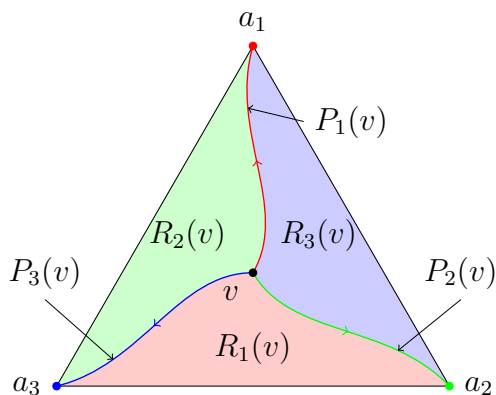


Figure 2.8: Paths and regions for vertex v defined by a Schnyder wood of a planar triangulation.

2.4 Planar drawings from Schnyder woods

In [50, 51] the concept of *barycentric embedding* is introduced. We proceed to define this concept and then relate it to the regions defined by a Schnyder wood. A *barycentric embedding* of a graph G is an injective function $f : V(G) \rightarrow \mathbb{R}^3$, $v \mapsto (v_1, v_2, v_3)$, so that the following two conditions hold.

- For each $v \in V(G)$, $v_1 + v_2 + v_3 = 2n - 5$, and
- for every $uv \in E(G)$ and $w \in V(G) \setminus \{u, v\}$ there is $k \in \{1, 2, 3\}$ so that $u_k, v_k < w_k$.

We now state a known result about barycentric embeddings.

Theorem 2.4.1 (Schnyder [50, 51]). *Each barycentric embedding of a graph defines a planar drawing of the graph in the plane $x + y + z = 2n - 5$.*

Barycentric embeddings for planar triangulations can be obtained from Schnyder woods. To prove this, we begin by showing the following lemma.

Lemma 2.4.2. *Let T be a planar triangulation equipped with a Schnyder wood S and let u and v be interior vertices. If $u \in R_i(v)$ then $R_i(u) \subsetneq R_i(v)$. Furthermore, there is exactly one face in $R_i(v) \setminus R_i(u)$ if and only if there exists $w \in R_i(v)$ such that $uvw \in R_i(v)$ and $(v, u), (v, w), (u, w) \in S$.*

Proof. Let us begin by defining vertices x and y . If $u \in P_{i+1}(v)$ then we let $x := u$. Otherwise, we choose x to be the first vertex of $P_{i+1}(u)$ other than u that is in $P_{i-1}(v) \cup P_{i+1}(v)$ while traversed from u to a_{i+1} . Note that x is not a vertex of $P_{i-1}(v)$ as this would contradict the interior vertex property (D1) at x , therefore x is a vertex of $P_{i+1}(v)$ and $x \neq v$. In an analogous fashion we define vertex y , for $i - 1$ instead of $i + 1$. Thus y is a vertex in $P_{i-1}(v)$. From this it follows that $R_i(u) \subseteq R_i(v)$, see Figure 2.9.

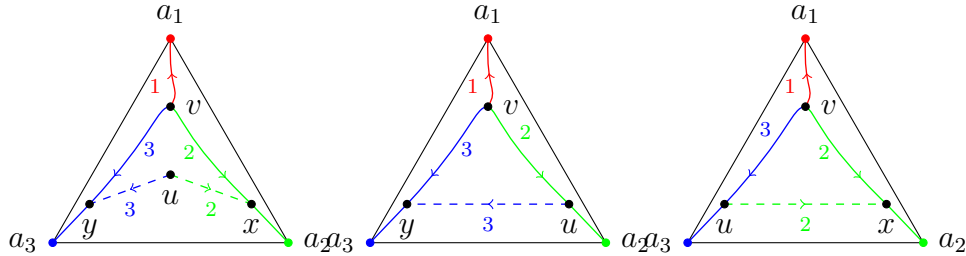


Figure 2.9: Three possible ways of having vertices x and y , in each case we have $R_i(u) \subseteq R_i(v)$.

To prove the inclusion is proper let us begin by noting that $x \neq y$. This implies that at least one of x and y , say x , is different from u . If x' denotes the vertex preceding x in $P_{i+1}(v)$, then the face incident to (x', x) that is in $R_i(v)$ is not in $R_i(u)$. A similar argument can be used for the case where $y \neq u$. Therefore the inclusion is proper.

Let us now show that there is exactly one face in $R_i(v) \setminus R_i(u)$ if and only if there exists $w \in R_i(v)$ such that $uvw \in R_i(v)$ and $(v, u), (v, w), (u, w) \in S$. Suppose there is no vertex $w \in R_i(v)$ such that $uvw \in \mathcal{F}(T)$ and $(v, u), (v, w), (u, v) \in S$. We consider the following 2 possibilities.

1. Assume $uv \notin E$. Suppose it is the case that $u \in P_{i+1}(v) \cup P_{i-1}(v)$, say $u \in P_{i+1}(v)$. Let x' be the predecessor of u in $P_{i+1}(v)$ and let x'' be the predecessor of x' in $P_{i+1}(v)$. Then the edges $x''x$ and $x'u$ bound faces in $R_i(v)$ that are not in $R_i(u)$. Now, if $u \notin P_{i+1}(v) \cup P_{i-1}(v)$ then the arcs outgoing u in colours $i + 1$ and $i - 1$ bound faces in $R_i(v)$ that are not in $R_i(u)$. It follows from (D1) that the faces are distinct, since the outgoing arc at u of colour i appears between the other two outgoing arcs.
2. For the case where $uv \in E$ we have the following. Let $w \in R_i(v)$ be a common neighbour of u and v . If uvw is a not a facial cycle in T , then uvw is a separating triangle. Therefore there are at least three faces enclosed by uvw and such faces are in $R_i(v) \setminus R_i(u)$. Finally, if uvw is a facial triangle two possible cases arise. First

$(v, u) \notin S$, and thus $(u, v) \in S$. In this case the two faces incident to uv are in $R_i(v) \setminus R_i(u)$. Finally, if $(u, w) \notin S$, then $(w, u) \in S$. In this case the two faces incident to wu are in $R_i(v) \setminus R_i(u)$.

□

In [50, 51] it is shown that given a planar triangulation T on n vertices equipped with a Schnyder wood S we can obtain a barycentric embedding defined in terms of S . One can consider the map $f : V(T) \rightarrow \mathbb{R}^3$, where $f(a_i) = (2n - 5)e_i$, where e_i denotes the i -th standard basis vector in \mathbb{R}^3 , and for each interior vertex v , $f(v) = (v_1, v_2, v_3)$, where v_i denotes the number of faces contained inside region $R_i(v)$.

Dhandapani noted in [25] that the previous result holds more generally. Before proving such result we introduce some terminology. A *weight distribution* is a function $\mathbf{w} : \mathcal{F}(T) \rightarrow (0, 2n - 5)$ that assigns to each face in $\mathcal{F}(T)$ a positive weight, such that $\sum_{f \in \mathcal{F}(T)} \mathbf{w}(f) = 2n - 5$. Let us now show how barycentric embeddings can be obtained from Schnyder woods and weight distributions.

Theorem 2.4.3 (Schnyder). *If S is a Schnyder wood of a planar triangulation T on n vertices and $\mathbf{w} : \mathcal{F}(T) \rightarrow (0, 2n - 5)$ is a weight distribution, then the function $f : V(T) \rightarrow \mathbb{R}^3$ defined by*

$$f(v) = \begin{cases} (2n - 5)e_i & \text{if } v = a_i \\ (v_1, v_2, v_3) & \text{if } v \text{ is an interior vertex} \end{cases}$$

is a barycentric embedding of T . Here e_i denotes the i -th standard basis vector in \mathbb{R}^3 and $v_i := \sum_{g \in R_i(v)} \mathbf{w}(g)$.

Proof. Clearly f satisfies the first condition in the definition of a barycentric embedding, this follows from the definition of f and that of a weight distribution. We now show that the second condition holds, noting that injectivity follows from this condition. First note that no vertex other than a_i is mapped to $(2n - 5)e_i$, thus if we are given an edge $uv \in E(T - a_i)$ then $u_i, v_i < 2n - 5$, so the second condition of the definition of a barycentric embedding holds whenever w is an exterior vertex.

Now, let $uv \in E(T)$ and suppose $w \in V(T) \setminus \{u, v\}$, with w an interior vertex. It follows from the planarity of T that $uv \in R_i(w)$ for some $i \in \{1, 2, 3\}$. If u is an exterior vertex, then clearly $u \neq a_i$ and therefore $u_i < w_i$, since $u_i = 0$ in this case. A similar assertion holds if v is an exterior vertex. Now, if u is an interior vertex then by Lemma 2.4.2 we have that $u_i < w_i$ since $R_i(u)$ is properly contained in $R_i(w)$ and the weights are all positive.

Similarly we obtain that $v_i < w_i$ whenever v is an interior vertex. In either case the second condition of the definition of barycentric embedding is satisfied. This concludes the proof. \square

A consequence of the previous theorem is that whenever we are given a Schnyder wood S of a planar triangulation T together with a weight distribution \mathbf{w} , there is a planar drawing that can be obtained from S and \mathbf{w} . We call such drawing of T the *Schnyder drawing induced by \mathbf{w} and S* .

Recall that in the definition of barycentric embedding, one of the conditions requires that for any edge $uv \in E(G)$ and $x \in V(G) \setminus \{u, v\}$, there is a coordinate $k \in \{1, 2, 3\}$, such that $u_k, v_k < w_k$. As noted in the previous proof, this condition is fulfilled by Schnyder drawings. This property will be of use in other results, so we state it explicitly here.

(R) Let T be a planar triangulation and let S be a Schnyder wood of T . Then, for any edge $uv \in E(T)$ and any $w \in V \setminus \{u, v\}$, there is $k \in \{1, 2, 3\}$ so that $u, v \in R_k(w)$. Consequently, in the corresponding Schnyder drawing we have $u_k, v_k < w_k$.

2.5 Face weights

As we saw in the previous section, given any Schnyder wood and a weight distribution we can obtain a planar drawing of the corresponding planar triangulation. The aim of this section is to prove that any drawing of a planar triangulation can be obtained from a Schnyder wood and some assignment of weights in the interior faces, where not necessarily all the weights are positive. The ideas presented in this section are based on a result of Felsner and Zickfeld [33, Theorem 9], they study the same system of linear equations that we do but in a different context.

Let T be a planar triangulation, let S be a Schnyder wood and let $\mathbf{w} : \mathcal{F}(T) \rightarrow \mathbb{R}$ be such that $\sum_{f \in \mathcal{F}(T)} \mathbf{w}(f) = 2n - 5$. We define the Schnyder drawing of T induced by S and \mathbf{w} as the drawing Γ in which each vertex is assigned the position (v_1, v_2, v_3) , where $v_i = \sum_{f \in R_i(v)} w(f)$. Our aim is to show how to obtain the weight function \mathbf{w} given a Schnyder wood S and the positions assigned to each vertex.

Let T be a planar triangulation and let S be a Schnyder wood of T . For an interior vertex v and a colour i , we define the *characteristic vector* of $R_i(v)$, $\chi_{R_i(v)}$, to be the $(0, 1)$ -vector with entries indexed by elements of $\mathcal{F}(T)$, where the entry indexed by $f \in \mathcal{F}(T)$ is equal to 1 if $f \in R_i(v)$ and 0 otherwise.

In this same context we define the *incidence matrix* of S with respect to colours i and j to be the $(2n - 5) \times (2n - 5)$ matrix given by

$$A = \begin{pmatrix} \chi_{R_i(v_1)} \\ \chi_{R_j(v_1)} \\ \chi_{R_i(v_2)} \\ \chi_{R_j(v_2)} \\ \vdots \\ \chi_{R_i(v_{n-3})} \\ \chi_{R_j(v_{n-3})} \\ \mathbf{1} \end{pmatrix},$$

here $\mathbf{1}$ denotes the all ones vector in \mathbb{R}^{2n-5} .

As we will see, given a Schnyder wood and a drawing of a planar triangulation we will need to solve a system of linear equations involving the incidence matrix to find the face weights that induce the given drawing. In the following result we show that the incidence matrix with respect to any two colours has rank $2n - 5$.

Lemma 2.5.1 (Felsner and Zickfeld [33]). *Let T be a planar triangulation and let S be a Schnyder wood of T . Then the incidence matrix of S with respect to colours i and j is invertible and its inverse has integer entries.*

Proof. Let T be a planar triangulation and let S be a Schnyder wood of T . We may assume without loss of generality that we are considering colours 1 and 2, otherwise we could just rename the colours. Let A be the incidence matrix of S with respect to colours 1 and 2. We show A is invertible by showing that it has rank $2n - 5$. It is clear that A has rank at most $2n - 5$.

Let f be an interior face of T , for such face we define χ_f to be the $(0, 1)$ -vector which has all entries equal to 0, except for the one indexed by f . To show that A has rank at least $2n - 5$ we will show that $\chi_f \in \text{row}(A)$. We consider three possible cases depending on the edges in S incident to f .

The first case we consider is when f is incident to an exterior edge, let u be the interior vertex incident to f . Say the exterior edge is a_1a_2 . Then $\chi_f = \chi_{R_3(u)} = \mathbf{1} - \chi_{R_1(u)} - \chi_{R_2(u)}$. For the case where the exterior edge is a_1a_3 or a_2a_3 we have $\chi_f = \chi_{R_2(u)}$ or $\chi_f = \chi_{R_1(u)}$ respectively. In either case $\chi_f \in \text{row}(A)$, as desired.

For the second case, we will assume that the edges of S incident to f form a directed cycle. Say $f = uvw$ and we have edges (u, v) , (v, w) and (w, u) of colours 1, 2 and 3

respectively. In this case we can observe that

$$\chi_f = \mathbf{1} - \chi_{R_2(u)} - \chi_{R_1(w)} - \chi_{R_3(v)}.$$

And since $\chi_{R_3(v)} = \mathbf{1} - \chi_{R_1(v)} - \chi_{R_2(v)}$ we get that

$$\chi_f = \chi_{R_1(v)} + \chi_{R_2(v)} - \chi_{R_2(u)} - \chi_{R_1(w)},$$

as desired.

Finally, we consider the case when the edges of S incident to f do not form an oriented cycle. In this case we must have two edges of the same colour pointing towards a vertex by Lemma 2.3.1. So if we assume $f = uvw$, we may assume without loss of generality that the edges in S incident to f are (u, v) and (w, v) in colour 1. Now, it may be the case that edge (u, w) has colour $i + 1$ or (w, u) has colour $i - 1$. The two cases can be handled similarly, so we will assume that (u, w) has colour $i + 1$ in S . Here we have the following

$$\chi_f = \mathbf{1} - \chi_{R_2(u)} - \chi_{R_3(w)} - \chi_{R_1(u)},$$

now, since $\chi_{R_3(w)} = \mathbf{1} - \chi_{R_1(w)} - \chi_{R_2(w)}$ we get that

$$\chi_f = \chi_{R_1(w)} + \chi_{R_2(w)} - \chi_{R_2(u)} - \chi_{R_1(u)},$$

therefore A is invertible.

As we can see from the expressions above each χ_f can be obtained as an integral linear combination of the rows of A , which implies that the inverse of A has integer entries. \square

We use Felsner and Zickfeld's result to derive a new lemma. We show that given any straightline drawing Γ of T and any Schnyder wood of T such that they have the same set of exterior vertices, we may find a weight distribution that induces Γ .

Lemma 2.5.2. *Let S be a Schnyder wood of a planar triangulation T on n vertices and let Γ be a straightline drawing of T that has the same exterior vertices as S . Then there exists a unique function $w : \mathcal{F} \rightarrow \mathbb{R}$ satisfying $\sum_{f \in \mathcal{F}} w(f) = 2n - 5$, such that S and w induce Γ . Furthermore, if the barycentric coordinates of the drawing Γ are integral, then the weights inducing such drawing are also integral.*

Proof. Let A be the incidence matrix of S with respect to colours 1 and 2. It follows from the definition of the induced drawing that finding such weight distribution w is equivalent to solving the system of linear equations $Aw = b$, where b is the vector obtained from Γ

by considering the first two barycentric coordinates of each vertex in the same order as in the rows of A , and $2n - 5$ as its last entry.

The result now follows from Lemma 2.5.1. The existence and uniqueness of w follow from the fact that A is an invertible matrix. We can also conclude that, since the inverse of A has integer entries, if the coordinates given by b are integral then the resulting weights given by w will also be integral. \square

A recognition algorithm for drawings of planar triangulations arising from an assignment of positive weights to the faces and a Schnyder wood can be derived by using the oriented half- Θ_6 -graph as defined in [17]¹.

2.6 Flipping triangles

In general, there may be exponentially many Schnyder woods for a fixed planar triangulation as proved in [32]. It has also been proved that the set of Schnyder woods is a distributive lattice [19, 30, 48]. In this distributive lattice, the basic operation to traverse it is by reversing cyclically oriented triangles and changing colours appropriately, we call this operation a *flip* and we describe it in detail at the end of this section. We also state a result which provides a bound on the distance between any two Schnyder woods in the lattice.

Let us begin by studying the structure of Schnyder woods within cyclically oriented separating triangles.

Lemma 2.6.1. *Let T be a planar triangulation and let S be a Schnyder wood of T . Assume there is a cyclically oriented separating triangle C in S . Then the restriction of S to the edges inside C defines a Schnyder wood of $T|_C$.*

Proof. It is clear that the interior vertex property (D1) is satisfied in $T|_C$. We are just left to show the exterior vertex property (D2). We may assume that C is cyclically oriented in counterclockwise order, say $C = b_1, b_2, b_3$. The case where C is clockwise will follow from a similar argument. We show that all interior edges of $T|_C$ at b_1 are incoming and have the same colour, the argument for b_2 and b_3 is analogous. Suppose, by way of contradiction, that there is an interior edge of $T|_C$ in S having colour i that is outgoing b_1 . Let j be the colour of (b_1, b_2) in S , clearly $j \neq i$ by the vertex property (D1). By property (P2) the path

¹Thank you to an anonymous reviewer for pointing out the relationship to half- Θ_6 -graphs

$P_i(b_1)$ ends at a_i , therefore it must leave C through b_2 or b_3 . Clearly $b_2 \notin P_i(b_1)$, otherwise this would contradict property (P1) for $P_i(b_1)$ and $P_j(b_1)$. Let j' be the colour of (b_3, b_1) and suppose $b_3 \in P_i(b_1)$. We can now see that $T_i^- \cup T_{j'}^-$ contains a cycle, which contradicts property (P1). Therefore all interior edges of $T|_C$ at b_1 are incoming. Furthermore, these edges must be of the same colour or else, by the vertex property (D1), there would be an outgoing edge towards the interior of C . To conclude the proof we show that the colours of interior edges of $T|_C$ at b_1 , b_2 and b_3 appear in the same cyclic order as the colours of the interior edges incident to a_1 , a_2 and a_3 . Let v be an interior vertex of $T|_C$ and suppose, without loss of generality, that $P_i(v)$ uses b_1 . It now follows that $P_{i+1}(v)$ and $P_{i-1}(v)$ leave through b_3 and b_2 respectively, otherwise, by the vertex property (D1) we would have that $P_{i+1}(v)$ and $P_{i-1}(v)$ would share a vertex, contradicting (P1). This concludes the proof. \square

In the following lemma we look at the structure of cyclically oriented separating triangles in a given Schnyder wood.

Lemma 2.6.2. *Let T be a planar triangulation and let S be a Schnyder wood of T . If S has a triangle C at which the edges are oriented cyclically, then C has an edge of each colour in S . Furthermore, if C is oriented counterclockwise then the edges along the cycle have colours i , $i - 1$ and $i + 1$ respectively.*

Proof. It follows from Lemma 2.3.1 that the result holds for the case where C is a facial cycle.

Let $C = b_1b_2b_3$ be a separating triangle and suppose the arcs forming C are $\alpha_1 = (b_1, b_2)$, $\alpha_2 = (b_2, b_3)$ and $\alpha_3 = (b_3, b_1)$. By property (P1) not all arcs have the same colour. If two of the arcs share colour i , say α_1 and α_2 , and α_3 has colour j , then $T_i^- \cup T_j^-$ contains a cycle, which contradicts property (P1). Therefore the colours of α_1 , α_2 and α_3 are pairwise distinct. Now, let us assume that C is oriented counterclockwise. Suppose without loss of generality that α_1 has colour i . It suffices to show that α_2 has colour $i - 1$ and by rotational symmetry the result will follow. Suppose, by contradiction that α_2 has colour $i + 1$. Then there are two interior edges of $T|_C$ that are outgoing b_2 , and this contradicts Lemma 2.6.1. Therefore α_2 must have colour $i - 1$. The result now follows. \square

Given a Schnyder wood S of a planar triangulation T , we can obtain another Schnyder wood S' of T different from S , provided that S contains a triangle $C = xyz$ which is cyclically oriented. We will assume that the edges of C are directed counterclockwise, and by symmetry, a similar procedure will also work for triangles directed clockwise. We describe how to obtain S' from S . We may assume without loss of generality and by

Lemma 2.6.2 that the directed edges in S are (x, y) , (y, z) and (z, x) , and that they are coloured 1, 3 and 2 respectively. We obtain S' from S in the following way:

1. Every edge having an endpoint outside xyz remains unchanged.
2. Edges on the cycle are reversed and colours change from i to $i - 1$.
3. Any interior edge of $T|_C$ remains with the same orientation and changes colour from i to $i + 1$.

We call such procedure a *flip* of the triangle xyz . We define a *flop* to be the analogous procedure applied to a clockwise directed triangle. The fact that performing a flip or a flop yields another Schnyder wood is a particular case of a result proven by Brehm [19, p. 44].

Theorem 2.6.3 (Brehm [19]). *Let T be a planar triangulation, let S be a Schnyder wood of T such that S contains a triangle which is oriented counterclockwise and let S' be as described above. Then S' is a Schnyder wood of T .*

This theorem provides a way to go from a Schnyder wood to another in the lattice. In fact, this is the basic step to traverse such structure. In the following section we derive a bound for the distance between any two Schnyder woods in the lattice.

2.7 Flip distance between Schnyder woods

The aim of this section is to provide a bound for the flip distance between any two Schnyder woods of a fixed planar triangulation. As noted by Miracle et al. [46], a bound of $O(n^2)$ can be obtained from Brehm's work [19] for the case of 4-connected planar triangulations, here n denotes the number of vertices of the triangulation. Here we observe that the same bound holds for any planar triangulation.

A triangle in a Schnyder wood S is called *flippable* if it is cyclically oriented counterclockwise. *Floppable* triangles are triangles whose edges are cyclically oriented clockwise in S . Let C be a flippable triangle in S and denote by S^C the Schnyder wood obtained from flipping C in S . We say C_1, C_2, \dots, C_k is a flip sequence if C_1 is flippable in $S_1 := S$, and C_i is flippable in S_i with $S_{i+1} := S_i^{C_i}$ for $1 \leq i \leq k - 1$. Note that if C_1, \dots, C_k defines a flip sequence, then C_k, \dots, C_1 defines a flop sequence. In a 4-connected planar triangulation T the flippable triangles are precisely the cyclically oriented faces of T , since T does not contain separating triangles.

The following result of Brehm will allow us to derive an upper bound for the length of a maximal flip sequence in any planar triangulation.

Proposition 2.7.1 (Brehm [19, p. 15]). *Let T be a 4-connected planar triangulation, let S be a Schnyder wood of T and let f be an interior face of T . If there is a flip sequence that contains f at least twice, then between any two flips of f , all the faces adjacent to f must be flipped.*

Let us observe that any maximal flip sequence starting at an arbitrary Schnyder wood ends at the unique Schnyder wood containing no flippable face. In fact we can derive the following bound, as suggested in [19, p. 15].

Theorem 2.7.2. *Let T be a 4-connected planar triangulation on n vertices with exterior face f^* . The length of any flip sequence F is bounded by the sum of the distances in the dual of T to f^* , that is,*

$$|F| \leq \sum_{f \in \mathcal{F}(T)} d(f, f^*) = O(n^2).$$

Furthermore, any maximal flip sequence terminates at \mathcal{L} , the Schnyder wood containing no flippable triangles.

Proof. Observe that any face adjacent to the exterior face cannot be flipped. By Proposition 2.7.1 it follows that the number of times a face f can be flipped is bounded by the distance from f to the exterior face f^* . Therefore the length of any flip sequence is $O(n^2)$, as claimed. Clearly any maximal flip sequence terminates at the Schnyder wood containing no flippable face, or otherwise it would contradict its maximality. \square

A 4-connected block of a graph G is a maximal 4-connected induced subgraph of G . If G_1, \dots, G_k denote the 4-connected blocks of a graph G then we say that they define a *decomposition of G into 4-connected blocks*. One more result that will be useful is the following.

Theorem 2.7.3 (Brehm [19, p. 37]). *Consider a planar triangulation T . Let T_1, \dots, T_k be a decomposition of T into 4-connected blocks. Then any flip sequence in S can be obtained by concatenating flip sequences S_1, S_2, \dots, S_k , where each S_i is flip sequence in T_i .*

We now derive an upper bound for the length of maximal flip sequences in planar triangulations.

Lemma 2.7.4. *Let T be a planar triangulation on n vertices. A maximal flip F sequence has length $O(n^2)$.*

Proof. Let T be a planar triangulation on n vertices. Consider a decomposition of T into 4-connected blocks T_1, \dots, T_k . Denote by n_i the number of interior vertices of T_i , $1 \leq i \leq k$. Therefore we have $3 + \sum_{i=1}^k n_i = n$. Observe that the length of a maximal flip sequence in the lattice of Schnyder woods of T_i is $O(n_i^2)$ from Theorem 2.7.2. By Theorem 2.7.3 the length of a maximal flip sequence in the lattice of Schnyder woods of T is $O(\sum_{i=1}^k n_i^2)$. We now have the following standard claim.

Claim. The value of $\sum_{i=1}^k n_i^2$ subject to $\sum_{i=1}^k n_i = n - 3$ and $n_i \geq 0$, is maximized when exactly one of the n_i is equal to $n - 3$ and all others are zero.

Proof of claim. Suppose at least two terms are non zero say $0 < n_1 \leq n_2$. Let us show how to increase the value of the sum.

$$\begin{aligned} (n_1 - 1)^2 + (n_2 + 1)^2 + \sum_{i=3}^k n_i^2 &= 2(n_2 - n_1 + 1) + \sum_{i=1}^k n_i^2 \\ &> \sum_{i=1}^k n_i^2. \end{aligned}$$

So the claim holds.

A consequence of the claim is that $O(\sum_{i=1}^k n_i^2) = O(n^2)$ and therefore the length of a maximal flip sequence in the lattice of Schnyder woods of T is $O(n^2)$. \square

Chapter 3

Morphing planar graph drawings with unidirectional moves

In this chapter we present an improvement on the result of Alamdari et al. [2]. We show an approach which simplifies that of [2] where the steps that describe the morph are a simpler type of morph, namely, *unidirectional morphs*. A *unidirectional morph* is a linear morph where every vertex moves parallel to the same line, i.e. there is a line L with unit direction vector $\bar{\ell}$ such that each vertex v moves at constant speed from initial position v_0 to position $v_0 + k_v \bar{\ell}$ for some $k_v \in \mathbb{R}$. Note that k_v may be positive, negative or zero, that different vertices may move different amounts along direction $\bar{\ell}$ and that vertices may move at different speeds. We call this an *L-directional morph*.

This chapter is structured as follows. First we present an overview of Cairns' [22] procedure in Section 3.1. Then, in Section 3.2 we provide an overview of the technique used in [2]. This technique can be analyzed in two phases. In Section 3.3 we focus on the first phase. We show that their first phase can be implemented using only unidirectional morphs. Finally in Section 3.4 we present a new approach for the second phase of the technique described in [2] that only uses unidirectional morphs.

3.1 Overview of Cairns' algorithm

In this section we provide a high-level description of Cairn's solution to the problem of morphing between any two straightline drawings of a planar triangulation.

Given a planar triangulation T , we call a vertex $v \in V(T)$ a *low degree vertex* if $\deg(v) \leq 5$. We now state a lemma which provides a lower bound on the number of low degree vertices in planar triangulations.

Lemma 3.1.1. *Let T be a planar triangulation. Then T has at least 4 low degree vertices.*

Given an n -gon P with vertices p_1, \dots, p_n in counterclockwise order we define the *kernel* of P , $\mathcal{K}(P)$, to be the set consisting of points inside or on P that are visible from any vertex of P (see Figure 3.1), or explicitly

$$\mathcal{K}(P) := \{p \in P \mid \overline{pp_i} \text{ lies entirely within } P \text{ for all } 1 \leq i \leq n\}.$$

We provide an alternative definition for $\mathcal{K}(P)$ in terms of half-planes. Let h_i be the half-plane defined by $p_i p_{i+1}$ which is to the left of the segment $p_i p_{i+1}$ while traversed from p_i to p_{i+1} . We call h_i the *interior half-plane* through $p_i p_{i+1}$. Then, $\mathcal{K}(P) := \bigcap_{i=1}^n h_i$.

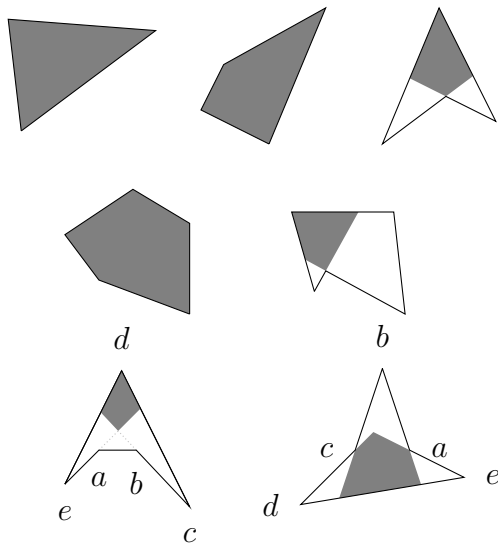


Figure 3.1: Some polygons with shaded regions representing their kernels.

If P is a k -gon with $k \leq n$ then we say P is a $\leq n$ -gon.

Lemma 3.1.2 (Cairns [22]). *Let P be a ≤ 5 -gon, then $\mathcal{K}(P) \neq \emptyset$. Furthermore, there is a vertex a of P such that $a \in \mathcal{K}(P)$.*

Proof. Note that the result is clearly true for triangles. Now, for the case of quadrilaterals, two possibilities arise. If the quadrilateral Q is convex, then the statement holds. However, if Q is not convex, then exactly one of its vertices is reflex. In such case, the reflex vertex is in the kernel.

Let us now prove the statement for a pentagon $P = abcde$, where its vertices are listed in counterclockwise order. Since the sum of the interior angles of P is 3π it follows that P cannot have more than two reflex vertices. When P has 0 or 1 reflex vertices, then any vertex or the reflex vertex is in $\mathcal{K}(P)$ respectively. Now, suppose P has two reflex vertices. Let us treat two possible subcases. We begin by considering the case where the reflex vertices are consecutive, say they are a and b , see bottom left of Figure 3.1. In this case we can observe that the vertex opposite to the segment ab , namely d , is in $\mathcal{K}(P)$. Finally, for the case where the reflex vertices are non consecutive, say a and c (bottom right in Figure 3.1), then at least one of them is in the kernel. This follows by observing that if none of a and c are in the kernel, then they must mutually obstruct their visibility to d and e respectively, which is not possible. \square

Let T be a planar triangulation and let Γ_0 and Γ_1 be two drawings of T such that the exterior face coincides in Γ_0 and Γ_1 . The first step in Cairns' inductive approach is to consider an interior vertex of low degree v . Such vertex exists by Lemma 3.1.1. Then, we focus on the polygons P_0 and P_1 defined by the neighbours of v in Γ_0 and Γ_1 respectively. By Lemma 3.1.2 there are neighbours u_0 and u_1 of v such that $u_0 \in \mathcal{K}(P_0)$ and $u_1 \in \mathcal{K}(P_1)$. We then consider the planar triangulations $T'_0 := T/u_0v$ and $T'_1 := T/u_1v$ together with two drawings Γ'_0 and Γ'_1 . In Γ'_i the positions of the vertices are those inherited from the positions in Γ_i , for $i \in \{0, 1\}$. A third drawing is also considered, this is a drawing Γ'_2 of $T - v$ where the polygon P_2 defined by the neighbours of v in Γ'_2 contains u_0 and u_1 its kernel.

The problem can then be solved inductively by obtaining a morph \mathcal{M}'_0 from Γ'_0 to Γ'_2 and a morph \mathcal{M}'_1 from Γ'_2 to Γ'_1 , this is the first phase of this procedure. Note that by putting \mathcal{M}'_0 and \mathcal{M}'_1 together we do not obtain a true morph, since some vertices become coincident. However, we may still obtain a morph from Γ_0 to Γ_1 by using \mathcal{M}'_0 and \mathcal{M}'_1 . We call this the second phase. The way to obtain such morph is to extend each drawing in \mathcal{M}'_0 and \mathcal{M}'_1 to a drawing of T . In Cairns' approach this is achieved by placing v at the barycenter of the kernel of the ≤ 5 -gon defined by the neighbours of v .

There are two aspects to be noted from Cairns' approach. The first one is that the number of steps required in total $T_C(n)$ satisfies the following recurrence

$$T_C(n) \leq T_C(n-1) + T_C(n-1).$$

This implies that $T_C(n) = O(2^n)$. The second aspect is that placing v at the barycenter of the kernel does not guarantee that the resulting morph will be linear, see appendix in [2]. The technique followed in [2] circumvents these two aspects as will be described in the following section.

3.2 The technique used by Alamdari et al.

In this section we provide an overview of the technique used in [2]. Like Cairns, they follow a two phase approach. The method in [2] provides two advantages over Cairns' approach, namely that only a polynomial number of steps is required and that each step is a linear morph.

Let us begin by introducing some terminology. Let T be a planar triangulation and let Γ be a planar drawing of T . Let $u \in V(T)$ and let P be the polygon defined by its neighbours. If there is a neighbour x of u in the kernel of P , $\mathcal{K}(P)$, then we define the *contraction* of u onto x as the family of drawings $\{\Gamma^t\}_{t \in [0,1]}$, where $\Gamma_0 = \Gamma$, Γ_1 is the drawing of $T_{u,x}$ where the position for vertices in $T_{u,x}$ is inherited from Γ , and as t goes from 0 to 1 the vertex u moves in a linear trajectory at constant speed from its position in Γ to the position of x in Γ . An *uncontraction* of u from x is defined in an analogous fashion as a contraction, where we are given a drawing of $T_{u,x}$ and u linearly moves away from x to some point in $\mathcal{K}(P)$. Note that any time a single vertex moves linearly this defines a unidirectional move, particularly in the case where we perform a contraction of u onto x or in an uncontraction of u from x the vertex u . We define a *pseudo morph* as a sequence of the following kinds of steps:

- a linear morph
- a contraction of a vertex u onto another vertex x , followed by a pseudo morph between the two reduced drawings, and then an uncontraction of u from x .

The number of steps in a pseudo morph is defined to be the number of linear morphs plus the number of contractions and uncontractions. As for the case of morphs, say a pseudo morph is *planar* if each of the linear morphs in the pseudo morph is planar. The first phase in the approach from [2] consists of finding a planar pseudo morph with $O(n^2)$ steps.

Recall that in Cairns' approach we morph to an intermediate drawing in which all feasible vertices are in the kernel of the ≤ 5 -gon P , here by feasible vertex we mean a

vertex that is in the kernel of P in at least one of two given drawings. This causes the procedure to have two recursive calls and thus have exponential running time. To avoid this, the alternative approach is to morph to a drawing that satisfies weaker conditions. The procedure requires to morph to a drawing Γ_2 such that $u_0, u_1 \in \mathcal{K}_{\Gamma_2}(P)$, where $u_0 \in \mathcal{K}_{\Gamma_0}(P)$ and $u_1 \in \mathcal{K}_{\Gamma_1}(P)$. In [2] they show that this takes $O(n)$ time. Then by using the recursive step from Cairns' approach, they show that the total number of steps required $T(n)$ satisfies

$$T(n) \leq T(n - 1) + O(n),$$

thus yielding that $T(n) = O(n^2)$.

In the second phase from [2] the pseudo morph is converted to a true morph that avoids coincident vertices. This requires a somewhat involved geometric argument that instead of contracting a vertex p to a neighbour, it is possible to move p close to the neighbour and keep it close during subsequent morphing steps without increasing the number of steps.

3.3 A pseudo morph with unidirectional morphing steps

Alamdari et al. [2] give a pseudo morph of $O(n^2)$ steps to go between any two drawings of a planar triangulation having the same exterior face. In this section we show that their pseudo morph can be implemented with unidirectional morphs. They show that the only thing that is needed is a solution to the following problem using $O(n)$ linear morphs:

PROBLEM 3.2. (4-GON CONVEXIFICATION) Given a planar triangulation T with a triangle boundary and a 4-gon $abcd$ in a straightline planar drawing of T such that neither ac nor bd is an edge outside of $abcd$ (i.e., $abcd$ does not have external chords), find a pseudo morph so that $abcd$ becomes convex.

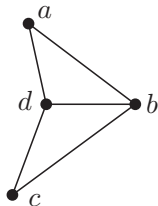


Figure 3.2: A 4-gon $abcd$.

The main idea is to use Cairns' approach, namely, find a low-degree vertex, contract it to a neighbour, and recurse on the resulting smaller graph. Note that each such contraction is a unidirectional morph. In general, not any low-degree vertex can be chosen to perform a contraction, as this would obstruct the 4-gon convexification process. A low-degree vertex p for which the contraction cannot be performed will be called a *problematic vertex*, and it satisfies one of the following:

1. p is a vertex of the boundary triangle z_1, z_2, z_3 .
2. p is a vertex of the 4-gon $abcd$ and is not on the boundary.
3. p is outside the 4-gon, is not on the boundary, has degree at most 5, and is adjacent to both a and c , and either a or c is in the kernel of the polygon formed by the neighbours of p . (In this case contracting p to a or c would create the edge ac outside the 4-gon.)

In [2] it is shown how to handle each type of problematic vertex. Here we go through the cases to show that unidirectional morphs suffice in each case.

Problematic vertices of type (2) and type (3) are handled (in their Sections 4.1 and 4.3) by moving linearly a single vertex at a time either by contracting or by moving a vertex very close to another vertex. Moving one vertex along a linear trajectory is clearly a unidirectional morph, so there is nothing to be done for these cases.

It remains to consider problematic vertices of type (1) which they do in Section 4.2. To handle this case they use an operation where one vertex of a separating triangle moves along a straight line and the other vertices inside the triangle follow along linearly. We will show that the resulting motion is in fact unidirectional. Note that the statement of the following lemma is slightly stronger than what we need to show, which is done with the intention of using the strengthened version later in this chapter.

Lemma 3.3.1. *Let a, b, c be the vertices of a triangle and let x be a point inside the triangle defined by the convex combination $\lambda_1 a + \lambda_2 b + \lambda_3 c$ where $\sum \lambda_i = 1$ and $\lambda_i \geq 0$. If $a, b,$ and c move linearly in the direction of the vector \bar{d} then so does x .*

Proof. Suppose the morph is indexed by $t \in [0, 1]$ and that the positions of the vertices at time t are a_t, b_t, c_t, x_t . Suppose that a moves by $k_1 \bar{d}$, b moves by $k_2 \bar{d}$, and c moves by $k_3 \bar{d}$. Thus

$$\begin{aligned} a_t &= a_0 + tk_1 \bar{d} \\ b_t &= b_0 + tk_2 \bar{d} \\ c_t &= c_0 + tk_3 \bar{d}. \end{aligned}$$

Then

$$\begin{aligned}
 x_t &= \lambda_1 a_t + \lambda_2 b_t + \lambda_3 c_t \\
 &= \lambda_1 a_0 + \lambda_2 b_0 + \lambda_3 c_0 + t(\lambda_1 k_1 + \lambda_2 k_2 + \lambda_3 k_3) \bar{d} \\
 &= x_0 + tk\bar{d},
 \end{aligned}$$

where $k = \lambda_1 k_1 + \lambda_2 k_2 + \lambda_3 k_3$. Thus x also moves linearly in direction \bar{d} . \square

In [2] it is proven that to handle problematic vertices of type (1) it suffices to handle the following two cases. We repeat their arguments, adding details of exactly how Lemma 3.3.1 gives unidirectional morphs.

A. There is a boundary vertex, say z_1 , of degree 3. See Figure 3.3(a).

Then z_1 must have a neighbour y that is adjacent to z_2 and z_3 . If $abcd$ lies entirely inside the triangle $C = yz_2z_3$ then we recursively morph $T|_C$. Otherwise $abcd$ must include at least one triangle outside C . It cannot have both triangles outside C because of the assumption that there is no edge ac . Thus we can assume without loss of generality that $abcd$ consists of triangle z_1yz_2 and an adjacent triangle inside C , see Figure 3.3(b). The solution is to move y towards z_1 to directly convexify $abcd$. As y is moved, the interior vertices of $T|_C$ follow along linearly. Thus, by Lemma 3.3.1 this is a unidirectional morph.

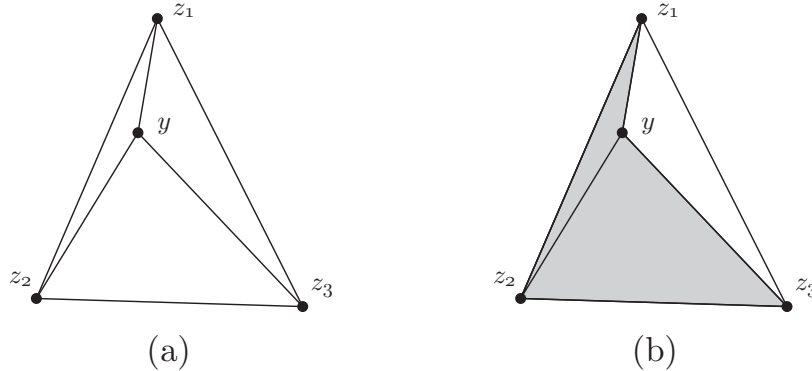


Figure 3.3: A boundary vertex of degree 3.

B. All three boundary vertices have degree 4. See Figure 3.4(a).

In this case there must exist an internal separating triangle $C = y_1y_2y_3$ containing all other interior vertices with y_i adjacent to z_j for $j \neq i$, with $i, j \in \{1, 2, 3\}$. If $abcd$

lies entirely inside C then we recursively morph $T|_C$. If $abcd$ lies entirely outside C then without loss of generality $abcd$ is $z_2z_1y_2y_3$. The solution is to move y_2 towards z_1 to directly convexify the 4-gon. As y_2 is moved, the interior vertices of $T|_C$ follow along linearly. Thus by Lemma 3.3.1 this is a unidirectional morph.

The final possibility is that $abcd$ consists of one triangle outside C and one triangle inside C . We may assume without loss of generality that $abcd$ consists of triangle $z_1y_3y_2$ and an adjacent triangle inside C , see Figure 3.4(b). We will convexify the 4-gon $z_1y_2y_1y_3$, which will necessarily also convexify $abcd$. The solution is to move y_1 towards z_2 to convexify the 4-gon while the interior vertices of $T|_C$ follow along linearly. Therefore by Lemma 3.3.1 this is a unidirectional morph.

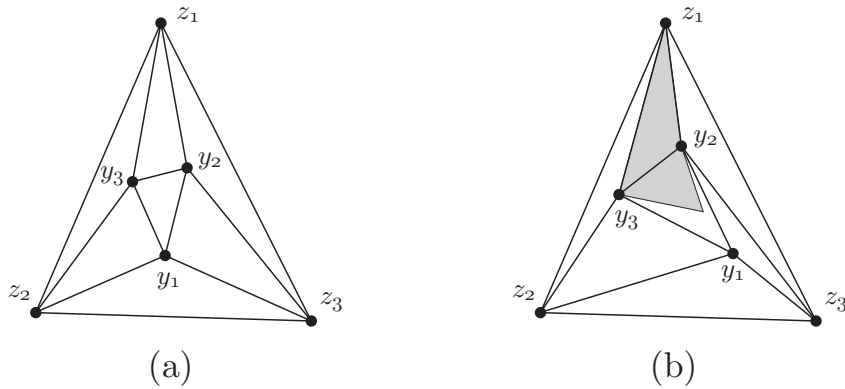


Figure 3.4: All three boundary vertices of degree 4.

This completes the argument that the pseudo morph of Alamdari et al. can be implemented with unidirectional morphs.

3.4 Avoiding coincident vertices

In this section we show how to convert a pseudo morph to a true morph that avoids coincident vertices. More precisely, we show that a pseudo morph of k steps that acts on a planar triangulation, preserves planarity, uses unidirectional morphing steps, and contracts vertices of degree at most 5 can be converted to a true morph that preserves planarity and consists of k unidirectional morphing steps. The key to simplifying the second phase presented in [2] is that in our approach we only allow unidirectional morphs. Let us begin by stating our main result of this section.

Theorem 3.4.1. *Let T be a planar triangulation and let Γ and Γ' be two planar drawings of T that have the same exterior face. If $\mathcal{M} = \langle \Gamma'_1, \dots, \Gamma'_k \rangle$ is a planar pseudo morph from Γ to Γ' that consists of unidirectional steps then there exists a planar morph $M = \langle \Gamma_1, \dots, \Gamma_k \rangle$ from Γ to Γ' that consists of unidirectional steps.*

To prove Theorem 3.4.1 we proceed by induction on the number of vertices, following an argument similar to that of [2]. Suppose the pseudo morph consists of the contraction of a non-boundary vertex p of degree at most 5 to a neighbour a , followed by a pseudo morph \mathcal{M} of the reduced graph $T_{p,a}$ and then an uncontraction of p . The pseudo morph \mathcal{M} consists of unidirectional morphing steps and by induction we can convert it to a morph M that consists of the same number of unidirectional morphing steps. We will show how to modify M to M^p by adding p and its incident edges back into each drawing of the morph sequence. To obtain the final morph, we replace the contraction of p to a by a unidirectional morph that moves p from its initial position to its position at the start of M^p , then follow the steps of M^p , and then replace the uncontraction of p by a unidirectional morph that moves p from its position at the end of M^p to its final position. The result is a true morph that consists of unidirectional morphing steps and the number of steps is the same as in the original pseudo morph.

Thus our main task is to modify a morph M to a morph M^p by adding a vertex p of degree at most 5 and its incident edges back into each drawing of the morph sequence, maintaining the property that each step of the morph sequence is a unidirectional morph. It suffices to look at the polygon P formed by the neighbours of p . We know that P has a vertex a that remains in the kernel of P throughout the morph. We will place p near a . We separate into the cases where P has 3 or 4 vertices and the case where P has 5 vertices, the second case being more involved. The following two lemmas handle these two cases, and together strengthen Lemmas 5.1 and 5.2 of [2] by adding the unidirectional condition. Furthermore, together they provide a proof of Theorem 3.4.1.

Lemma 3.4.2. *Let P be a ≤ 4 -gon and let $\Gamma_1, \dots, \Gamma_k$ be straightline planar drawings of P such that each morph $\langle \Gamma_i, \Gamma_{i+1} \rangle, i = 1, \dots, k - 1$ is unidirectional and planar, and vertex a of P is in the kernel of P at all times during the whole morph $\langle \Gamma_1, \dots, \Gamma_k \rangle$. Then we can augment each drawing Γ_i to a drawing Γ_i^p by adding vertex p at some point p_i inside the kernel of the polygon P in Γ_i and adding straightline edges from p to each vertex of P in such a way that each morph $\langle \Gamma_i^p, \Gamma_{i+1}^p \rangle$ is unidirectional and planar.*

Proof. Note that if P is a triangle then $\mathcal{K}(P)$ consists of all points inside P and on P . In this case, it follows from Lemma 3.3.1 that we can place p at a fixed convex combination of the vertices of P in each of the drawings Γ_i .

Now, let us consider the case where P is a 4-gon, say $abcd$. Here the line segment $\overline{ac} \subseteq \mathcal{K}(P)$. Again, by Lemma 3.3.1 we can place p at a fixed convex combination of a and c in each of the drawings Γ_i , noting that we can write p as a convex combination of a, b and c taking the coefficient of b to be 0. \square

The lemma that handles the case where P is a 5-gon is the following.

Lemma 3.4.3. *Let P be a 5-gon and let $\Gamma_1, \dots, \Gamma_k$ be straightline planar drawings of P such that each morph $\langle \Gamma_i, \Gamma_{i+1} \rangle, i = 1, \dots, k - 1$ is unidirectional and planar, and vertex a of P is in the kernel of P at all times during the whole morph $\langle \Gamma_1, \dots, \Gamma_k \rangle$. Then we can augment each drawing Γ_i to a drawing Γ_i^p by adding vertex p at some point p_i inside the kernel of the polygon P in Γ_i and adding straightline edges from p to each vertex of P in such a way that each morph $\langle \Gamma_i^p, \Gamma_{i+1}^p \rangle$ is unidirectional and planar.*

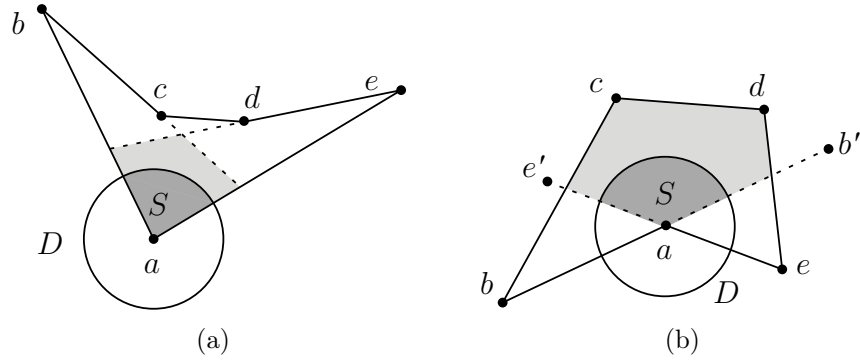


Figure 3.5: A disk D centered at a whose intersection with the kernel of P (the lightly shaded polygonal region) is a non-zero-area sector S (darkly shaded). (a) Vertex a is convex and S is a positive sector. (b) Vertex a is reflex and S is a negative sector.

The proof of Lemma 3.4.3 is more involved and we defer its proof until the end of this section. Let us begin by introducing some notation and proving some lemmas. Let P be the 5-gon $abcde$ labelled clockwise. We assume that vertex a is fixed throughout the morph. This is not a loss of generality because if a moves during an L -directional morph we can translate the whole drawing back in direction L so that a returns to its original position. An L -directional morph composed with a translation in direction L is again an L -directional morph, and planarity is preserved since the relative positions of vertices do not change.

Observe that at any time instant t during morph $\langle \Gamma_1, \dots, \Gamma_k \rangle$ there exists an $\varepsilon_t > 0$ such that the intersection between the disk D centered at a with radius ε_t and the kernel

of polygon P consists of a positive-area sector S of D . This is because a is a vertex of the kernel of P . Let $\varepsilon = \min_t \varepsilon_t$ be the minimum of ε_t among all time instants t of the morph.

Fix D to be the disk of radius ε centered at a . In case a is a convex vertex of P , the sector S is bounded by the edges ab and ae and we call it a *positive* sector. See Figure 3.5(a). In case a is a reflex vertex of P , the sector S is bounded by the extensions of edges ab and ae and we call it a *negative* sector. See Figure 3.5(b). More precisely, let b' and e' be points so that a is the midpoint of the segments bb' and ee' respectively. The negative sector is bounded by the segments ae' and ab' . Note that when an L -directional morph is applied to P , the points b' and e' also move at uniform speed in direction L .

The important property we use from now on is that any point in the sector S lies in the kernel of polygon P . Let the sector in drawing Γ_i be S_i for $i = 1, \dots, k$. Let the direction of the unidirectional morph $\langle \Gamma_i, \Gamma_{i+1} \rangle$ be L_i for $i = 1, \dots, k - 1$. In other words, $\langle \Gamma_i, \Gamma_{i+1} \rangle$ is an L_i -directional morph.

Our task is to choose for each i a position p_i for vertex p inside sector S_i so that all the L_i -directional morphs keep p inside the sector at all times. A necessary condition is that the line through $p_i p_{i+1}$ be parallel to L_i . We will first show that this condition is in fact sufficient (see Lemma 3.4.6). Then we will show that such points p_i exist.

To simplify our analysis we rotate and translate L_i so that it is horizontal and it goes through point a and distinguish the following two cases depending on how L_i and S_i intersect:

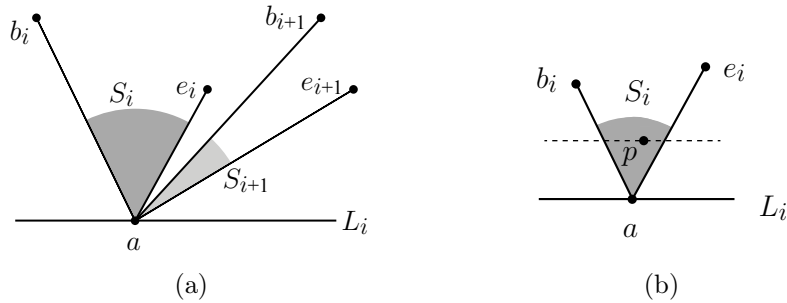


Figure 3.6: The one-sided case where S_i lies to one side of L_i , illustrated for a positive sector S_i . (a) An L_i -directional morph to S_{i+1} . (b) p remains inside the sector if and only if it remains inside D and between the two lines ba and ea .

one-sided case Points b_i and e_i lie in the same closed half-plane determined by L_i . In this case, whether the sector S_i is positive or negative, L_i does not intersect the interior

of S_i . See Figure 3.6. An L_i -directional morph keeps b_i and e_i on the same side of L_i so if S_i is positive it remains positive and if S_i is negative it remains negative.

two-sided case Points b_i and e_i lie on opposite sides of L_i . In this case L_i intersects the interior of the sector S_i . See Figure 3.7. During an L_i -directional morph the sector S_i may remain positive, or it may remain negative, or it may switch between the two, although it can only switch once.

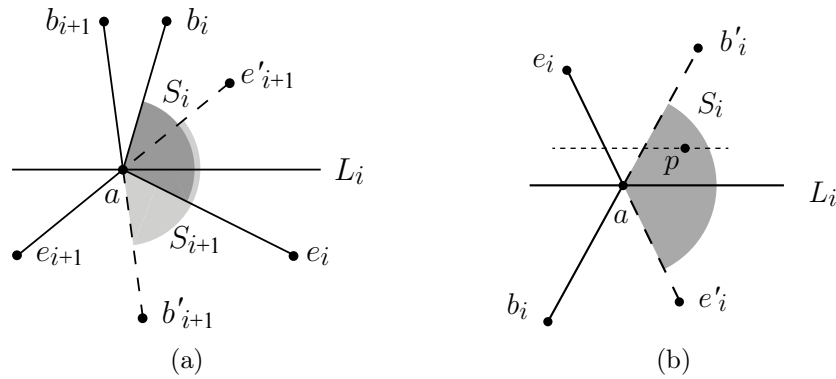


Figure 3.7: The two-sided case where S_i contains points on both sides of L_i . (a) An L_i -directional morph from the positive sector S_i bounded by $b_i a e_i$ to the negative sector S_{i+1} bounded by $e'_{i+1} a b'_{i+1}$. (b) p remains inside the sector if and only if it remains inside D and on the same side of the lines bb' and ee' .

As our main tool we will show that under the action of an L -directional morph any point p remains in the same half plane h of a line L' during the morph, provided $p \in h$ at time 0 and at time 1. This is shown in the following two results.

Lemma 3.4.4. *Let L be a horizontal line and x_0, x_1, y_0, y_1 be points in L . Consider a point x that moves at constant speed from x_0 to x_1 in one unit of time. If y_i is to the right of x_i , $i = 0, 1$, and y is a point that moves at constant speed from y_0 to y_1 in one unit of time then y remains to the right of x during their movement. Note that x_0 may lie to the right or left of x_1 and likewise for y_0 and y_1 .*



Figure 3.8: Points x and y move from x_0 to x_1 and from y_0 to y_1 respectively.

Proof. Let x_i and y_i , $i = 0, 1$, be points as described above, see Figure 3.8. Denote by x_t and y_t the positions of x and y for $0 < t < 1$. First note that

$$y_i = x_i + \delta_i \tag{3.1}$$

for $i = 0, 1$, with $\delta_i > 0$. Since x and y are moving at constant speed, we have $x_t = (1 - t)x_0 + tx_1$ and $y_t = (1 - t)y_0 + ty_1$. Now, using equation (3.1) in the expression for y_t we have

$$y_t = (1 - t)(x_0 + \delta_0) + t(x_1 + \delta_1) \tag{3.2}$$

$$= x_t + (1 - t)\delta_0 + t\delta_1, \tag{3.3}$$

where $(1 - t)\delta_0 + t\delta_1 > 0$. □

Corollary 3.4.5. *Consider an L -directional morph acting on points p, r and s . If p is to the right of the line through rs at the beginning and the end of the L -directional morph, then p is to the right of the line through rs throughout the L -directional morph.*

Proof. Let p_i, r_i, s_i , $i \in \{0, 1\}$ be the initial and final positions of points p, r and s respectively during the L -directional morph. Denote by p_t, r_t, s_t the position of p, r and s at time t , $t \in (0, 1)$, respectively. Let L'_t denote the line through r_t and s_t . Suppose $p_0 = (x_0, y_0)$ and $p_1 = (x_1, y_1)$. Note that the height of each point remains unchanged since we are assuming that L is a horizontal line. Therefore $y_0 = y_1$. Let h_t be the point on L'_t at height y_0 . By assumption p_i is to the right of h_i , $i \in \{0, 1\}$, so Lemma 3.4.4 implies that p_t is to the right of h_t throughout the morph. Consequently p_t is to the right of L'_t throughout the morph, as desired. □

We are now ready to prove our main lemma about the relative positions of points p_i and p_{i+1} .

Lemma 3.4.6. *If point p_i lies in sector S_i and point p_{i+1} lies in sector S_{i+1} and the line $p_i p_{i+1}$ is parallel to L_i then an L_i -directional morph from S_i, p_i to S_{i+1}, p_{i+1} keeps the point in the sector at all times.*

Proof. We use the notation that b moves from b_i to b_{i+1} , p moves from p_i to p_{i+1} , and similarly for the remaining points a, c, d, e .

We begin by considering the one-sided case. Note that it suffices to consider only the case where the sector S_i is positive, as the case where S_i is negative follows by a similar argument. Observe that a point p remains in the sector during an L_i -directional morph

if and only if it remains in the disc D and remains between the lines ba and ea . See Figure 3.6(b). Since p_i and p_{i+1} both lie in the disc D , we have that the line segment joining them lies in the disc D . Therefore p remains in the disc throughout the morph. In the initial configuration, p_i lies between the lines $b_i a$ and $e_i a$, and in the final configuration p_{i+1} lies between the lines $b_{i+1} a$ and $e_{i+1} a$. Therefore by Corollary 3.4.5 p remains between the lines throughout the L_i -directional morph. Thus p remains inside the sector throughout the morph.

Now consider the two-sided case. Observe that a point p remains in the sector during an L_i -directional morph if and only if it remains on the same side of the lines bb' and ee' . Note that this is true even when the sector changes between positive and negative. See Figure 3.7(b). As in the one-sided case, p remains in the disc throughout the morph. Also, p is on the same side of the lines bb' and ee' in the initial and final configurations, and therefore by Corollary 3.4.5 p remains on the same side of the lines throughout the morph. Thus p remains inside the sector throughout the morph. \square

We now focus on proving the existence of the points p_i . We call the possible positions for p_i inside sector S_i , $1 \leq i \leq k$, the *nice* points, defined formally as follows:

- All points in the interior of S_k are nice.
- For $1 \leq i \leq k - 1$, a point p_i in the interior of S_i is nice if there is a nice point p_{i+1} in S_{i+1} such that $p_i p_{i+1}$ is parallel to L_i .

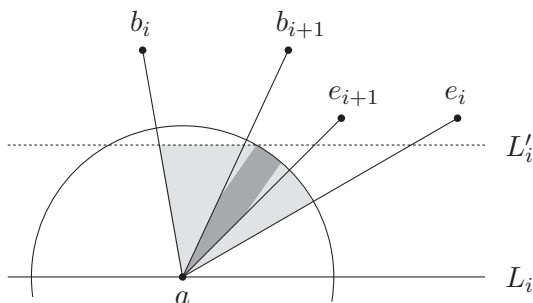


Figure 3.9: N_i (lightly shaded) is an L_i -truncation of S_i in the one-sided case. N_{i+1} is darkly shaded. L_i and L'_i are the slab boundaries for N_i .

By Lemma 3.4.6 it suffices to show that each of the nice sets is non-empty. We proceed to characterize the sets. Given a line L , an L -truncation of a sector S is the intersection of

S with an open slab that is bounded by two lines parallel to L and contains all points of S in a small neighbourhood of a . In particular, an L -truncation of a sector is non-empty.

Lemma 3.4.7. *The set of nice points in S_i is an L_i -truncation of S_i for $i = 1, \dots, k$.*

Proof. Let N_i denote the nice points in S_i . The proof is by induction as i goes from k to 1. All the points in the interior of S_k are nice. Suppose by induction that N_{i+1} is an L_{i+1} -truncation of S_{i+1} .

First let us consider the one-sided case, see Figure 3.9. Let us assume without loss of generality that the sector N_{i+1} lies above L_i . The slab determining N_i consists of all lines parallel to L_i that go through a point of N_{i+1} . The line L_i itself forms one boundary of the slab. The other line delimiting the slab is given by the line L'_i parallel to L_i and of maximum height that goes through a point of N_{i+1} . Note that this slab is non-empty since N_{i+1} contains all of S_{i+1} in a small neighbourhood of a . Thus the slab contains all points of S_i in a neighbourhood of a , and therefore N_i is an L_i -truncation of S_i .

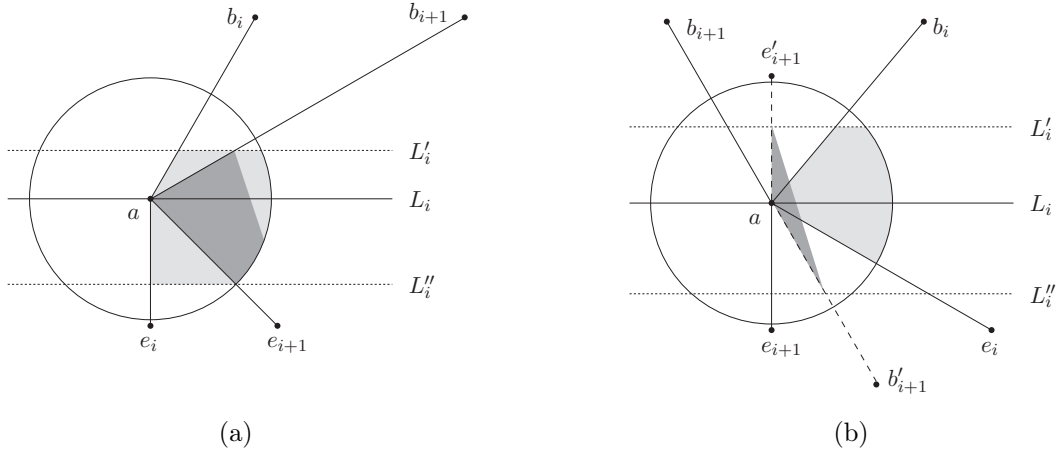


Figure 3.10: N_i (lightly shaded) is an L_i -truncation of S_i in the two-sided case. N_{i+1} is darkly shaded. L'_i and L''_i are the slab boundaries for N_i .

Now let us consider the two-sided case, see Figure 3.10. The slab determining N_i consists of all lines parallel to L_i that go through a point of N_{i+1} . Similar to the previous case, here we note that the slab is bounded by the lines L'_i and L''_i parallel to L_i having maximum and minimum height respectively. Since N_{i+1} contains all of S_{i+1} around a small neighbourhood of a , it follows that the line L_i is strictly below L'_i and strictly above L''_i .

Thus the slab contains all points of S_i around a small neighbourhood of a and therefore N_i is an L_i -truncation of S_i . \square

We are now in position to prove Lemma 3.4.3.

Proof of Lemma 3.4.3. From Lemma 3.4.7 we know that there exist nice points p_1, \dots, p_k . We claim that it suffices to place p at p_i in Γ_i and morph in a unidirectional fashion from p_i to p_{i+1} , $1 \leq i \leq k-1$. The fact that placing p at these positions during the morph satisfies the desired conditions follows from Lemma 3.4.6 and the fact that the points p_1, \dots, p_k are nice. \square

As mentioned at the beginning of this section, the proof of Theorem 3.4.1 follows from Lemmas 3.4.2 and 3.4.3. We now present an algorithm resulting from Theorem 3.4.1. This algorithm takes as input a planar pseudo morph $\mathcal{M} = \langle \Gamma'_1, \dots, \Gamma'_k \rangle$ of a planar triangulation T consisting of unidirectional steps and returns a planar morph $M = \langle \Gamma_1, \dots, \Gamma_k \rangle$ consisting of unidirectional steps, where $\Gamma_i = \Gamma'_i$, $i \in \{1, k\}$.

Algorithm 1 Obtain a true planar morph from a given planar pseudo morph

1: **procedure** CONVERT PSEUDO MORPH TO UNIDIRECTIONAL MORPH(\mathcal{M})

Require: $\mathcal{M} = \langle \Gamma'_1, \dots, \Gamma'_k \rangle$ a planar pseudo morph of a planar triangulation.

2: **if** \mathcal{M} consists of only linear morphing steps **then**
 return \mathcal{M} $\triangleright \mathcal{M}$ is already a true planar morph.

3: **end if** \triangleright If there are steps other than linear morphs, then there must be edge contractions.

4: Let ap be the first edge that is contracted during \mathcal{M} . \triangleright Say p is contracted onto a .

5: Let k_1 be the step number during \mathcal{M} at which p is contracted onto a .

6: Let k_2 be the step number during \mathcal{M} at which p is uncontracted from a .

7: Let $\langle \Gamma''_{k_1} \dots, \Gamma''_{k_2} \rangle = \text{CONVERT PSEUDO MORPH TO UNIDIRECTIONAL MORPH}(\langle \Gamma'_{k_1} \dots, \Gamma'_{k_2} \rangle)$
 \triangleright Here we use a recursive call so that $\langle \Gamma'_1, \dots, \Gamma'_{k_1-1}, \Gamma''_{k_1}, \dots, \Gamma''_{k_2}, \Gamma'_{k_2+1}, \dots, \Gamma_k \rangle$ is a true planar morph of $T_{p,a}$.

8: Let $\mathcal{M}' := \langle \Gamma'_1, \dots, \Gamma'_{k_1-1}, \Gamma''_{k_1}, \dots, \Gamma''_{k_2}, \Gamma'_{k_2+1}, \dots, \Gamma_k \rangle$.

9: **if** $\deg_T(p) = 3$ **then**

10: Augment each drawing in \mathcal{M}' to contain p as a fixed convex combination of its neighbours (see Lemma 3.4.2) and let M be the resulting morph.

11: **else if** $\deg_T(p) = 4$ **then**

12: Augment each drawing in \mathcal{M}' to contain p as a fixed convex combination of two of its neighbours (see Lemma 3.4.2) and let M be the resulting morph.

13: **else if** $\deg_T(p) = 5$ **then**

14: Augment each drawing in \mathcal{M}' to contain p in the corresponding set of nice points (see Lemma 3.4.3) and let M be the resulting morph.

15: **end if**

16: **return** M

17: **end procedure**

Chapter 4

Morphing from one Schnyder drawing to another

As we saw in Chapter 2, given a Schnyder wood and a weight distribution (a positive assignment weights to the set of interior faces) we can obtain a planar drawing of the corresponding planar triangulation. Also recall from Chapter 2, that for a given planar triangulation there may be exponentially many Schnyder woods. The aim of this chapter is to show that it is possible to morph between any two drawings obtained from a Schnyder wood and a weight distribution, even in the case where the corresponding Schnyder woods differ. The resulting morph can be expressed as $\langle \Gamma_1, \dots, \Gamma_k \rangle$, where each Γ_i is a weighted Schnyder drawing, the intermediate drawings are on a grid of size $O(n) \times O(n)$ and $k = O(n^2)$, where n denotes the number of vertices of the planar triangulation. In Chapter 5 we discuss how the morph resulting from flipping a facial triangle can be implemented using 3 unidirectional morphs.

This chapter is structured as follows. In the following section we begin by showing that it is possible to morph, while preserving planarity, between two drawings obtained from a fixed Schnyder wood and two weight distributions. Section 4.2 is devoted to showing that planarity is preserved when morphing linearly between two drawings obtained from Schnyder woods that differ by a face flip and any weight distribution. In Figure 4.1 we show the intermediate drawings from the morph resulting from performing some facial flips. In Section 4.3 we show that it is possible to obtain a planar morph consisting of at most 3 linear morphing steps between any two weighted Schnyder drawings arising from Schnyder woods that differ by a flip of a separating triangle. Finally, in Section 4.4 we prove that there exists a sequence of linear morphs of polynomial length between any two Schnyder drawings of a planar triangulation where each intermediate drawing is realizable

in an $O(n) \times O(n)$ grid. The last section also features the algorithm that morphs between any two given Schnyder drawings.

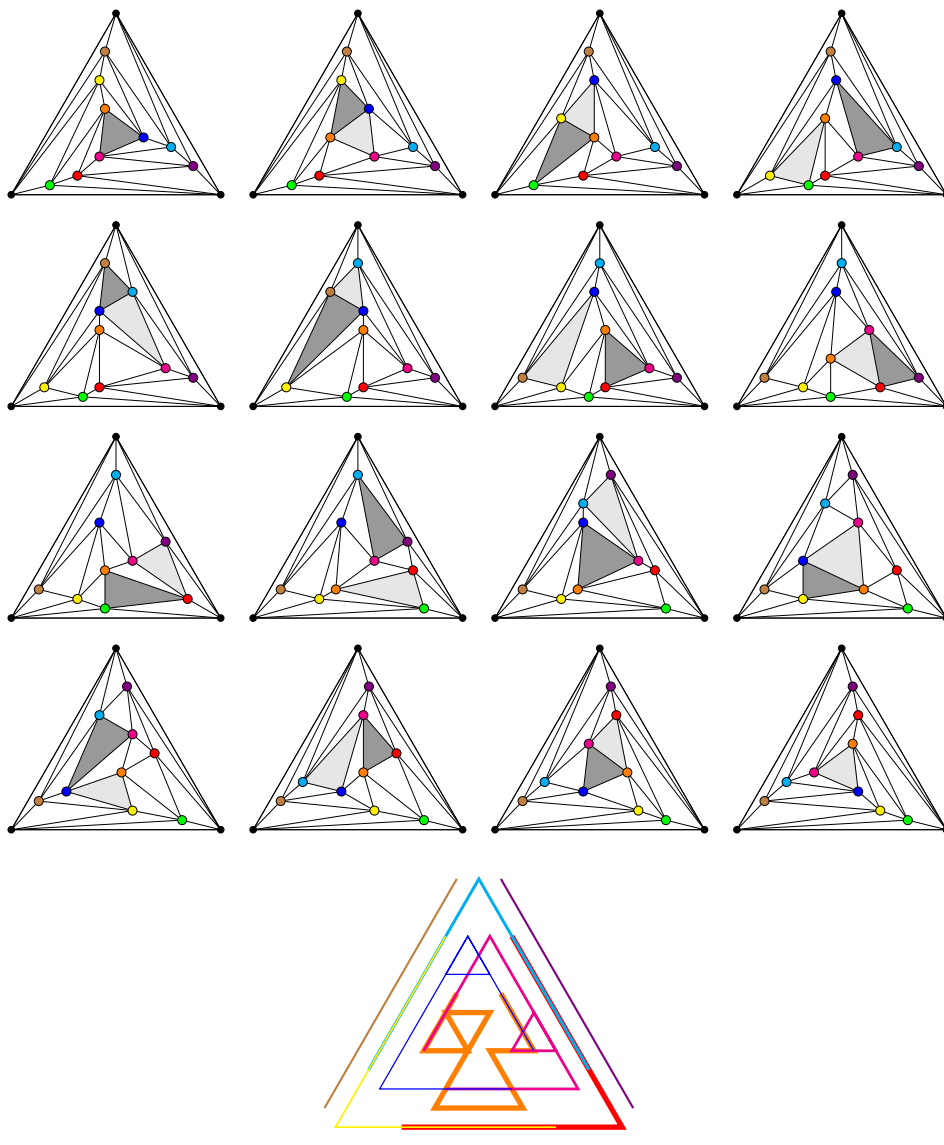


Figure 4.1: A sequence of triangle flips. In each drawing the triangle to be flipped is darkly shaded, and the one most recently flipped is lightly shaded. The linear morph from each drawing to the next one is planar. At the bottom we illustrate the piecewise linear trajectories followed by vertices during the sequence of flips.

4.1 Planar morphs from weight distributions

In this section we prove that if we are given a Schnyder wood of a planar triangulation and two weight distributions \mathbf{w} and \mathbf{w}' on the set of interior faces, then morphing linearly between the corresponding drawings defines a planar morph. This type of morph will be used in this chapter at two different stages. The first stage is when we flip separating triangles. Here a weight distribution satisfying a special condition will be required, thus redistributing weight will be of use. The second stage will be for our main result in this chapter, as it might be the case that the given drawings are not realizable in an $O(n) \times O(n)$ grid. Thus, as a first step we will redistribute weights so that all weights are the same and thus the drawings are realizable in an $O(n) \times O(n)$ grid.

We begin by proving that redistributing weights defines a linear morph. Here we are only concerned with showing that the resulting morph is linear and not with planarity, thus some faces may be assigned negative weights.

Lemma 4.1.1. *Let T be a planar triangulation and let S be a Schnyder wood of T . Consider two weight assignments \mathbf{w} and \mathbf{w}' , and denote by Γ and Γ' the drawings of T induced by \mathbf{w} and \mathbf{w}' respectively. Then the family of drawings induced by $\mathbf{w}^t = (1-t)\mathbf{w} + t\mathbf{w}'$ as t goes from 0 to 1 corresponds to the linear morph $\langle \Gamma, \Gamma' \rangle$.*

Proof. Let $r_i^t(x) = \sum_{f \in R_i(x)} \mathbf{w}^t(f)$ and note that $r_i^t(x) = (1-t)r_i^0(x) + tr_i^1(x)$. The position of x at time t , x^t , is given by

$$\begin{aligned} x^t &= (r_1^t(x), r_2^t(x), r_3^t(x)) \\ &= (1-t)(r_1^0(x), r_2^0(x), r_3^0(x)) + t(r_1^1(x), r_2^1(x), r_3^1(x)) \\ &= (1-t)x^0 + tx^1. \end{aligned}$$

Therefore each vertex x moves linearly from its position in Γ to its position as Γ' , as desired. \square

Let Γ and Γ' be drawings induced by two weight distributions and a fixed Schnyder wood. In the following result we show that the linear morph $\langle \Gamma, \Gamma' \rangle$ preserves planarity.

Lemma 4.1.2. *Let T be a planar triangulation and let S be a Schnyder wood of T . Consider two weight distributions \mathbf{w} and \mathbf{w}' , and denote by Γ and Γ' the Schnyder drawings of T induced by \mathbf{w} and \mathbf{w}' respectively. Then the linear morph $\langle \Gamma, \Gamma' \rangle$ is planar.*

Proof. Consider the family of functions $\{\mathbf{w}^t\}_{t \in [0,1]}$, defined as

$$\mathbf{w}^t(f) = (1 - t)\mathbf{w}(f) + t\mathbf{w}'(f).$$

By Lemma 4.1.1 it follows that the drawings induced by \mathbf{w}^t define a linear morph, and this linear morph must be $\langle \Gamma, \Gamma' \rangle$. Note that $\mathbf{w}^0 = \mathbf{w}$ and $\mathbf{w}^1 = \mathbf{w}'$ are weight distributions. This is also the case for any $t \in [0, 1]$, since $\mathbf{w}^t(f) > 0$ for any $f \in \mathcal{F}(T)$ and $t \in [0, 1]$, and

$$\sum_{f \in \mathcal{F}(T)} \mathbf{w}^t(f) = \sum_{f \in \mathcal{F}(T)} (1 - t)\mathbf{w}(f) + \sum_{f \in \mathcal{F}(T)} t\mathbf{w}'(f) = 2n - 5,$$

for any $t \in [0, 1]$. Therefore by Theorem 2.4.3 each drawing is planar. Thus the resulting linear morph is planar. \square

The previous result only applies provided the Schnyder wood is fixed. In what follows we will show how to morph between any two induced Schnyder drawings, even if they are induced by two different Schnyder woods.

4.2 Flips on faces define morphs

This section is devoted to the analysis of flips of faces in Schnyder woods. We begin by investigating how the regions for each vertex change and use this to derive the variation of the barycentric coordinates induced by the Schnyder wood. We finalize the section by proving that morphing linearly from one Schnyder drawing to another one obtained by flipping a cyclically oriented face, both drawings given by a fixed weight distribution, defines a planar morph. We note that our result does not make any assumptions about the weight distributions, thus the fact that the drawings are realizable in an $O(n) \times O(n)$ grid depends only on the given Schnyder drawings.

Let us begin by introducing some notation. Consider a planar triangulation T equipped with a Schnyder wood S . Suppose there is a cyclically oriented face xyz in S . Without loss of generality we will assume that xyz is oriented counterclockwise and that (x, y) has colour 1. Let S' be the Schnyder wood obtained from S by flipping xyz . Let \mathbf{w} be a weight distribution and let (v_1, v_2, v_3) denote the Schnyder coordinates for vertex v obtained from S and \mathbf{w} , and let (v'_1, v'_2, v'_3) denote the Schnyder coordinates for vertex v obtained from S' and \mathbf{w} . We use $P'_i(v)$ and $R'_i(v)$ to denote the outgoing path from v in colour i and the i -th region of i in S' respectively. For an interior edge pq of T , we define $\Delta_i(pq)$ to be the set of faces bounded by the edge pq and the paths outgoing p and q in colour i . Observe

that if $pq \in E(T)$ and $p \in D_i(q)$ then $\Delta_i(pq)$ is empty. For an interior edge pq we also define $\delta_i(pq) = \sum_{f \in \Delta_i(pq)} \mathbf{w}(f)$.

Throughout this section, we will use S and S' to denote the Schnyder woods described above. We also use $f = xyz$ to denote the face in S which is flipped to obtain S' . Given a weight distribution \mathbf{w} , the Schnyder woods S and S' induce different Schnyder drawings of T in the plane. We begin by identifying properties of S and S' .

Lemma 4.2.1. *Let T be a planar triangulation and let S and S' be Schnyder woods of T such that S' is obtained from S by flipping a counterclockwise cyclically oriented face xyz with (x, y) coloured 1. Then the following conditions hold:*

1. $R_1(x) = R'_1(x)$, $R_3(y) = R'_3(y)$ and $R_2(z) = R'_2(z)$.
2. $D_1(x) = D'_1(x)$, $D_2(z) = D'_2(z)$ and $D_3(y) = D'_3(y)$.
3. The sets $D_1(x)$, $D_2(z)$ and $D_3(y)$ are pairwise disjoint.

Proof. For each of the conditions we just show the first result, since the other can be derived by analogous arguments.

1. Let us show that $R_1(x) = R'_1(x)$. Note that the only path outgoing x that changes is $P_1(x)$ (see Figure 4.2), that is, $P_2(x) = P'_2(x)$ and $P_3(x) = P'_3(x)$ and therefore $R_1(x) = R'_1(x)$.
2. We claim $D_1(x) = D'_1(x)$. This is an immediate consequence of 1, since no edges of S in $R_1(x)$ changed from S to S' .
3. We now show that $D_1(x) \cap D_2(z) = \emptyset$. First note that $R_1(x)$ and $R_2(z)$ only share vertices which are in $P_3(x)$ and $P_3(z)$, see Figure 4.2. Note that $x \notin P_3(z)$ otherwise, since $x \in P_2(z)$, this would contradict (P1). Finally, for any $v \in D_1(x) \setminus \{x\}$ we have that $v \notin P_3(x)$, or else this would contradict (P1) as $T_1^- \cup T_2 \cup T_3^-$ would contain a cycle through x and v . This implies in particular that $v \notin D_2(z)$. Therefore $D_1(x) \cap D_2(z) = \emptyset$.

□

Now, we study the difference between the coordinates of the Schnyder drawings corresponding to S and S' .

Lemma 4.2.2. *Let T be a planar triangulation and let S and S' be Schnyder woods of T such that S' is obtained from S by flipping a counterclockwise cyclically oriented face $f = xyz$ with (x, y) coloured 1 in S . Consider a weight distribution \mathbf{w} and let Γ and Γ' be the drawings induced by S and \mathbf{w} , and S' and \mathbf{w} respectively. Then the following relation holds for each $v \in V(T)$:*

$$(v'_1, v'_2, v'_3) = \begin{cases} (v_1, v_2, v_3) & \text{if } v \notin D_1(x) \cup D_2(z) \cup D_3(y) \\ (v_1, v_2 - (\delta_1(yz) + \mathbf{w}(f)), v_3 + \delta_1(yz) + \mathbf{w}(f)) & \text{if } v \in D_1(x) \\ (v_1 + \delta_2(xy) + \mathbf{w}(f), v_2, v_3 - (\delta_2(xy) + \mathbf{w}(f))) & \text{if } v \in D_2(z) \\ (v_1 - (\delta_3(xz) + \mathbf{w}(f)), v_2 + \delta_3(xz) + \mathbf{w}(f), v_3) & \text{if } v \in D_3(y), \end{cases}$$

where (v_1, v_2, v_3) and (v'_1, v'_2, v'_3) denote the coordinates of v in Γ and Γ' respectively.

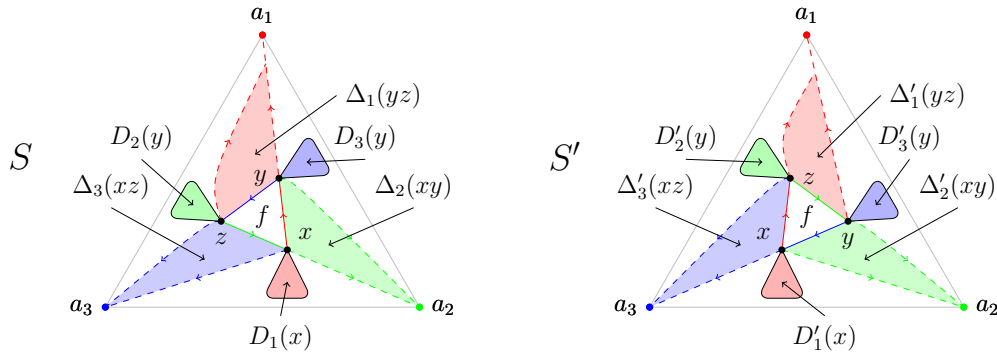


Figure 4.2: A flip of a counterclockwise oriented face triangle xyz showing changes to the regions. Observe that $\Delta_1(yz) \cup \{f\}$ leaves $R_2(v)$ and joins $R'_3(v)$ for any $v \in D_1(x)$.

Proof. It is clear that the coordinates do not change for any of the exterior vertices. Now, let us analyze how the coordinates change for each interior vertex. First observe that the 3 outgoing paths at every interior vertex v of T use at most one edge in total from (x, y) , (y, z) and (z, x) , as otherwise this would imply that the corresponding paths share a vertex different from v , thus contradicting property (P1). Let $v \notin D_1(x) \cup D_2(z) \cup D_3(y)$. Note that its regions remain unchanged, since none of the outgoing paths at v changed, and its coordinates remain unchanged, as the weights remain fixed. Therefore for such vertex v we have $(v'_1, v'_2, v'_3) = (v_1, v_2, v_3)$. Now we analyze how the coordinates change from Γ to Γ' for the vertices in $D_1(x) \cup D_2(z) \cup D_3(y)$, see Figure 4.2. By Lemma 4.2.1 we have that the sets $D_1(x)$, $D_2(z)$ and $D_3(y)$ are pairwise disjoint and by symmetry we may just consider the case $v \in D_1(x)$. First observe that the face f is contained in $R_2(v)$ in S ,

whereas in S' it is contained in $R'_3(v)$. It is not only f but also the faces in $\Delta_1(yz)$ that are in $R_2(v)$ in S , and in $R'_3(v)$ in S' , as shown in Figure 4.2. As in Lemma 4.2.1 we have $R_1(v) = R'_1(v)$. These are the only changes in the regions corresponding to v . Therefore $R'_1(v) = R_1(v)$, $R'_2(v) = R_2(v) \setminus (\Delta_1(yz) \cup \{f\})$ and $R'_3(x) = R_3(x) \cup \Delta_1(yz) \cup \{f\}$. This implies that the relation between the Schnyder coordinates of x in Γ and Γ' is given by

$$(v'_1, v'_2, v'_3) = (v_1, v_2 - (\delta_1(yz) + \mathbf{w}(f)), v_3 + \delta_1(yz) + \mathbf{w}(f)).$$

The cases when $v \in D_2(x)$ and $v \in D_3(x)$ follow from an analogous argument, so the result now follows. \square

Now that we know how the coordinates change from one Schnyder drawing to the other, we use this to prove that morphing linearly between the drawings does not cause any face in the region $R_1(x)$ to collapse. This is done in the following lemma.

Lemma 4.2.3. *Let S be a Schnyder wood of a planar triangulation T that contains a face $f = xyz$ bounded by a counterclockwise directed triangle with (x, y) coloured 1, and let S' be the Schnyder wood obtained from S by flipping f . Denote by Γ and Γ' the Schnyder drawings induced by S and S' respectively and by a fixed weight distribution \mathbf{w} . Then during the morph $\langle \Gamma, \Gamma' \rangle$ no face in $R_1(x)$ collapses.*

Proof. Let bce be a face in $R_1(x)$ and suppose at least one vertex of b , c and e is in $D_1(x)$, otherwise all vertices remain fixed by Lemma 4.2.2. Therefore at least one of the vertices b, c, e is moving at constant speed and with direction parallel to the line segment a_2a_3 , as the first coordinate remains unchanged during the morph. Since the movement is monotone, no face collapses, as otherwise this would need to be undone by $t = 1$. We analyze this in detail by discarding the possibility that bce collapses during the morph in each of the following cases.

Case 1: The three vertices b, c and e move.

Case 2: Two vertices of b, c and e move, while one remains fixed.

Case 3: Only one of c, b and e moves.

In each case we formulate algebraically the fact that the face bce collapses and proceed by contradiction.

Case 1: Let us start by considering the case where $b, c, e \in D_1(x)$. We prove that there is no time $r \in (0, 1)$ such that b, c and e are collinear in Γ^r . Assume there is $s \in \mathbb{R}$ and $r \in (0, 1)$ so that

$$b^r = se^r + (1 - s)c^r. \quad (4.1)$$

By Lemma 4.2.2 this is equivalent to the following system of equations

$$\begin{aligned} b_1 - (se_1 + (1 - s)c_1) &= 0 \\ b_2 - r(\delta_1(yz) + \mathbf{w}(f)) - (s(e_2 - r(\delta_1(yz) + \mathbf{w}(f))) + (1 - s)(c_2 - r(\delta_1(yz) + \mathbf{w}(f)))) &= 0 \\ b_3 + r(\delta_1(yz) + \mathbf{w}(f)) - (s(e_3 + r(\delta_1(yz) + \mathbf{w}(f))) + (1 - s)(c_3 + r(\delta_1(yz) + \mathbf{w}(f)))) &= 0. \end{aligned}$$

By simplifying the last two equations we obtain

$$\begin{aligned} b_2 - (se_2 + (1 - s)c_2) &= 0 \\ b_3 - (se_3 + (1 - s)c_3) &= 0. \end{aligned}$$

This implies that b, c and e are collinear in Γ , which contradicts the planarity of Γ .

Case 2: Now let us consider the case where exactly two vertices of the face are in $D_1(x)$, say $e, c \in D_1(x)$. Again, we proceed by contradiction. We consider two subcases.

1. First we consider the case in which there is a point in time $r \in (0, 1)$ where the fixed vertex b^r lies in the line segment joining c^r and e^r . We can reformulate this assumption as equation (4.1) for some $s \in [0, 1]$ and $r \in (0, 1)$. By Lemma 4.2.2, if we write the explicit system of equations we obtain

$$b_1 - (se_1 + (1 - s)c_1) = 0 \quad (4.2)$$

$$b_2 - (s(e_2 - r(\delta_1(yz) + \mathbf{w}(f))) + (1 - s)(c_2 - r(\delta_1(yz) + \mathbf{w}(f)))) = 0 \quad (4.3)$$

$$b_3 - (s(e_3 + r(\delta_1(yz) + \mathbf{w}(f))) + (1 - s)(c_3 + r(\delta_1(yz) + \mathbf{w}(f)))) = 0. \quad (4.4)$$

Note that $c, e \in R_j(b)$, for some $j \in \{1, 2, 3\}$, by property (R). Since the edges in $R_1(x)$ and $R'_1(x)$ coincide, by Lemma 4.2.1, we have that $c, e \in R'_j(b)$. Therefore $b_j > e_j, c_j, e'_j, c'_j$ by property (R). This implies that if $j = 1$ then equation (4.2) does not hold. Now, if $j = 2$, then $b_2 > c_2, e_2$ which implies that

$$b_2 > c_2 - r(\delta_1(yz) + \mathbf{w}(f)), e_2 - r(\delta_1(yz) + \mathbf{w}(f)).$$

So equation (4.3) does not hold. Finally, if $j = 3$ then

$$b_3 > c_3 + (\delta_1(yz) + \mathbf{w}(f)), e_3 + (\delta_1(yz) + \mathbf{w}(f))$$

which implies that

$$b_3 > c_3 + r(\delta_1(yz) + \mathbf{w}(f)), e_3 + r(\delta_1(yz) + \mathbf{w}(f))$$

and therefore equation (4.4) does not hold. Thus there is no $r \in (0, 1)$ such that b^r lies in the line segment joining c^r and e^r .

2. Now we consider the case where one of the two vertices that are moving, say c , lies in the line segment joining the fixed vertex and the second moving vertex. Suppose by contradiction that at time $r \in (0, 1)$ we have that c^r is in the line segment joining b^r and e^r . This can be written as

$$c^r = sb^r + (1 - s)e^r,$$

for some $s \in [0, 1]$ and $r \in (0, 1)$. Writing the explicit system of equations yields

$$c_1 - (sb_1 + (1 - s)e_1) = 0 \quad (4.5)$$

$$c_2 - r(\delta_1(yz) + \mathbf{w}(f)) - (sb_2 + (1 - s)(e_2 - r(\delta_1(yz) + \mathbf{w}(f)))) = 0 \quad (4.6)$$

$$c_3 + r(\delta_1(yz) + \mathbf{w}(f)) - (sb_3 + (1 - s)(e_3 + r(\delta_1(yz) + \mathbf{w}(f)))) = 0. \quad (4.7)$$

Note that, by property (R), vertices b and e must lie in some region j , $j \in \{1, 2, 3\}$, of vertex c in S . The edges in $R_1(x)$ and $R'_1(x)$ coincide, by Lemma 4.2.1, so we have that $b, e \in R'_j(c)$. Therefore $c_j > b_j, e_j$ and $c'_j > b_j, e'_j$, by property (R) and since $b_j = b'_j$. If $j = 1$ then equation (4.5) does not hold. Now, if $j = 2$, since $c_2 > e_2$, then $c_2 - r(\delta_1(yz) + \mathbf{w}(f)) > e_2 - r(\delta_1(yz) + \mathbf{w}(f))$. This together with $c_2 - r(\delta_1(yz) + \mathbf{w}(f)) > c'_2 > b_2$ implies that equation (4.6) does not hold. Finally, if $j = 3$, then $c_3 > e_3$ implies $c_3 + r(\delta_1(yz) + \mathbf{w}(f)) > e_3 + r(\delta_1(yz) + \mathbf{w}(f))$ and $c_3 > b_3$ implies $c_3 + r(\delta_1(yz) + \mathbf{w}(f)) > b_3$. This implies equation (4.7) does not hold. Therefore there is no $r \in (0, 1)$ such that one of the two vertices that are moving lie in the line segment joining the second moving vertex and the fixed vertex b .

Case 3: We now consider the case where two vertices are fixed, say b and c , and one vertex is moving, say e . As in the previous case, we consider two possible subcases.

1. Let us begin by showing that it cannot be possible for e^r to land in the line segment joining b^r and c^r . If this is the case, then $r \in (0, 1)$, as Γ and Γ' are planar drawings. Now, let us assume by contradiction that there is $r \in (0, 1)$

and $s \in [0, 1]$ such that

$$e_1 - (sb_1 + (1 - s)c_1) = 0 \quad (4.8)$$

$$e_2 - r(\delta_1(yz) + \mathbf{w}(f)) - (sb_2 + (1 - s)c_2) = 0 \quad (4.9)$$

$$e_3 + r(\delta_1(yz) + \mathbf{w}(f)) - (sb_3 + (1 - s)c_3) = 0. \quad (4.10)$$

Recall that vertices b and c lie in some region of e by property (R), say $b, c \in R_j(e)$. It also follows from property (R) that $e_j > b_j, c_j$. Since edges in $R_1(x)$ are the same as edges in $R'_1(x)$ by Lemma 4.2.1 and property (R), we have that $e'_j > b_j, c'_j$. Now, if $j = 1$ then $e_1 > b_1, c_1$ and so equation 4.8 does not hold. Let us assume $j = 2$. In this case we use $e'_2 > b_2, c_2$. Since $e'_2 = e_2 - (\delta_1(xy) + \mathbf{w}(f))$ we have that

$$e_2 - r(\delta_1(xy) + \mathbf{w}(f)) \geq e_2 - (\delta_1(xy) + \mathbf{w}(f)) > sb_2 + (1 - s)c_2,$$

so equation (4.9) cannot be satisfied. Now, if $j = 3$ we have $e_3 > b_3, c_3$ and therefore

$$e_3 + r(\delta_1(yz) + \mathbf{w}(f)) \geq e_3 > sb_3 + (1 - s)c_3,$$

which implies that equation (4.10) does not hold. Therefore we cannot have that the face bce collapses by having e^r along the line segment joining b^r and c^r .

2. We now show that it is not possible for one of the fixed vertices, say b , to land along the line segment joining the other two vertices, c and e in this case. Suppose by contradiction that there is $r \in (0, 1)$ such that b^r is in the line segment $c^r e^r$. Algebraically we have

$$b_1 - (se_1 + (1 - s)c_1) = 0 \quad (4.11)$$

$$b_2 - (s(e_2 - r(\delta_1(yz) + \mathbf{w}(f))) + (1 - s)c_2) = 0 \quad (4.12)$$

$$b_3 - (s(e_3 + r(\delta_1(yz) + \mathbf{w}(f))) + (1 - s)c_3) = 0, \quad (4.13)$$

for some $r \in (0, 1)$ and $s \in [0, 1]$. Let j be the index such that $c, e \in R_j(b)$ and $b_j > c_j, e_j$, this follows from property (R). If $j = 1$ then we have $b_1 > c_1, e_1$ and therefore equation (4.11) cannot be satisfied. Now, if $j = 2$ then we have $b_2 > c_2, e_2$. This implies $b_2 > e_2 - r(\delta_1(yz) + \mathbf{w}(f))$, therefore

$$b_2 > e_2 - r(\delta_1(yz) + \mathbf{w}(f)), c_2,$$

so equation (4.12) cannot hold. For the case $j = 3$ we have $b_3 > c_3, e_3$ and $b_3 = b'_3 > e'_3$. Since $e'_3 = e_3 + (\delta_1(xy) + \mathbf{w}(f))$ we have that

$$b_3 > e_3 + r(\delta_1(yz) + \mathbf{w}(f)), c_3,$$

so equation (4.13) cannot hold.

□

We are now in position to prove the main result of this section.

Theorem 4.2.4. *Let S be a Schnyder wood of a planar triangulation T that contains a face f bounded by a counterclockwise directed triangle, and let S' be the Schnyder wood obtained from S by flipping f . Denote by Γ and Γ' the Schnyder drawings induced by S and S' respectively and by a fixed weight distribution. Then $\langle \Gamma, \Gamma' \rangle$ is a planar morph.*

Proof. Let $\{\Gamma^t\}_{t \in [0,1]} = \langle \Gamma, \Gamma' \rangle$. Clearly $\Gamma = \Gamma^0$ and $\Gamma' = \Gamma^1$ are planar drawings. It suffices to show that Γ^t is planar for all $t \in (0, 1)$. Let us assume, without loss of generality, that $f = xyz$ with (x, y) having colour 1 in S . Note that the set of descendants of x , $D_1(x)$, remains unchanged from S to S' , and also recall that $R_1(x) = R'_1(x)$, by Lemma 4.2.1. First let us observe that among the vertices that change position, see Lemma 4.2.2, those in $D_1(x)$ remain in the region of the plane bounded by $x^0, x^1, P_3(x)$ and $P_2(x)$, see Figure 4.3. This follows from the fact that for $t = 0$ and $t = 1$ each of these vertices belongs to $R_1(x)$ and that the trajectory followed by each vertex is monotone. This implies that if any face collapses, then the face must belong to one of $R_1(x)$, $R_2(z)$ or $R_3(y)$, or it must be xyz .

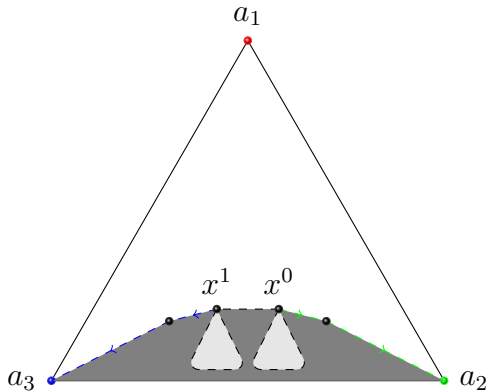


Figure 4.3: Region in which x and its descendants move.

It follows from Lemma 4.2.3 that no face collapses in $R_i(x)$ during the morph, here $i \in \{1, 2, 3\}$.

There is only one last possible source of faces collapsing, namely xyz . Let us show that there is no point in time $r \in [0, 1]$ such that a vertex of xyz , say x , lies in the line segment determined by the other two points, in this case yz . Since (x, y) has colour 1 in S ,

it follows that $x \in R_1(y)$. Similarly, since (z, x) has colour 2 in S , we have that $x \in R_1(z)$. Therefore $x_1 < y_1, z_1$. Now, in S' we have that (x, z) has colour 1 and (y, x) has colour 3. This implies $x \in R'_1(z)$ and $x \in R'_1(y)$. Hence $x'_1 < y'_1, z'_1$. Thus we have $x_1 < y_1, z_1$ and $x'_1 < y'_1, z'_1$ at times 0 and 1 respectively. Now, since $x_1 = x'_1$ it follows that for any $r \in (0, 1)$ and $s \in [0, 1]$ we will have $x_1 < s((1-r)y_1 + ry'_1) + (1-s)((1-r)z_1 + rz'_1)$. Thus x^r cannot be in the line segment joining z^r and y^r . The result now follows. \square

4.3 Morphs from flips in separating triangles

As we saw in Section 2.6, given a Schnyder wood with a cyclically oriented triangle, it is possible to flip such triangle to obtain a second Schnyder wood. In the previous section we showed that when such triangle is a face, we can obtain a planar linear morph between the two Schnyder drawings. In this section we obtain a similar result for the case where the triangle is a separating triangle, the difference is that in this case morphing linearly might not preserve planarity (see Figure 4.4). We will give a planar morph that uses at most 3 steps, each of which is a linear morph.

We make one remark about the complications caused by separating triangles. It is tempting to simply combine morphs of the outside and the inside of each separating triangle. Essentially, this assigns coordinates to each vertex relative to the Schnyder wood of the 4-connected block containing the vertex. The difficulty with this approach is that separating triangles can be nested $c \cdot n$ deep, and we lose control of the grid size, see Figure 4.5. An upper bound for the grid size following this approach is $O(n^c) \times O(n^c)$. Since we wish that each intermediate drawing can be realized in an $O(n) \times O(n)$ grid we only consider coordinates with respect to the three exterior vertices of the planar triangulation.

Let us begin by introducing some notation. Throughout this section we let S and S' be Schnyder woods of a planar triangulation T such that S' is obtained from S after flipping a counterclockwise oriented separating triangle $C = xyz$, with (x, y) coloured 1 in S . Consider the uniform weight distribution \mathbf{u} and the two drawings Γ and Γ' induced by S and \mathbf{u} and S' and \mathbf{u} respectively. For the main result of this section, it suffices to consider a uniform weight distribution because we can get to it via a single planar linear morph, as shown in Section 4.1. However, for the intermediate results of the section we need more general weight distributions. We now give an outline of the strategy we follow. As noted above, morphing linearly from Γ to Γ' may cause faces inside C to collapse. However, we can show that there is a “nice” weight distribution that prevents this from happening. Our

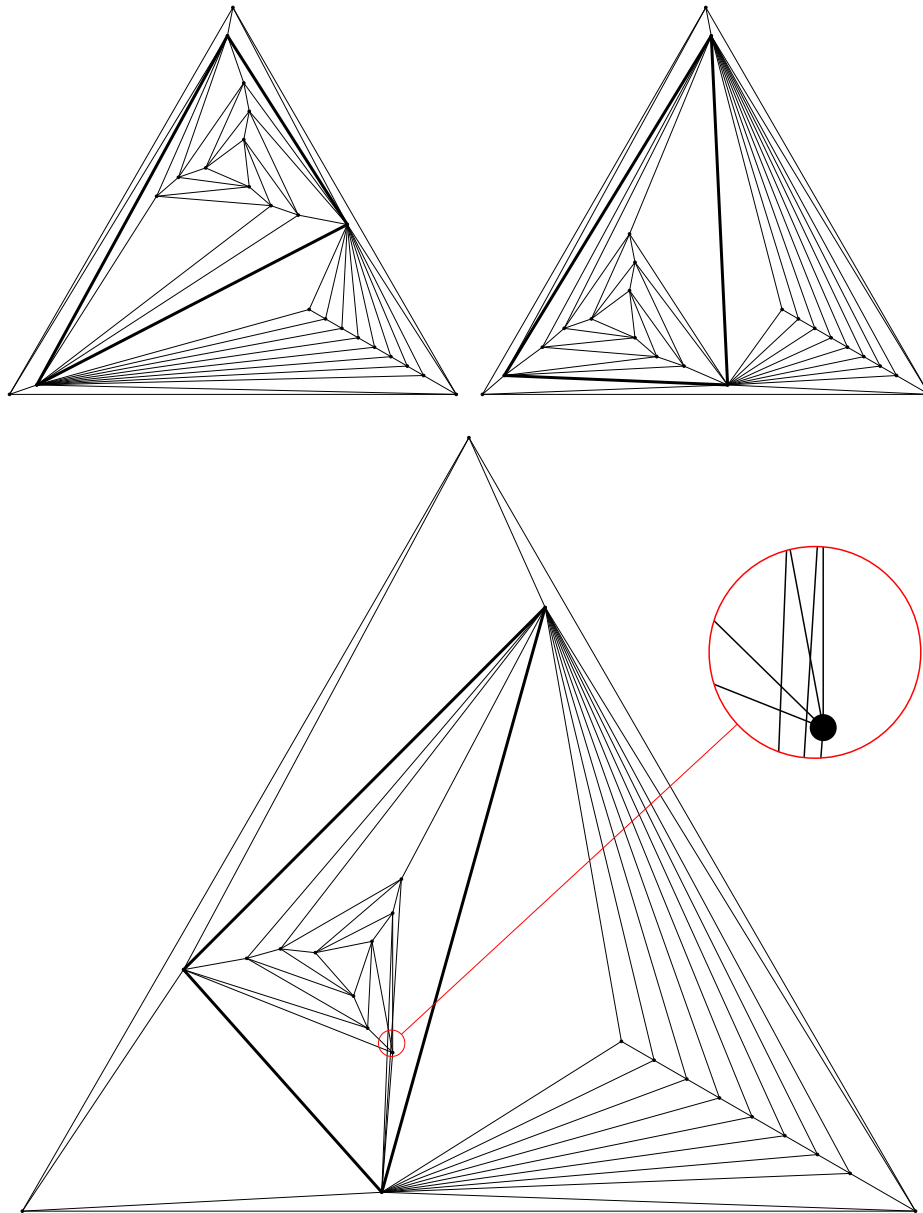


Figure 4.4: The linear morph defined by a flip of a separating triangle might not be planar if weights are not distributed appropriately. Here we illustrate the flip of the separating triangle in thick edges. Snapshots at $t = 0$, and $t = 1$ are the top. The bottom drawing corresponds to $t = 0.7$, note the edge crossings.

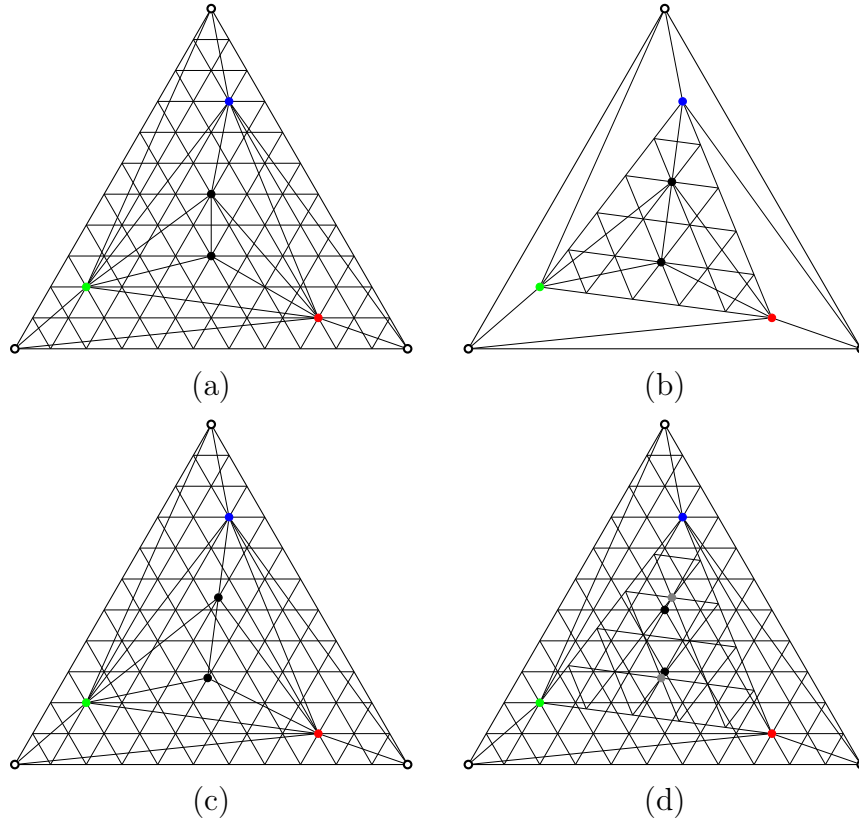


Figure 4.5: (a): Positions given by the Schnyder wood of the whole graph, the barycentric grid is also shown. (b): Black vertices assigned coordinates with respect to the Schnyder wood of the separating triangle, the local barycentric grid is displayed too. (c): Same position assignment for black vertices as in (b) with grid from (a). (d): Simultaneous drawing of (a) and (b).

plan, therefore, is to morph linearly from Γ to a drawing $\bar{\Gamma}$ with a nice weight distribution, then morph linearly to drawing $\bar{\Gamma}'$ to effect the separating triangle flip. A final change of weights back to the uniform distribution gives a linear morph from $\bar{\Gamma}'$ to Γ' .

This section is structured as follows. First we study how the coordinates change between drawings induced by S and S' and some weight distribution. We then show that no interior face of $T|_C$ collapses while morphing linearly between $\bar{\Gamma}$ and $\bar{\Gamma}'$, where these drawings are defined in terms of a special weight distribution, see Lemma 4.3.6. After this, we show that the morph $\langle \bar{\Gamma}, \bar{\Gamma}' \rangle$ is planar. We then prove the main result of this section, which is the following.

Theorem 4.3.1. *Let T be a planar triangulation and let S and S' be two Schnyder woods of T such that S' is obtained from S by flipping a counterclockwise cyclically oriented separating triangle $C = xyz$ in S . Let Γ and Γ' be weighted Schnyder drawings obtained from S and S' , respectively, with uniform weight distribution. Then there exist weighted Schnyder drawings $\bar{\Gamma}$ and $\bar{\Gamma}'$ on a $(6n - 15) \times (6n - 15)$ integer grid such that the morph $\langle \Gamma, \bar{\Gamma}, \bar{\Gamma}', \Gamma' \rangle$ is planar.*

Let us begin by writing down the coordinates in Γ for interior vertices of $T|_C$. Let b be an interior vertex of $T|_C$ and denote by β_i the i -th coordinate of b in $T|_C$ when considering the restriction of S to $T|_C$ with weight distribution \mathbf{w} . By analyzing Figure 4.6, we can see that the coordinates for b in Γ are

$$\begin{aligned} (b_1, b_2, b_3) &= (x_1 + \delta_3(xz) + \beta_1, z_2 + \delta_1(yz) + \beta_2, y_3 + \delta_2(xy) + \beta_3) \\ &= (x_1, z_2, y_3) + (\delta_3(xz), \delta_1(yz), \delta_2(xy)) + (\beta_1, \beta_2, \beta_3), \end{aligned} \quad (4.14)$$

We now analyze how the coordinates of vertices change from Γ to Γ' .

Lemma 4.3.2. *Let T be a planar triangulation and let S and S' be Schnyder woods of T such that S' is obtained from S by flipping a counterclockwise cyclically oriented separating triangle $C = xyz$, with (x, y) coloured 1 in S . Consider a weight distribution \mathbf{w} and let Γ and Γ' be the drawings induced by S and \mathbf{w} , and S' and \mathbf{w} respectively. Let $b \in V(T)$, and let (b_1, b_2, b_3) and (b'_1, b'_2, b'_3) denote the coordinates of b in Γ and Γ' respectively. Then the following relation holds:*

$$(b'_1, b'_2, b'_3) = \begin{cases} (b_1, b_2 - (\delta_1(yz) + \mathbf{w}_C), b_3 + \delta_1(yz) + \mathbf{w}_C) & \text{if } b \in D_1(x) \\ (b_1 + \delta_2(xy) + \mathbf{w}_C, b_2, b_3 - (\delta_2(xy) + \mathbf{w}_C)) & \text{if } b \in D_2(z) \\ (b_1 - (\delta_3(xz) + \mathbf{w}_C), b_2 + \delta_3(xz) + \mathbf{w}_C, b_3) & \text{if } b \in D_3(y) \\ (x_1, z_2, y_3) + (\delta_2(xy), \delta_3(xz), \delta_1(yz)) + (\beta_3, \beta_1, \beta_2) & \text{if } b \text{ is an interior vertex of } T_C \\ (b_1, b_2, b_3) & \text{otherwise,} \end{cases}$$

where $\mathbf{w}_C = \sum_{f \in \mathcal{F}(T|_C)} \mathbf{w}(f)$, and $(\beta_1, \beta_2, \beta_3)$ denotes the coordinates of b in $T|_C$ with respect to \mathbf{w} and $S|_C$.

Proof. Consider a planar triangulation T with a cyclically oriented separating triangle C in a Schnyder wood S . Let S' be the Schnyder wood obtained from S by flipping C .

Consider the planar triangulation $T \setminus C$. We associate to $T \setminus C$ the two Schnyder woods obtained from S and S' by restricting them to the interior edges of $T \setminus C$. We also consider

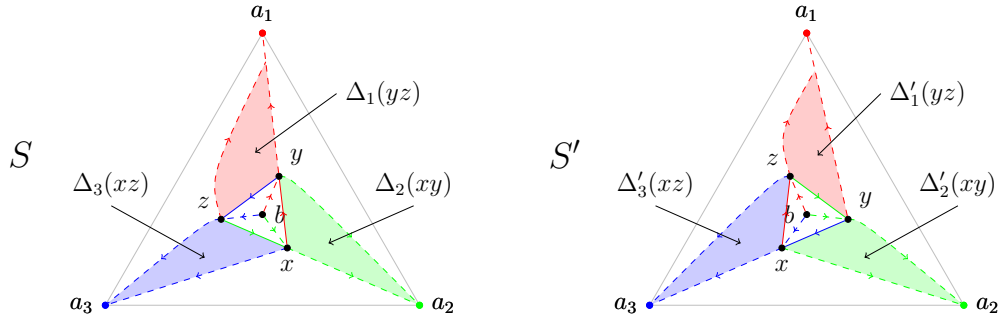


Figure 4.6: A flip of a counter-clockwise oriented separating triangle xyz .

a weight distribution for $T \setminus C$ where the weight of the face xyz is equal to $\sum_{f \in \mathcal{F}(T_C)} \mathbf{w}(f)$ and the weight of the remaining faces is given by \mathbf{w} . The first three and the last part of the result now follow from Lemma 4.2.2 applied to $T \setminus C$ considering the Schnyder woods and weight distributions described above.

It only remains to analyze how the coordinates change for an interior vertex b of $T|_C$. As before, let β_i denote the i -th coordinate of b in $T|_C$. The coordinates of b in $T|_C$ are given by (4.14). Denote by β'_i the i -th coordinate of b in $T|_C$. Similar to (4.14), see Figure 4.6, the coordinates for b in Γ' are given by

$$\begin{aligned} (b'_1, b'_2, b'_3) &= (x_1 + \delta_2(xy) + \beta'_1, z_2 + \delta_3(xz) + \beta'_2, y_3 + \delta_1(yz) + \beta'_3) \\ &= (x_1, z_2, y_3) + (\delta_2(xy), \delta_3(xz), \delta_1(yz)) + (\beta'_1, \beta'_2, \beta'_3). \end{aligned}$$

Considering that the colours of the interior edges of $T|_C$ change from i to $i + 1$ we have that $\beta'_i = \beta_{i-1}$. We can then rewrite the coordinates for b in Γ' as

$$(b'_1, b'_2, b'_3) = (x_1, z_2, y_3) + (\delta_2(xy), \delta_3(xz), \delta_1(yz)) + (\beta_3, \beta_1, \beta_2).$$

This concludes the proof. \square

Our aim in this section is to show that morphing linearly from Γ to Γ' while preserving planarity is possible under certain conditions. In the following lemma we show that, for an arbitrary weight distribution, no interior face of $T|_C$ that is not incident to exterior vertices of $T|_C$ collapses during the linear morph from Γ to Γ' .

Lemma 4.3.3. *No face formed by interior vertices of $T|_C$ collapses in the morph $\langle \Gamma, \Gamma' \rangle$.*

Proof. Let $b, c, e \in V(T|_C)$ be interior vertices of $T|_C$ such that bce is an interior face of $T|_C$. We proceed by contradiction by assuming there is a time $r \in (0, 1)$ during the linear

morph such that bce collapses, say b^r is in the line segment joining c^r and e^r . That is, assume that

$$b^r = se^r + (1-s)c^r \quad (4.15)$$

for some $r \in (0, 1)$ and $s \in [0, 1]$. By (4.14) and Lemma 4.3.2, the left hand side of (4.15) can be written as

$$(x_1, z_2, y_3) + (1-r)(\delta_3(xz), \delta_1(yz), \delta_2(xy)) + r(\delta_2(xy), \delta_3(xz), \delta_1(yz)) + \beta^r,$$

where $\beta^r = (1-r)(\beta_1, \beta_2, \beta_3) + r(\beta_3, \beta_1, \beta_2)$. Similar to what we have above, by using (4.14) and Lemma 4.3.2, we can rewrite the right hand side of (4.15) as

$$(x_1, z_2, y_3) + (1-r)(\delta_3(xz), \delta_1(yz), \delta_2(xy)) + r(\delta_2(xy), \delta_3(xz), \delta_1(yz)) + s\varepsilon^r + (1-s)\gamma^r,$$

where ε^r and γ^r are defined analogously to β^r . So, equation (4.15) is equivalent to

$$\beta^r - ((1-s)\varepsilon^r + s\gamma^r) = (0, 0, 0).$$

This can be rewritten as

$$(1-r)\beta^0 + r\beta^1 - ((1-s)((1-r)\varepsilon^0 + r\varepsilon^1) + s((1-r)\gamma^0 + r\gamma^1)) = (0, 0, 0),$$

and rearranging terms yields

$$(1-r)(\beta^0 - ((1-s)\varepsilon^0 + s\gamma^0)) + r(\beta^1 - ((1-s)\varepsilon^1 + s\gamma^1)) = (0, 0, 0).$$

This is equivalent to the following system of equations

$$\begin{aligned} (1-r)(\beta_1 - ((1-s)\varepsilon_1 + s\gamma_1)) + r(\beta_3 - ((1-s)\varepsilon_3 + s\gamma_3)) &= 0 \\ (1-r)(\beta_2 - ((1-s)\varepsilon_2 + s\gamma_2)) + r(\beta_1 - ((1-s)\varepsilon_1 + s\gamma_1)) &= 0 \\ (1-r)(\beta_3 - ((1-s)\varepsilon_3 + s\gamma_3)) + r(\beta_2 - ((1-s)\varepsilon_2 + s\gamma_2)) &= 0. \end{aligned}$$

To simplify the following arguments, we let $Q_i = \beta_i - ((1-s)\varepsilon_i + s\gamma_i)$. So the system of equations now becomes

$$(1-r)Q_1 + rQ_3 = 0 \quad (4.16)$$

$$(1-r)Q_2 + rQ_1 = 0 \quad (4.17)$$

$$(1-r)Q_3 + rQ_2 = 0, \quad (4.18)$$

Since these coordinates were obtained from a Schnyder drawing, we know there is $i \in \{1, 2, 3\}$ so that $\beta_i > \gamma_i, \varepsilon_i$ by property (R). We may assume without loss of generality that

$i = 1$. This implies in particular that $Q_1 > 0$. We now multiply equation (4.17) by r and subtract it from equation (4.18) multiplied by $(1 - r)$ to obtain $(1 - r)^2 Q_3 - r^2 Q_1 = 0$, or

$$Q_3 = \frac{r^2}{(1 - r)^2} Q_1.$$

Using this in equation (4.16) we get $(1 - r + r^3/(1 - r)^2)Q_1 = 0$. Since $Q_1 > 0$ we must have

$$(1 - r)^3 + r^3 = 0.$$

Simplifying the right hand side we get $3r^2 - 3r + 1$, which has no real roots. This contradicts our assumption that $r \in (0, 1)$ so the result follows. \square

In the following lemma we show that no interior face of $T|_C$ incident to an exterior edge of $T|_C$ collapses, provided that the given weight distribution \mathbf{w} satisfies $\delta_1(yz) = \delta_2(xy) = \delta_3(xz)$. We prove this only for the interior face of $T|_C$ incident to xy , as the proof for the other two faces follows by an analogous argument. For simplicity, let us use δ_1 , δ_2 and δ_3 to denote $\delta_1(yz)$, $\delta_2(xy)$ and $\delta_3(xz)$ respectively in what remains of this section.

Lemma 4.3.4. *Let \mathbf{w} be a weight distribution for the interior faces of T such that $\delta_1 = \delta_2 = \delta_3$. The interior face of $T|_C$ incident to xy does not collapse during $\langle \Gamma, \Gamma' \rangle$.*

Proof. Let bxy be the interior face of $T|_C$ incident with xy . Assume, by contradiction, that there is a time $r \in (0, 1)$ during the morph such that b , x and y are collinear. That is $b^r = (1 - s)x^r + sy^r$. Since (b, x) has colours 2 and 3 in S and S' respectively, it follows that $x \in R_1(b)$ and $x \in R'_1(b)$. Thus, property (R) implies $x_1^0 < b_1^0$ and $x_1^0 = x_1^1 < b_1^1$. Similarly $y_3 < b_3^0, b_3^1$. Hence for any $r \in [0, 1]$, the first coordinate of b is greater than x_1 and the third coordinate of b is greater than y_3 . Therefore $s \in (0, 1)$, as otherwise at least one of these conditions would not hold.

We write the equation from above explicitly, using (4.14) and Lemma 4.3.2:

$$\begin{aligned} & (x_1, z_2, y_3) + (1 - r)(\delta_3, \delta_1, \delta_2) + r(\delta_2, \delta_3, \delta_1) + (1 - r)(\beta_1, \beta_2, \beta_3) + r(\beta_3, \beta_1, \beta_2) = \\ (1 - s) & \left[(x_1, z_2, y_3) + (1 - r)(0, \delta_3 + \delta_1, \delta_2) + r(0, \delta_3, \delta_2 + \delta_1) + (1 - r)(0, \mathbf{w}_C, 0) + r(0, 0, \mathbf{w}_C) \right] \\ & + s \left[(x_1, z_2, y_3) + (1 - r)(\delta_2 + \delta_3, \delta_1, 0) + r(\delta_2, \delta_1 + \delta_3, 0) + (1 - r)(\mathbf{w}_C, 0, 0) + r(0, \mathbf{w}_C, 0) \right], \end{aligned}$$

here $\mathbf{w}_C := \sum_{f \in \mathcal{F}(T|_C)} \mathbf{w}(f)$. By simplifying and analyzing each coordinate separately we obtain the following system of equations

$$(1-r)(\delta + \beta_1 - s(2\delta + \mathbf{w}_C)) + r(\delta + \beta_3 - s\delta) = 0 \quad (4.19)$$

$$(1-r)(\beta_2 - (1-s)(\delta + \mathbf{w}_C)) + r(\beta_1 - s(\delta + \mathbf{w}_C)) = 0 \quad (4.20)$$

$$(1-r)(\delta + \beta_3 - (1-s)\delta) + r(\delta + \beta_2 - (1-s)(2\delta + \mathbf{w}_C)) = 0, \quad (4.21)$$

where $\delta = \delta_1 = \delta_2 = \delta_3$. Now, since we have that $\delta + \beta_3 - s\delta > 0$ then from (4.19) we conclude that $\delta + \beta_1 - s(2\delta + \mathbf{w}_C) < 0$. Therefore

$$\beta_1 - s(\delta + \mathbf{w}_C) < -(1-s)\delta < 0. \quad (4.22)$$

A similar analysis on equation (4.21) yields

$$\beta_2 - (1-s)(\delta + \mathbf{w}_C) < -s\delta < 0. \quad (4.23)$$

It now follows from inequalities (4.22) and (4.23) that there is no $r \in [0, 1]$ satisfying (4.20). The result now follows. \square

We are only left to discard one more possible source of faces collapsing within $T|_C$, namely faces incident to two interior vertices of $T|_C$ and an exterior vertex of $T|_C$. As in the previous lemma, we require that $\delta_1 = \delta_2 = \delta_3$. We prove this for the case when the exterior vertex of $T|_C$ is x , since the other two cases follow from an analogous argument.

Lemma 4.3.5. *Consider a weight distribution \mathbf{w} for the interior faces of T such that $\delta_1 = \delta_2 = \delta_3$. Then during the linear morph from the corresponding induced Schnyder drawings Γ to Γ' with respect to S and S' no face incident to two interior vertices of $T|_C$ and x collapses.*

Proof. We proceed by contradiction. Let us assume that the face abc collapses at time r , with $c \in R_1(b)$ and $b \in R_3(c)$ in S . This and property (R) imply in particular that $\gamma_1 < \beta_1$ and that $\beta_3 < \gamma_3$.

We will show that b cannot be in the line segment xc at any time r during the morph. So we have $b^r = (1-s)x^r + sc^r$, with $r \in (0, 1)$ and $s \in (0, 1)$. By an analogous argument, it will follow that c cannot be in the line segment xb .

We write the previous equation explicitly. From (4.14) and Lemma 4.3.2 we obtain:

$$\begin{aligned} & (x_1, z_2, y_3) + (1-r)(\delta_3, \delta_1, \delta_2) + r(\delta_2, \delta_3, \delta_1) + (1-r)(\beta_1, \beta_2, \beta_3) + r(\beta_3, \beta_1, \beta_2) = \\ & (1-s)((x_1, z_2, y_3) + (0, \delta_3, \delta_2) + (1-r)(0, \delta_1 + \mathbf{w}_C, 0) + r(0, 0, \delta_1 + \mathbf{w}_C)) \\ & + s((x_1, z_2, y_3) + (1-r)(\delta_3, \delta_1, \delta_2) + r(\delta_2, \delta_3, \delta_1) + (1-r)(\gamma_1, \gamma_2, \gamma_3) + r(\gamma_3, \gamma_1, \gamma_2)) \end{aligned}$$

By simplifying and writing equations for each coordinate we obtain the following system of equations

$$(1-r)(\delta + \beta_1 - s(\delta + \gamma_1)) + r(\delta + \beta_3 - s(\delta + \gamma_3)) = 0 \quad (4.24)$$

$$(1-r)(\beta_2 - (1-s)(\delta + \mathbf{w}_C) - s\gamma_2) + r(\beta_1 - s\gamma_1) = 0 \quad (4.25)$$

$$(1-r)(\beta_3 - s\gamma_3) + r(\beta_2 - (1-s)(\delta + \mathbf{w}_C) - s\gamma_2) = 0, \quad (4.26)$$

where $\delta = \delta_1 = \delta_2 = \delta_3$. Now, since $\beta_1 > \gamma_1$ from (4.24) we get that $\delta + \beta_1 - s(\delta + \gamma_1) > 0$ and therefore $\delta + \beta_3 - s(\delta + \gamma_3) < 0$. From the previous inequality we get $\beta_3 - s\gamma_3 < -(1-s)\delta < 0$. Now, using this in equation (4.26) we get that $\beta_2 - (1-s)(\delta + \mathbf{w}_C) - s\gamma_2 > 0$. Finally, using the previous inequality in (4.25) we obtain that $\beta_1 - s\gamma_1 < 0$, contradicting our original assumption that $\beta_1 > \gamma_1$. So the result follows. \square

We require the condition that $\delta_1 = \delta_2 = \delta_3$, as otherwise there are instances for which the linear morph between the drawings induced by S and S' contains non planar drawings, see Figure 4.4. We can now show that morphing linearly between drawings Γ and Γ' defines a planar morph. Here the drawings Γ and Γ' are induced by S and S' respectively together with a weight distribution for which $\delta_1 = \delta_2 = \delta_3$. This is done in the following lemma.

Lemma 4.3.6. *Let T be a planar triangulation and let S and S' be two Schnyder woods of T such that S' is obtained from S by flipping a counterclockwise directed separating triangle $C = xyz$ in S . Let \mathbf{w} be a weight distribution on $\mathcal{F}(T)$ such that $\delta_1 = \delta_2 = \delta_3$ and let Γ and Γ' be the Schnyder drawings induced by \mathbf{w} and S and S' respectively. Then $\langle \Gamma, \Gamma' \rangle$ defines a planar morph.*

Proof. It follows from Lemma 4.3.3, 4.3.4 and 4.3.5 that no interior face of $T|_C$ collapses during the morph $\langle \Gamma, \Gamma' \rangle$. In particular, during the morph every interior vertex of $T|_C$ is in the interior of the triangle $x^t y^t z^t$. Therefore faces collapsing, if any, must arise from of $\mathcal{F}(T \setminus C) \setminus \{xyz\}$. Finally, Theorem 4.2.4 implies that no face collapses in $T \setminus C$. We conclude that $\langle \Gamma, \Gamma' \rangle$ defines a planar morph. \square

We are now ready to prove the main result of this section.

Proof of Theorem 4.3.1. Our aim is to provide a description for the planar drawings $\bar{\Gamma}$ and $\bar{\Gamma}'$. We will show each of these drawings can be realized in a grid which is three times finer than the $(2n-5) \times (2n-5)$ grid. For that purpose, we consider drawings in an $(6n-15) \times (6n-15)$ grid and with weight distributions \mathbf{w} such that $\sum_{f \in \mathcal{F}(T)} \mathbf{w}(f) = 6n-15$. Under this setup, the uniform weight distribution takes a value of 3 in each interior face.

Note that if $\delta_1 = \delta_2 = \delta_3$ then $\Gamma = \bar{\Gamma}$ and $\Gamma' = \bar{\Gamma}'$, and by Lemma 4.3.6 $\langle \Gamma, \Gamma' \rangle$ is planar. Let us now handle the case in which $\delta_1 = \delta_2 = \delta_3$ does not hold. Our approach will be the following. We will define a new weight distribution \mathbf{w}' such that all weights are integers and $\delta_1 = \delta_2 = \delta_3$. This weight distribution is used twice together with Lemma 4.1.2 to obtain two drawings, namely $\bar{\Gamma}$ and $\bar{\Gamma}'$.

Let us now begin by defining the weight distribution \mathbf{w}' . We require that all the weights are integers and that the regions, Δ_1, Δ_2 and Δ_3 , have weight $\delta := (\delta_1 + \delta_2 + \delta_3)/3$. For each $i, i \in \{1, 2, 3\}$, we will define sets $E_i, F_i, G_i \subseteq \Delta_i$. The idea is to take away two units of weight from faces in E_i , and one unit of weight from the face in F_i if $\delta_i > \delta$. For the case where $\delta_i < \delta$ we will transfer weight to the face in G_i .

Define the excess weight of region Δ_i to be $\epsilon_i := \delta_i - \delta$, note that ϵ_i is an integer. If $\epsilon_i = 0$ we let $E_i = F_i = G_i = \emptyset$, as in this case the weight of Δ_i should remain unchanged. If ϵ_i is positive and even then we let E_i be any subset of $\epsilon_i/2$ faces of Δ_i and $F_i = G_i = \emptyset$. If ϵ_i is positive and odd, then we begin by letting E_i be any subset of Δ_i consisting of $\lfloor \epsilon_i/2 \rfloor$ faces of Δ_i , then we define F_i to consist of any face in $\Delta_i \setminus E_i$ and $G_i = \emptyset$. If $\epsilon_i < 0$ we let G_i be any set consisting of one face in Δ_i and $E_i = F_i = \emptyset$. Finally, let $E = \cup_{i \in \{1,2,3\}} E_i$, $F = \cup_{i \in \{1,2,3\}} F_i$ and $G = \cup_{i \in \{1,2,3\}} G_i$. Now, we define \mathbf{w}' as follows.

$$\mathbf{w}'(f) = \begin{cases} \mathbf{w}(f) & \text{if } f \notin E \cup F \cup G \\ \mathbf{w}(f) - 2 & \text{if } f \in E \\ \mathbf{w}(f) - 1 & \text{if } f \in F \\ \mathbf{w}(f) - \epsilon_i & \text{if } f \in G_i. \end{cases}$$

It is clear that \mathbf{w}' is a weight distribution, as the weight of an interior face is at least 1. It can also be seen that the weights given by \mathbf{w}' are integers. Let us show that it satisfies $\delta'_i = \delta$, here δ'_i refers to the total weight in Δ_i given by \mathbf{w}' , $i \in \{1, 2, 3\}$. Note that if $\epsilon_i = 0$ then no weight was taken or added in from Δ_i in \mathbf{w}' , as the sets E_i, F_i and G_i are empty in this case. Now, suppose ϵ_i is positive and even. Then we have $|E_i| = \epsilon_i/2$, $|F_i| = |G_i| = 0$. Therefore precisely ϵ_i units of weight were taken away from Δ_i , two units from each face in E_i . Therefore $\delta'_i = \delta$. For the case where ϵ_i is positive and odd, observe that $G_i = \emptyset$. In this case $2\lfloor \epsilon_i/2 \rfloor$ units of weight were taken from faces in E_i and 1 unit of weight from the face in F_i . This amounts to a total of $2\lfloor \epsilon_i/2 \rfloor + 1 = \epsilon_i$ units of weight taken away from Δ_i , as desired. Finally, if $\epsilon_i < 0$, then the amount of weight added to the face in G_i is $-\epsilon_i$. In any case we get that $\delta'_i = \delta$, as desired.

Let Γ and $\bar{\Gamma}$ be the drawings induced by \mathbf{w} and \mathbf{w}' , and S respectively. Similarly let $\bar{\Gamma}'$ and Γ' be the drawings induced by \mathbf{w}', \mathbf{w} , and S' . By Lemma 4.1.2 we have that the

morphs $\langle \Gamma, \bar{\Gamma} \rangle$ and $\langle \bar{\Gamma}', \Gamma' \rangle$ are planar. Now, by Lemma 4.3.6 we have that $\langle \bar{\Gamma}, \bar{\Gamma}' \rangle$ is planar. The result now follows. \square

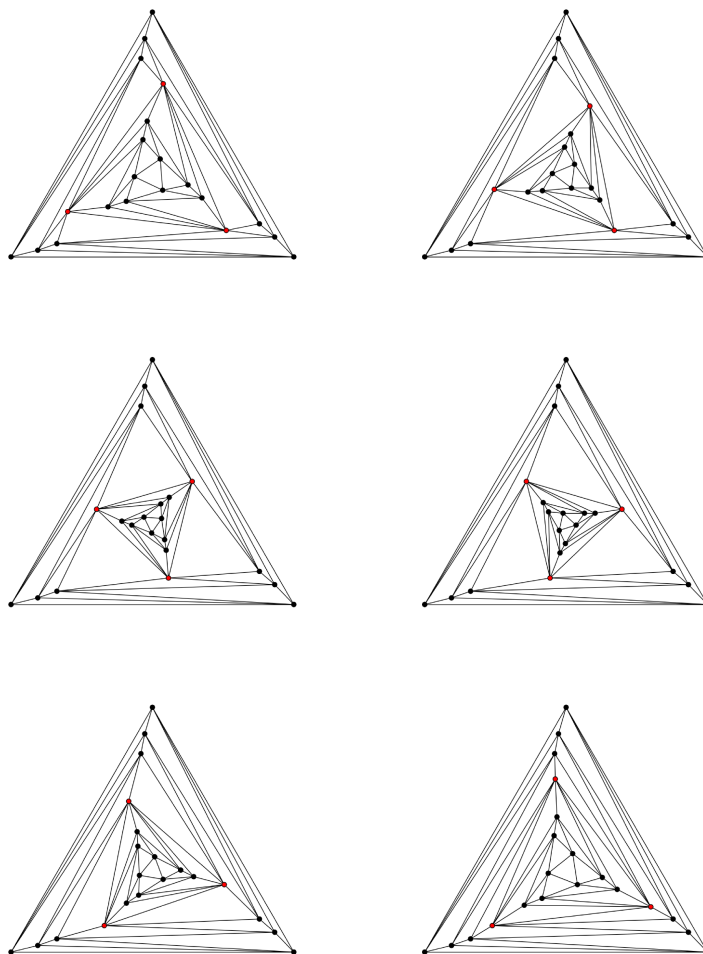


Figure 4.7: The morph resulting from flipping a separating triangle.

4.4 Traversing the Schnyder lattice

The main result of this section shows that it is possible to morph between any two Schnyder drawings in $O(n^2)$ linear morphing steps while preserving planarity throughout the morph. The intermediate drawings in the morph are realizable in an $O(n) \times O(n)$ grid.

Consider a planar triangulation T . Let S and S' be two Schnyder woods such that S' can be obtained from S by flipping a cyclically oriented triangle C . Let \mathbf{u} denote the uniform weight distribution and consider the drawings Γ and Γ' induced by S and S' respectively together with the weight distribution \mathbf{u} . In Section 4.2 we have shown that it is possible to morph linearly, while preserving planarity, from Γ to Γ' provided that C is an interior face of T . In Section 4.3 we proved that there exists a sequence of at most 4 drawings starting at Γ and ending at Γ' so that we can morph linearly between consecutive drawings while preserving planarity, whenever C is a separating triangle. As shown by Felsner in [30] these are the only two operations that are required to traverse the lattice of Schnyder woods. In this section we use the results from Sections 4.2 and 4.3 to show that given any two Schnyder drawings $\bar{\Gamma}$ and $\bar{\Gamma}'$ induced by any two Schnyder woods S and S' and any two weight distributions \mathbf{w} and \mathbf{w}' respectively, there exists a sequence of drawings of length $O(n^2)$ starting at $\bar{\Gamma}$ and ending at $\bar{\Gamma}'$ with the property that linearly morphing between consecutive drawings preserves planarity and each intermediate drawing is realizable in an $O(n) \times O(n)$ grid.

Theorem 4.4.1. *Let T be a planar triangulation and let S and S' be Schnyder woods of T . Consider the drawings Γ and Γ' induced by S and S' together with weight distributions \mathbf{w} and \mathbf{w}' respectively. There exists a sequence of drawings $\Gamma_1, \dots, \Gamma_k$ such that $k = O(n^2)$, $\Gamma = \Gamma_1$, $\Gamma' = \Gamma_k$, the linear morph $\langle \Gamma_i, \Gamma_{i+1} \rangle$ is planar, $1 \leq i \leq k - 1$, and the intermediate drawings in the sequence can be realized in an $O(n) \times O(n)$ sized grid. Furthermore, these drawings can be obtained in polynomial time.*

Proof. Let T be a planar triangulation on n vertices and let S and S' be Schnyder woods of T . Since it may be the case that Γ or Γ' are not realizable in an $O(n) \times O(n)$ grid, we consider the drawings of T $\bar{\Gamma}$ and $\bar{\Gamma}'$ obtained from the uniform weight distribution and S and S' respectively. It just remains to show that we can morph from $\bar{\Gamma}$ to $\bar{\Gamma}'$ in $O(n^2)$ steps while realizing each drawing in an $O(n) \times O(n)$ grid. This follows from the fact that $\langle \Gamma, \bar{\Gamma} \rangle$ and $\langle \bar{\Gamma}', \Gamma' \rangle$ are planar by Lemma 4.1.2.

By Lemma 2.7.4 the flip distance between S and S' in the lattice of Schnyder woods is $O(n^2)$. Therefore, there is a path in the lattice of Schnyder woods, $P = S_1, \dots, S_k$, such that S_i differs from S_{i+1} by a triangle flip, $i = 1, \dots, k$, with $k = O(n^2)$. Note that we can morph between drawings associated to consecutive Schnyder woods in P in at most 4 steps by Theorems 4.2.4 and 4.3.1. Therefore the total length of the sequence of drawings is $O(n^2)$.

Also note that the drawings in the sequence can be realized in an $O(n) \times O(n)$ grid. This clearly holds for the drawings obtained from uniform weight distributions by Theorem 2.4.3.

For the drawings obtained from redistributing weight to perform a separating triangle flip, this holds by Theorem 4.3.1. Finally, note that the intermediate drawings in the morph can be obtained in $O(n^2)$ time, $O(n)$ time per drawing. \square

To conclude this section we give pseudocode for the algorithm that yields a planar morph between any two Schnyder drawings that consists of $O(n^2)$ linear morphing steps. Let T be a planar triangulation on n vertices and let Γ_1 and Γ_2 be two Schnyder drawings of T . We begin by presenting the procedure SCHNYDER MORPH NO FLIP. This procedure obtains a planar morph consisting of $O(n^2)$ linear morphing steps from any Schnyder drawing Γ to the Schnyder drawing induced by the Schnyder wood with no flippable faces and the uniform weight distribution, denoted by \mathbf{u} .

Algorithm 2 Morph to Schnyder drawing with no flippable triangle.

```

1: procedure SCHNYDER MORPH NO FLIP( $\Gamma$ )
Require:  $\Gamma$  a Schnyder drawing of a planar triangulation.
2:   Let  $S$  be the Schnyder wood associated to  $\Gamma$ .
3:   Let  $\Gamma_0 := \Gamma$ 
4:   Let  $\Gamma_1$  be the drawing induced by  $S$  and  $\mathbf{u}$ 
5:    $i := 2$ 
6:   while  $S$  has a flippable triangle  $xyz$  do
7:     if  $xyz$  is a facial triangle then
8:       Redefine  $S$  as the Schnyder wood resulting from flipping  $xyz$  in  $S$ 
9:       Let  $\Gamma_i$  be the drawing induced by  $S$  and  $\mathbf{u}$ 
10:       $i := i + 1$ 
11:    else if  $xyz$  is a separating triangle then
12:      Let  $\mathbf{w}$  be a weight distribution with  $\delta_1 = \delta_2 = \delta_3$ 
           $\triangleright \delta_1, \delta_2$  and  $\delta_3$  depend on  $xyz$ , see Lemmas 4.3.4–4.3.6
13:      Let  $\Gamma_i$  be the drawing induced by  $S$  and  $\mathbf{w}$ 
14:      Redefine  $S$  as the Schnyder wood resulting from flipping  $xyz$  in  $S$ 
15:      Let  $\Gamma_{i+1}$  be the drawing induced by  $S$  and  $\mathbf{w}$ 
16:      Let  $\Gamma_{i+2}$  be the drawing induced by  $S$  and  $\mathbf{u}$ 
17:       $i := i + 3$ 
18:    end if
19:  end while
    return  $\langle \Gamma_0, \dots, \Gamma_{i-1} \rangle$ 
20: end procedure

```

We now present the main algorithm of this chapter. It is an algorithm that obtains a

morph between any two Schnyder drawings of a planar triangulation. We use the procedure SCHNYDER MORPH NO FLIP as a subroutine.

Algorithm 3 Morphing between any two Schnyder drawings

1: **procedure** SCHNYDER MORPH(Γ_1, Γ_2)

Require: Γ_1 and Γ_2 Schnyder drawings of a planar triangulation.

2: Let M_1 be the morph resulting from SCHNYDER MORPH NO FLIP(Γ_1)

3: Let M_2 be the morph resulting from SCHNYDER MORPH NO FLIP(Γ_2)

4: Let M'_2 be the morph resulting from reversing M_2

5: Let M be the morph resulting from concatenating M_1 and M'_2

return M

6: **end procedure**

Chapter 5

Morphing from a planar drawing to a Schnyder drawing

In this chapter we show how to morph, using only unidirectional morphs, from an arbitrary drawing of a planar triangulation to a Schnyder drawing obtained from a positive weight distribution. We use this result together with our main result from Chapter 4 to prove that given two drawings Γ_1 and Γ_2 of a planar triangulation we can find a planar morph consisting of $O(n^2)$ linear morphs from Γ_1 to Γ_2 . This result provides an alternate solution to the morphing problem to that presented in Chapter 3.

The first result will be proved by induction on the number of vertices of the planar triangulation T . Observe that the result clearly holds for the planar triangulation K_4 . The inductive step will consist of an edge contraction, where the edge ux to be contracted is such that the resulting graph, $T_{u,x}$, is 3-connected and u is a low-degree interior vertex. The property that $T_{u,x}$ is 3-connected will imply that it is a planar triangulation with one fewer vertex, and the property that u is a low-degree vertex will simplify the task of obtaining a Schnyder wood and a suitable weight distribution for T by using that of $T_{u,x}$. In the following section we discuss the existence of a contractible edge. In Section 5.2 we show how to obtain a Schnyder wood for T that preserves most of the edges of the Schnyder wood of $T_{u,x}$. Then, in Section 5.3 we show how to obtain a suitable weight distribution that preserves the positions of all vertices except one. As we will see, in Sections 5.2 and 5.3 we omit an exceptional case. Section 5.4 will be devoted to handling that exceptional case. The exceptional case requires that we prove that if we allow a certain face to be assigned a weight of 0 we may still obtain a planar drawing from a Schnyder wood. Then in Section 5.5 we put together our results from previous sections to show that we can extend a Schnyder drawing of $T_{u,x}$ to a Schnyder drawing of T by performing a constant number of

unidirectional morphs and an uncontraction. Section 5.6 is devoted to stating and proving the main result of this chapter. Finally, in Section 5.7 we present two algorithms. The first algorithm produces a morph from an arbitrary drawing to a Schnyder drawing, and the second algorithm morphs between any two drawings of a planar triangulation. The approach used in the second algorithm consists of morphing each of the input drawings to Schnyder drawings and then using our morphing algorithm from Chapter 4 to morph between the Schnyder drawings.

5.1 Existence of a contractible edge

The inductive step in the proof of the main result of this chapter requires that we reduce the number of vertices by 1. In order to achieve this, we need to guarantee that there exists a suitable interior edge to contract. To simplify the argument that follows the inductive step, we add the condition that one of the endpoints of the edge to contract is a low-degree interior vertex. In this section we show that there always exists a suitable edge to contract.

Let us begin by formulating precisely what we mean by a suitable contractible edge. We use notation introduced in Section 2.2 for edge contraction. Let $T = (V, E)$ be a planar triangulation on n vertices and let Γ be a straightline drawing of T . We call an interior edge $ux \in E$ *contractible* if the following three conditions hold.

- (C1) Vertex u is a low-degree interior vertex, that is $\deg(u) \leq 5$,
- (C2) the graph $T_{u,x}$ is a planar triangulation on $n - 1$ vertices, and
- (C3) the positions of the vertices given by Γ define a straightline drawing of $T_{u,x}$.

Let us now show that there always exists a contractible edge.

Theorem 5.1.1 (Cairns [22]). *For any planar triangulation $T = (V, E)$ and any straightline drawing Γ of T , there exists a contractible edge.*

Proof. By Lemma 3.1.1 there is at least one low-degree interior vertex, call it u . Let $N(u)$ denote the set of neighbours of u and let P be the ≤ 5 -gon in Γ defined by the vertices in $N(u)$.

By Lemma 3.1.2 there is a vertex $x \in N(u)$ that is in the kernel of P , $\mathcal{K}(P)$. Let us show that ux is the desired contractible edge. Note that vertex u satisfies (C1) by construction.

Let y_1 and y_2 denote the two vertices in P so that y_1, x, y_2 are consecutive in that order around u . We claim that $N(u) \cap N(x) = \{y_1, y_2\}$. Since $x \in \mathcal{K}(P)$, every vertex of P is visible from x . If there were a third vertex of P , say w , such that $wx \in E$, then since $x \in \mathcal{K}(P)$ the edge wx is contained in P and would therefore cross one of uy_1 or uy_2 . Thus, by Lemma 2.2.1, $T_{u,x}$ is a planar triangulation on $n - 1$ vertices, so (C2) is satisfied. Finally, one can see that since $x \in \mathcal{K}(P)$ we have that condition (C3) is also satisfied. The result now follows. \square

5.2 Extending the Schnyder wood

In this section we show that given a contractible edge ux , with u a vertex of degree at most 4, there is a unique way to extend a Schnyder wood S' of $T_{u,x}$ to a Schnyder wood S of T , where the arcs of S are arcs of S' , except for the arcs incident to u . For the case where u is a vertex of degree 5, we will see that there exist three possibilities, depending on the type of arcs incident to x , and in two of these three cases, we obtain a similar result as above. The third case will be handled in Section 5.4. The intuition as to why the existence of these Schnyder woods is relevant, is that they preserve the structure of the regions for each interior vertex, thus simplifying the process of recovering a suitable weight distribution for our morph as we will see in the following section. The idea in the proofs of the lemmas in this section is similar to that of the proof of Theorem 2.2.3 in that an edge is uncontracted to obtain the new Schnyder wood. The difference in our approach is that in general it is not the case that an endpoint of the contracted edge is an exterior vertex.

We begin by considering the case where u has degree at most 4.

Lemma 5.2.1. *Let $T = (V, E)$ be a planar triangulation and let $e = ux \in E$ be a contractible edge with $\deg(u) \leq 4$. If S' is a Schnyder wood of $T_{u,x}$ then there exists a unique Schnyder wood S of T such that the arcs of S , except for those incident with u , are arcs of S' .*

Proof. To obtain the desired Schnyder wood for T we use most of the arcs in S' . After this we assign orientation and colours to the remaining edges, the ones incident to u in T .

Let us first consider the case where $\deg(u) = 3$, suppose that x, y and z are the neighbours of u . Then xyz is a face of $T_{u,x}$. We may assume without loss of generality that x, y, z is the clockwise order around u of its neighbours.

We begin by adding all arcs of S' to S . As a consequence, the arcs in S not incident with u, x, y or z satisfy conditions (D1) and (D2) from the definition of Schnyder wood.

We are only left to add the arcs in S incident with u , for these we proceed as follows. Let us consider the case where $(y, x) \in S'$, the case where $(x, y) \in S'$ can be handled by a similar argument. We may assume without loss of generality that (y, x) has colour 1, see Figure 5.1. Since $\deg(u) = 3$ the three arcs at u must be outgoing. Observe that since (y, x) has colour 1, if condition (D2) is to hold at x then (u, x) must have colour 1, any other colour would generate two consecutive incoming arcs at x of different colours. Now, we must have that the colours of (u, y) and (u, z) must be 2 and 3 if condition (D2) is to hold at u . Here we observe that (y, x) uniquely determined S . Now that we have defined S , note that the order of the arcs in S around u, x and y satisfy condition (D1) from the definition of Schnyder wood. Now, since S' is a Schnyder wood, it follows from Lemma 2.3.1 that (z, x) has colour 1 or (x, z) has colour 3. In either case, the order of the arcs in S around z also satisfy condition (D1) from the definition of a Schnyder wood. An analogous argument can be used for the case where (x, y) has colour 1 in S' , in this case we let (u, x) , (u, y) and (u, z) have colours 3, 1 and 2 respectively.

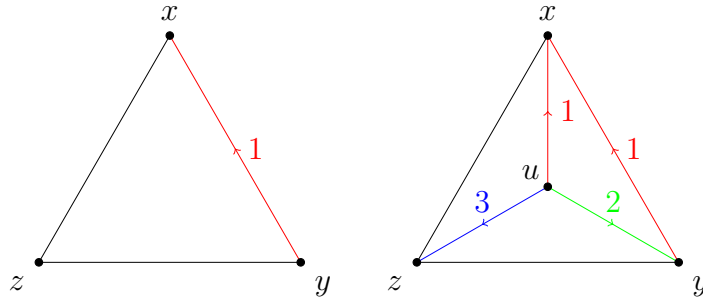


Figure 5.1: The case where $\deg(u) = 3$, and $(y, x) \in S'$ has colour 1.

Now let us consider the case where $\deg(u) = 4$. Let w, x, y , and z be the neighbours of u in clockwise order. Then xyz and wxz are faces in $T_{u,v}$ that share the edge xz . We use the arcs in S' other than (x, z) and (z, x) for S . Let us consider the case where $(x, z) \in S'$, the case with $(z, x) \in S'$ can be handled similarly. Without loss of generality we may assume that (x, z) has colour 1, see Figure 5.2. If this is the case and if condition (D1) is to hold at x in S , then there must be an outgoing arc of colour 1 at x in S . Therefore (x, u) must be of colour 1. Now given that (x, u) has colour 1 and if condition (D1) must hold at u , it follows that $(u, y), (u, z), (u, w) \in S$ and they must have colours 3, 1 and 2 respectively. At this point we make the observation that the resulting set S , if a Schnyder wood, is unique. The set of arcs S we have defined satisfies condition (D1) at vertices $V \setminus \{w, y, z\}$. It follows from Lemma 2.3.1 applied to S' and faces xyz and wxz that (y, z) has colour 1 or (z, y) has colour 3, and (w, z) has colour 1 or (z, w) has colour 2 in S . Therefore (u, z)

being of colour 1 is compatible with the colours of the arcs around z and so condition (D1) holds at z in S . Again, from Lemma 2.3.1 applied to S' and to the face xyz we have that (y, z) has colour 1 or (z, y) has colour 3, and (x, y) has colour 3 or (y, x) has colour 2. Thus (u, y) being of colour 3 is compatible with the ordering of the arcs around y and therefore condition (D1) holds at y . An analysis similar to the one used for y can be used for z to conclude that (D1) holds at z . Therefore S is a Schnyder wood. \square

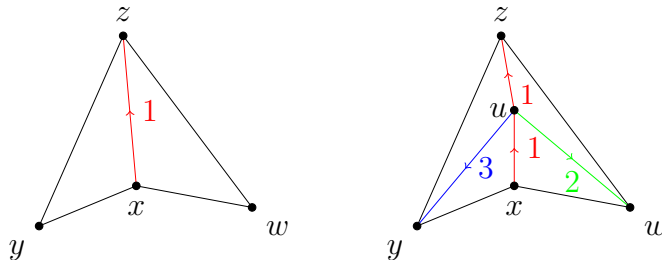


Figure 5.2: The case where $\deg(u) = 4$, and $(x, z) \in S'$ has colour 1.

Next we address the case where u has degree 5. There will be one exceptional subcase, which we will treat in Section 5.4.

Lemma 5.2.2. *Let $T = (V, E)$ be a planar triangulation and let $e = ux \in E$ be a contractible edge with $\deg(u) = 5$. Say v, w, x, y and z are the neighbours of u in T listed in clockwise order. If S' is a Schnyder wood of $T_{u,x}$ with at least one of (v, x) and (z, x) in S' , then there exists a unique Schnyder wood S of T such that the arcs of S , except for those incident with u , are arcs of S' .*

Proof. As in the proof of the previous lemma, to obtain the desired Schnyder wood for T we use most of the arcs in S' . After this we assign orientation and colours to the remaining edges, the ones incident to u in T . Note that if both (v, x) and (z, x) are in S' then they must have the same colour since they are consecutive arcs around x . Let us assume without loss of generality that the arcs incoming to x from $\{v, z\}$ have colour 1.

We begin by considering the case where both (v, x) and (z, x) are in S' , see Figure 5.3. Let us now define S . Begin by taking all arcs in S' , except (v, x) and (z, x) , and adding them to S . As for the arcs in S incident to u , we let (u, x) , (v, u) , and (z, u) be of colour 1, (u, y) be of colour 2 and (u, w) be of colour 3. Note that conditions (D1) and (D2) are satisfied at $V \setminus \{w, x, y\}$. Note that in S' (x, y) has colour 2 or (y, x) has colour 1, therefore the arcs at x and y have the proper colours and orientations in S . A similar assertion holds

for z , where (x, z) has colour 3 or (z, x) has colour 1. Thus S is a Schnyder wood. The uniqueness of S in this case follows from the fact that in S we must have (v, u) and (z, u) of colour 1, which forces the three other arcs at u to be outgoing and of the colours given above.

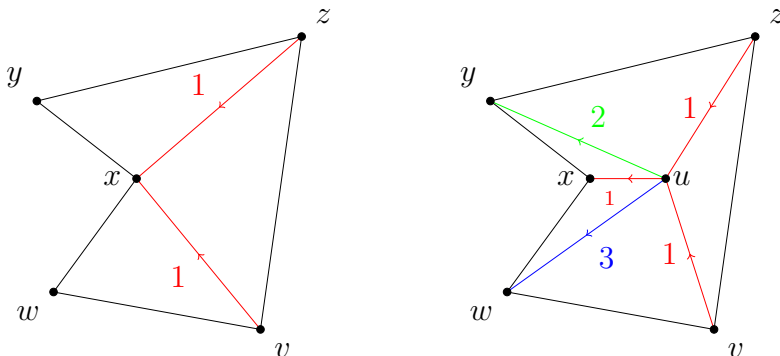


Figure 5.3: Arcs $(v, x), (z, x) \in S'$ have colour 1.

Now, let us consider the case where there is only one incoming arc to x from $\{v, z\}$ in S' . Assume without loss of generality that such incoming arc is (z, x) , see Figure 5.4. It follows that (x, v) is of colour 3. We take all arcs in S' , except (z, x) and (z, v) , and add them to S . We let the arcs incident to u in S be the following. Take (z, u) and (u, w) in colour 1, (u, y) in colour 2, and (x, u) and (u, v) in colour 3. It now follows that conditions (D1) and (D2) hold for vertices in $V \setminus \{w, x, y\}$. Finally, note that (w, x) has colour 2 or (x, w) has colour 1 and similarly for (x, y) and (y, x) . Therefore the arcs at w, x and y satisfy the conditions in the definition of a Schnyder wood. We arrive to the conclusion that S is a Schnyder wood. Here the uniqueness follows from the fact that in S we must have (x, u) of colour 3 and (z, u) of colour 1. Thus the remaining arcs at u must be outgoing and their colours are determined. \square

5.3 Finding the weight distribution

Let T be a planar triangulation. One of the steps of the morphing procedure presented in this chapter consists of performing a sequence of “uncontractions” while maintaining a weighted Schnyder drawing. In other words, starting from a weighted Schnyder drawing of $T_{u,x}$, where ux is a contractible edge, we aim to obtain a weighted Schnyder drawing of T .

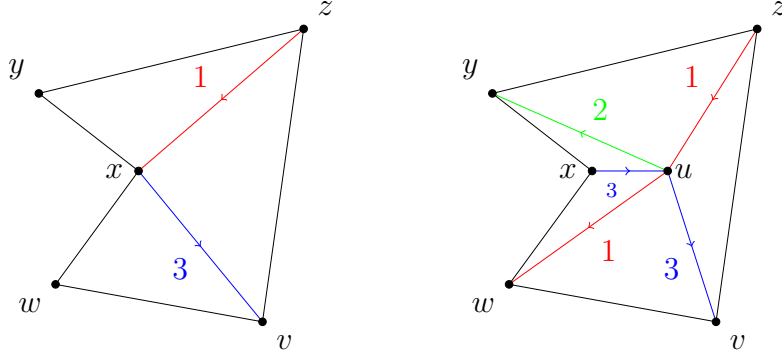


Figure 5.4: Arcs $(x, v), (z, x) \in S'$ have colours 3 and 1 respectively.

Recall that a weight distribution is an assignment of positive weights to the interior faces. This section is devoted to showing how to obtain suitable weight distributions for the Schnyder woods of T obtained from Lemmas 5.2.1 and 5.2.2 from weight distributions for Schnyder woods of $T_{u,x}$, so that the positions of all vertices of $T_{u,x}$ are preserved. We begin with Lemma 5.3.1 where we analyze the case where u has degree at most 4. Then in Lemma 5.3.2 and Lemma 5.3.3 we consider two cases where the degree of u is 5.

Lemma 5.3.1. *Let $T = (V, E)$ be a planar triangulation and let $e = ux \in E$ be a contractible edge with $\deg(u) \leq 4$. Assume that Γ' is a weighted Schnyder drawing of $T_{u,x}$ induced by S' and \mathbf{w}' . Then there exists a weighted Schnyder drawing Γ of T such that the position of each vertex of $T_{u,x}$ is preserved from Γ' to Γ .*

Proof. Since we are interested in obtaining a weighted Schnyder drawing of T in which the positions of vertices of T' as given by Γ' are preserved, our aim will be to use the Schnyder wood from Lemma 5.2.1 and find a suitable weight distribution that induces the desired drawing. Most of the weights to obtain the drawing of T will be the same as the ones assigned by \mathbf{w}' , except at the faces incident to u . Let S be the Schnyder wood given by Lemma 5.2.1. Our aim is to obtain a weight distribution \mathbf{w} for T such that

$$\sum_{f \in R_i(v)} \mathbf{w}(f) = \sum_{f \in R'_i(v)} \mathbf{w}'(f) \quad (5.1)$$

for all $v \in V \setminus \{u\}$.

First let us consider the case where $\deg(u) = 3$ and let us assume without loss of generality that the arc (u, x) has colour 1 in S . In this case xyz is a face in $T_{u,x}$, so let $a := \mathbf{w}'(xyz)$. Let p, q and r denote the weights of uxz, uxy and uyz respectively assigned

by \mathbf{w} , see Figure 5.5. For each face f of $T_{u,x}$ different from $\{xyz\}$, we let $\mathbf{w}(f) := \mathbf{w}'(f)$. Since the total weight is $2n - 5$, we must have $p + q + r = a$, so taking $p = q = r = a/3$ yields a weight distribution. Furthermore, for a given vertex $v \in V \setminus \{u\}$ if $xyz \notin R'_i(v)$, then clearly (5.1) holds. On the other hand, $xyz \in R'_i(v)$ if and only if $uxz, uxy, uyz \in R_i(v)$, thus (5.1) also holds in this case. We can now conclude the Schnyder drawing of T , Γ , obtained from S and \mathbf{w} has each vertex from $T_{u,x}$ preserve its position from Γ' .

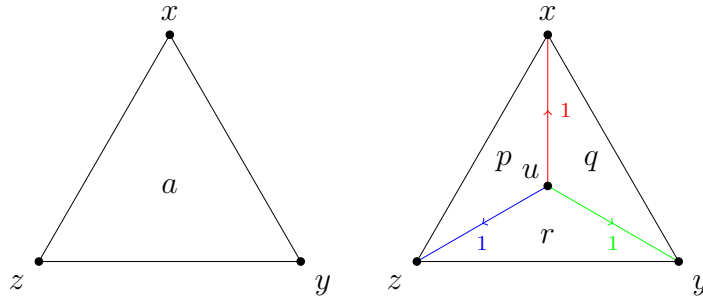


Figure 5.5: 3-gon

Now, we move on to the case where $\deg(u) = 4$. Let us assume without loss of generality that (x, z) has colour 1 in S' , thus $(x, u), (u, z)$ have colour 1 in S . Let a and b be the weights given by \mathbf{w}' and let p, q, r and s be the weights given by \mathbf{w} to the faces shown in Figure 5.6. Let us begin by setting $\mathbf{w}(f) := \mathbf{w}'(f)$ for all faces of $T_{u,x}$ that are faces of T .

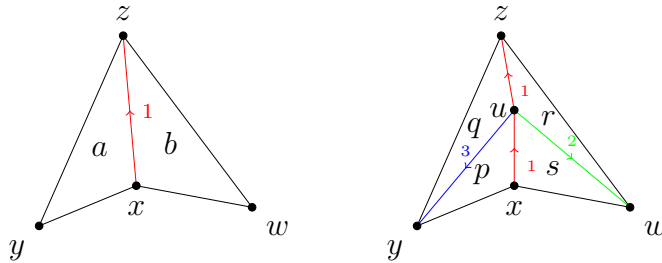


Figure 5.6: 4-gon

Now, since the total weight is $2n - 5$, we must have that $a + b = p + q + r + s$. Note that for every vertex $v \in V \setminus \{u\}$ we have that $xyz \in R'_i(v)$ if and only if $uxy, uyz \in R_i(v)$. Likewise for wxz and uwz . Thus we must have $a = p + q$ and $b = s + t$. Note that taking $p = q = a/2$ and $s = t = b/2$ yields a weight distribution. Consider the weighted Schnyder drawing Γ of T obtained from S and \mathbf{w} . We now show that Γ satisfies the required

conditions. Let v be an interior vertex of T , $v \neq u$. If $xyz, wxz \notin R'_i(v)$, then since \mathbf{w} and \mathbf{w}' coincide in $R'_i(v)$ we have that $\sum_{f \in R_i(v)} \mathbf{w}(f) = \sum_{f \in R'_i(v)} \mathbf{w}'(f)$. Therefore in this case the i -th coordinate of v is preserved from Γ' to Γ . Three more cases can arise, and in each of these at least one of xyz and wxz is in $R'_i(v)$. We only consider one of those three cases, noting that the remaining two can be proved in a similar way. Suppose $xyz, wxz \in R'_i(v)$. Let $A = \{uwx, uwz, uxy, uyz\}$ and $A' = \{xyz, wxz\}$. Here we have

$$\begin{aligned} \sum_{f \in R_i(v)} \mathbf{w}(f) &= p + q + r + s + \sum_{f \in R_i(v) \setminus A} \mathbf{w}(f) \\ &= a + b + \sum_{f \in R'_i(v) \setminus A'} \mathbf{w}'(v) \\ &= \sum_{f \in R'_i(v)} \mathbf{w}'(v). \end{aligned}$$

Therefore the i -th coordinate is also preserved in this case. Thus the positions of vertices in $T_{u,x}$ are preserved from Γ' to Γ , as desired. \square

We now consider one case where u has degree 5.

Lemma 5.3.2. *Let $T = (V, E)$ be a planar triangulation and let $e = ux \in E$ be a contractible edge with $\deg(u) = 5$. Say v, w, x, y and z are the neighbours of u in T listed in clockwise order. If S' denotes a Schnyder wood of $T_{u,x}$ where both (v, x) and (z, x) are in S' then for any weighted Schnyder drawing Γ' of $T_{u,x}$ given by S' , there exists a weighted Schnyder drawing Γ of T such that the position of each vertex of $T_{u,x}$ is preserved from Γ' to Γ .*

Proof. We use a similar approach as in the proof of the previous lemma, again the goal is to find a weighted Schnyder drawing of T such that the position of each vertex of $T_{u,x}$ is preserved. To obtain the weight distribution for the drawing of T we use most of the weights as given by \mathbf{w}' , except for faces incident to u . We may assume without loss of generality that (v, x) and (z, x) have colour 1 in S' . Let S be the Schnyder wood given by Lemma 5.2.2 for the case where $(v, x), (z, x) \in S'$, $A = \mathcal{F}(T) \setminus \mathcal{F}(T_{u,x}) = \{uvw, wvz, wwx, uxy, uyz\}$ and $A' = \mathcal{F}(T_{u,x}) \setminus \mathcal{F}(T) = \{vwx, vxz, xyz\}$.

We begin by finding a suitable weight distribution \mathbf{w} for T and then show that the drawing induced by \mathbf{w} and S satisfies the requirements from the statement. Let \mathbf{w}' be a weight distribution for T' and let Γ' be the Schnyder drawing given by S' and \mathbf{w}' . First we define $\mathbf{w}(f) := \mathbf{w}'(f)$ for each face $f \in \mathcal{F}(T) \cap \mathcal{F}(T_{u,x})$. We just need to define $\mathbf{w}(f)$ for

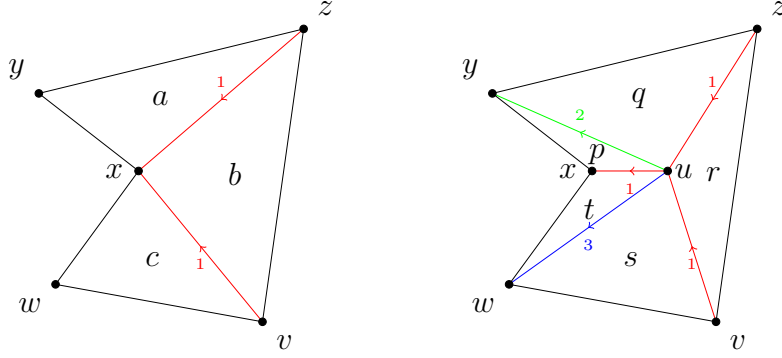


Figure 5.7: 5-gon case 1. The weights a, b and c assigned by \mathbf{w}' on the left, and the weights p, q, r, s and t assigned by \mathbf{w} on the right.

$f \in A$. Let a, b, c and p, q, r, s, t denote the weights given by \mathbf{w}' and \mathbf{w} to the faces in A' and A , see Figure 5.7. In other words it only remains to define p, q, r, s and t . Let us take $p = q = a/2, r = b$ and $s, t = c/2$. We have that

$$\begin{aligned}
 \sum_{f \in \mathcal{F}(T)} \mathbf{w}(f) &= p + q + r + s + t + \sum_{f \in \mathcal{F}(T) \setminus A} \mathbf{w}(f) \\
 &= a + b + c + \sum_{f \in \mathcal{F}(T_{u,x}) \setminus A'} \mathbf{w}'(f) \\
 &= \sum_{f \in \mathcal{F}(T_{u,x})} \mathbf{w}'(f) = 2n - 5.
 \end{aligned}$$

Therefore \mathbf{w} is a weight distribution.

Let Γ be the Schnyder drawing obtained from S and \mathbf{w} . Let us show that Γ preserves the positions of the vertices of $T_{u,x}$ from Γ' . Let α be an interior vertex of $T_{u,x}$, we show that the i -th coordinate of α is preserved from Γ' to Γ . We will consider several cases, depending whether $R'_i(\alpha)$ has (v, x) or (z, x) in its boundary. The first possibility is that none of (v, x) and (z, x) is in the boundary of $R'_i(\alpha)$ and here we must have that $A' \cap R'_i(\alpha) = \emptyset$ or $A' \subseteq R'_i(\alpha)$ (cases 1 and 2 below). If $R'_i(\alpha)$ uses (v, x) then $\alpha \in D_1(v)$. Here we could have two possibilities, either $A' \cap R'_i(\alpha) = \{vwx\}$ when $i = 2$ or $A' \cap R'_i(\alpha) = \{vzx, xyz\}$ when $i = 3$ (cases 3 and 4 below). For the case where $R'_i(\alpha)$ uses (z, x) we have $\alpha \in D_1(z)$, and this can be handled in a similar fashion as the case where $\alpha \in D_1(v)$. Finally, we note that no vertex has both arcs (v, x) and (z, x) bounding a given region, since regions are bounded by directed paths and here the aforementioned arcs are both incoming to x . Thus, we only consider the following four cases.

1. Assume $R'_i(\alpha) \cap A' = \emptyset$, or equivalently $A \cap R_i(\alpha) = \emptyset$. In this case we have that

$$\sum_{f \in R_i(\alpha)} \mathbf{w}(f) = \sum_{f \in R'_i(\alpha)} \mathbf{w}'(f).$$

Thus the i -th coordinate of α is preserved from Γ' to Γ .

2. Now suppose $A' \subseteq R'_i(\alpha)$ in S' , or equivalently $A \subseteq R_i(\alpha)$ in S . We have

$$\begin{aligned} \sum_{f \in R_i(\alpha)} \mathbf{w}(f) &= p + q + r + s + t + \sum_{f \in R_i(\alpha) \setminus A} \mathbf{w}(f) \\ &= a + b + c + \sum_{f \in R'_i(\alpha) \setminus A'} \mathbf{w}'(f) \\ &= \sum_{f \in R'_i(\alpha)} \mathbf{w}'(f). \end{aligned}$$

Thus, in this case the i -th coordinate of α is preserved from Γ' to Γ .

3. Now let us assume that $A' \cap R'_i(\alpha) = \{vwx\}$. By the structure of S we have that this is equivalent to $A \cap R_i(\alpha) = \{uvw, uwx\}$, since the 1-path of α in S' contains (v, x) if and only if it contains (v, u) and (u, x) in S . We can now deduce that

$$\begin{aligned} \sum_{f \in R_i(\alpha)} \mathbf{w}(f) &= s + t + \sum_{f \in R_i(\alpha) \setminus \{A\}} \mathbf{w}(f) \\ &= c + \sum_{f \in R'_i(\alpha) \setminus A'} \mathbf{w}'(f) \\ &= \sum_{f \in R'_i(\alpha)} \mathbf{w}'(f), \end{aligned}$$

as desired.

4. Finally, let us consider the case where $A' \cap R'_i(\alpha) = \{vxz, xyz\}$. Again, we use the fact that the 1-path of α in S' contains (v, x) if and only if it contains (v, u) and (u, x) in S , so $A' \cap R'_i(\alpha) = \{vxz, xyz\}$ is equivalent to $A \cap R_i(\alpha) = \{uvw, uxy, uxz\}$.

In this case we have that

$$\begin{aligned}
\sum_{f \in R_i(\alpha)} \mathbf{w}(f) &= p + q + r + \sum_{f \in R_i(\alpha) \setminus \{A\}} \mathbf{w}(f) \\
&= a + b + \sum_{f \in R'_i(\alpha) \setminus A'} \mathbf{w}'(f) \\
&= \sum_{f \in R'_i(\alpha)} \mathbf{w}'(f).
\end{aligned}$$

That is, the i -th coordinate of α is preserved from Γ' to Γ .

Therefore Γ is the desired weighted Schnyder drawing. \square

Let T be a planar triangulation and let $wx \in E(T)$. Recall that given a Schnyder wood S of T , we use $\Delta_i(wx)$ to denote the region enclosed by the edge wx and the i -paths in S outgoing x and w . If we are given a weight assignment of $\mathcal{F}(T)$, then we use $\delta_i(wx)$ to denote the sum of the weights of the faces in $\Delta_i(wx)$. Note that it might be the case that $\Delta_i(wx)$ is empty if (x, w) or (w, x) are in S and have colour i , in such case we also have that $\delta_i(wx) = 0$. Now we consider the second case where u has degree 5, in which exactly one of (v, x) and (z, x) is in S' . We will note that unlike in the previous cases, we require that the weight distribution satisfies a certain condition, which involves the weight $\delta_i(wx)$. The two cases considered in the statement of Lemma 5.3.3 exhaust all possibilities when exactly one of (v, x) and (z, x) is in S' .

Lemma 5.3.3. *Let $T = (V, E)$ be a planar triangulation and let $e = ux \in E$ be a contractible edge with $\deg(u) = 5$. Say v, w, x, y and z are the neighbours of u in T listed in clockwise order. Let S' be a Schnyder wood of $T_{u,x}$, \mathbf{w}' be a weight distribution of $\mathcal{F}(T_{u,x})$ and Γ' be the Schnyder drawing given by S' and \mathbf{w}' . If exactly one of (v, x) and (z, x) is in S' , then we have one of the following.*

1. Suppose $(z, x) \in S'$ and $(x, v) \in S'$. Let i denote the colour of (z, x) . If

$$\mathbf{w}'(xyz) > \mathbf{w}'(vwx)/2 + \delta_i(wx)$$

then there exists a weighted Schnyder drawing Γ of T such that the position of each vertex of $T_{u,x}$ is preserved from Γ' to Γ .

2. Suppose $(v, x) \in S'$ and $(x, z) \in S'$. Let i denote the colour of (v, x) . If

$$\mathbf{w}'(vwx) > \mathbf{w}'(xyz)/2 + \delta_i(xy)$$

then there exists a weighted Schnyder drawing Γ of T such that the position of each vertex of $T_{u,x}$ is preserved from Γ' to Γ .

Proof. Our aim for this proof is to find a weight distribution \mathbf{w} and a Schnyder wood S for T that yield the desired drawing Γ in each case. For this we use most weights as given by \mathbf{w}' , except at faces incident to u . Clearly cases 1 and 2 are mutually exclusive. We only prove the result for case 1, as case 2 can be proved by using an analogous argument, so assume that $(z, x) \in S'$. Without loss of generality we may assume (z, x) has colour 1, thus by condition (D1) (x, v) has colour 3 in S' , see Figure 5.8. Let S be the Schnyder wood given by Lemma 5.2.2 for the case where $(z, x) \in S'$ and $(v, x) \notin S'$, $A = \mathcal{F}(T) \setminus \mathcal{F}(T_{u,x}) = \{uvw, uvz, uwx, uxy, uyz\}$ and $A' = \mathcal{F}(T_{u,x}) \setminus \mathcal{F}(T) = \{vwx, vxz, xyz\}$.

We begin by finding the weight distribution \mathbf{w} . Let a, b, c and p, q, r, s, t be the weights given by \mathbf{w}' and \mathbf{w} of the faces shown in Figure 5.8. Now, let us define \mathbf{w} in terms of

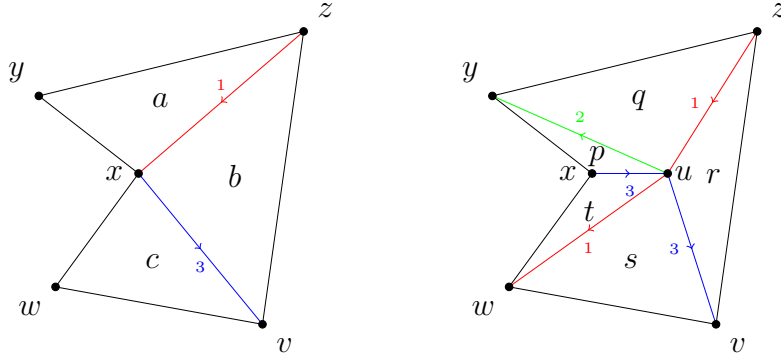


Figure 5.8: 5-gon case 2

\mathbf{w}' . Let $\mathbf{w}(f) := \mathbf{w}'(f)$ for all $f \in \mathcal{F}(T) \cap \mathcal{F}(T_{u,x})$. Take $p = q = (a - c/2 - \delta_1(wx))/2$, $r = b + c/2 + \delta_1(wx)$ and $s = t = c/2$. We can now deduce that

$$\begin{aligned} \sum_{f \in \mathcal{F}(T)} \mathbf{w}(f) &= p + q + r + s + t + \sum_{f \in \mathcal{F}(T) \setminus A} \mathbf{w}(f) \\ &= a + b + c + \sum_{f \in \mathcal{F}(T_{u,x}) \setminus A'} \mathbf{w}'(f) \\ &= \sum_{f \in \mathcal{F}(T_{u,x})} \mathbf{w}'(f), \end{aligned}$$

and since the weight of each face is positive, we can conclude that \mathbf{w} is a weight distribution.

Now, let Γ be the Schnyder drawing given by \mathbf{w} and S . We just need to show that the positions of vertices of $T_{u,x}$ are preserved from Γ' to Γ . Let α be an interior vertex of $T_{u,x}$. Let us prove that the i -th coordinate of α is preserved from Γ' to Γ . As in the proof of Lemma 5.3.2, we consider several cases. These cases will depend on whether $R'_i(\alpha)$ is bounded by (z, x) or (x, v) . The case where $R_i(\alpha)$ is bounded by none of (z, x) and (x, v) implies that either $A' \cap R'_i(\alpha) = \emptyset$ or $A' \subseteq R'_i(\alpha)$ and this can be handled in a similar way to how case 1 and 2 were handled in the proof of Lemma 5.3.2. Here we focus on the cases where $R'_i(\alpha)$ is bounded by exactly one of (z, x) and (x, v) , noting that it is not possible that both arcs (z, x) and (x, v) bound $R'_i(\alpha)$. If $R'_i(\alpha)$ uses (x, v) then $\alpha \in D_3(x)$. Here we could have two possibilities, either $A' \cap R'_i(\alpha) = \{vwx\}$ when $i = 2$ or $A' \cap R'_i(\alpha) = \{vxxz, xyz\}$ when $i = 1$ (cases 1 and 2 below). Now, if $R'_i(\alpha)$ uses (z, x) then $\alpha \in D_1(z)$. In this case we could have two possibilities, either $A' \cap R'_i(\alpha) = \{xyz\}$ when $i = 2$ or $A' \cap R'_i(\alpha) = \{vwx, vxxz\}$ when $i = 3$ (cases 3 and 4 below).

1. Suppose $A' \cap R'_i(\alpha) = \{vwx\}$. This occurs if and only if $A \cap R_i(\alpha) = \{uvw, uwx\}$. Thus

$$\begin{aligned} \sum_{f \in R_i(\alpha)} \mathbf{w}(f) &= s + t + \sum_{f \in R_i(\alpha) \setminus A} \mathbf{w}(f) \\ &= c + \sum_{f \in R'_i(\alpha) \setminus A'} \mathbf{w}'(f) \\ &= \sum_{f \in R'_i(\alpha)} \mathbf{w}'(f). \end{aligned}$$

2. Now assume that $A' \cap R'_i(\alpha) = \{vxxz, xyz\}$. This is true if and only if $A \cap R_i(\alpha) = \{uvz, uxy, uyz\}$. Therefore

$$\begin{aligned} \sum_{f \in R_i(\alpha)} \mathbf{w}(f) &= p + q + r + \sum_{f \in R_i(\alpha) \setminus A} \mathbf{w}(f) \\ &= a + b + \sum_{f \in R'_i(\alpha) \setminus A'} \mathbf{w}'(f) \\ &= \sum_{f \in R'_i(\alpha)} \mathbf{w}'(f). \end{aligned}$$

3. Now let us consider the case where $A' \cap R'_i(\alpha) = \{xyz\}$. Note that this implies $A \cap R_i(\alpha) = \{uwx, uxy, uyz\}$, furthermore $R_i(\alpha) \setminus R'_i(\alpha) = \Delta_1(wx) \cup \{uwx, uxy, uyz\}$. This implies that

$$\begin{aligned}
\sum_{f \in R_i(\alpha)} \mathbf{w}(f) &= p + q + t + \delta_1(wx) + \sum_{f \in R_i(\alpha) \setminus A} \mathbf{w}(f) \\
&= a + \sum_{f \in R'_i(\alpha) \setminus A'} \mathbf{w}'(f) \\
&= \sum_{f \in R'_i(\alpha)} \mathbf{w}'(f).
\end{aligned}$$

4. Finally, for the case where $A' \cap R'_i(\alpha) = \{vwx, vxz\}$, we have that $A \cap R_i(\alpha) = \{uvw, uvz\}$ and $R'_i(\alpha) \setminus R_i(\alpha) = \Delta_1(wx) \cup \{vwx, vxz\}$. Therefore

$$\begin{aligned}
\sum_{f \in R_i(\alpha)} \mathbf{w}(f) &= s + r + \sum_{f \in R_i(\alpha) \setminus A} \mathbf{w}(f) \\
&= b + c + \delta_1(wx) + \sum_{f \in R_i(\alpha) \setminus A} \mathbf{w}(f) \\
&= b + c + \sum_{f \in R'_i(\alpha) \setminus A'} \mathbf{w}'(f) \\
&= \sum_{f \in R'_i(\alpha)} \mathbf{w}'(f).
\end{aligned}$$

Thus in each case the coordinates from Γ' are preserved on Γ , as desired. \square

5.4 Handling the exceptional case with $\deg(u) = 5$

Let T be a planar triangulation. In the previous section we showed how to obtain a weighted Schnyder drawing of T from a weighted Schnyder drawing of $T_{u,x}$ while preserving the positions of the vertices of $T_{u,x}$. However this was only done for the case where $\deg(u) \leq 4$ or $\deg(u) = 5$ subject to some constraints. In this section we show that it is still possible to obtain a straightline drawing for the remaining case where $\deg(u) = 5$.

The exceptional case where $\deg(u) = 5$ and no arc is incoming to x in the Schnyder wood of $T_{u,x}$ requires a technical lemma. We must show that if we assign a weight of 0 to

a transitive interior face f of a Schnyder wood S and a positive weight to all remaining faces, such that the total weight is $2n - 5$, then we still obtain a planar drawing of T from S . Let $g \in \mathcal{F}(T)$ be a face incident to three interior vertices. An assignment of weights \mathbf{w} such that $\mathbf{w}(f) > 0$ for all $f \in \mathcal{F}(T) \setminus \{g\}$, $\mathbf{w}(g) = 0$ and $\sum_{f \in \mathcal{F}(T)} \mathbf{w}(f) = 2n - 5$ is called a *near weight distribution* of $\mathcal{F}(T) \setminus \{g\}$. The lemma we prove is a slightly stronger version that does not require the interior face g to be transitive. The proof is a modification of Schnyder's original argument in [51]. We now state the technical lemma.

Lemma 5.4.1. *Let T be a planar triangulation, let S be a Schnyder wood of T and let g be an interior face of T incident to three interior vertices. If \mathbf{w} is a near weight distribution of $\mathcal{F} \setminus \{g\}$ then the drawing defined by S and \mathbf{w} is planar.*

Proof. Let Γ be the drawing induced by S and \mathbf{w} . Recall that this is a drawing of T in the plane $r + s + t = 2n - 5$. We consider two possible cases depending on the type of face that g is, see Figure 2.6. In case 1 below we consider the case where g is a transitive face, type (i) or (ii) in Figure 2.6. Then, in case 2 we treat the case where g is a cyclically oriented face, type (iii) or (iv) in Figure 2.6.

1. Suppose g is a transitive face, type (i) or (ii) in Figure 2.6. Let us show that Γ is a planar drawing by showing that each of the three projections of Γ to the planes $r = 0$, $s = 0$ and $t = 0$ are planar, here we use r , s and t to denote the axis in 3-space. Suppose without loss of generality that $g = xyz$ is of type (i) as illustrated in Figure 2.6, and let us only consider one of the projections Π , say to the $t = 0$ plane. Recall that if all weights were to be positive, then property (R) (p. 21) guarantees that for each edge ab and a vertex $c \notin \{a, b\}$, there is a coordinate $k \in \{1, 2, 3\}$ such that $a_k, b_k < c_k$. Observe that by setting $\mathbf{w}(g) = 0$ this fails only for edge xz and vertex y . Thus we separate this special case in our analysis.

We begin by showing that no two edges ab and cd cross in Π whenever at least one of them does not have y as an endpoint or at least one of them is not xz . First we prove the following claim.

Claim. If the edge ab defines a segment with negative slope as in the figure below, then no other vertex is mapped to the shaded triangle from Figure 5.9.

Prof of Claim. Suppose by way of contradiction that there is a vertex c mapped to the shaded region. This implies there is $t \in [0, 1]$ such that

$$(1 - t)b_1 + ta_1 \leq c_1 \leq a_1 \tag{5.2}$$

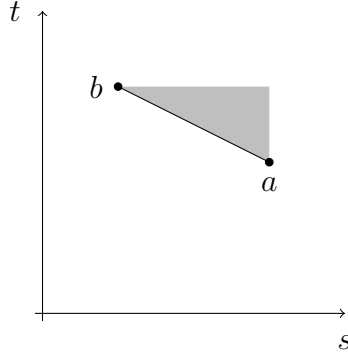


Figure 5.9: No vertex mapped to the shaded triangle

and

$$(1 - t)b_2 + ta_2 \leq c_2 \leq b_2. \quad (5.3)$$

Now, by our assumptions on the edges ab and cd we have that there is a coordinate k such that $c_k > a_k, b_k$. Therefore $t \in (0, 1)$. Now, since we have $c_1 \leq a_1$ and $c_2 \leq b_2$ then we must have $k = 3$. Thus $c_3 > a_3, b_3$. Therefore the previous inequality together with the left-hand inequalities from (5.2) and (5.3) imply

$$c_1 + c_2 + c_3 > (1 - t)b_1 + ta_1 + (1 - t)b_2 + ta_2 + (1 - t)b_3 + ta_3 = 2n - 5,$$

which yields a contradiction to $c_1 + c_2 + c_3 = 2n - 5$. Thus the claim follows. \square

We now use the previous claim to show that no two such edges ab and cd cross. Suppose by contradiction that the edges cross. Without loss of generality suppose a is the vertex with largest first coordinate. There must be $i, j, k \in \{1, 2, 3\}$ such that $cd \in R_i(b)$, $ab \in R_j(c)$ and $ab \in R_k(d)$. This will imply in particular that $b_i > c_i, d_i$, $c_j > a_j, b_j$ and $d_k > a_k, b_k$. Since the edges cross, we cannot have $b_1 > c_1, d_1$. Therefore $i, j, k \in \{2, 3\}$, and we must have $j = k$. If $j = 2$ then we would not have an edge crossing, therefore $i = 2$ and $j = k = 3$. Thus $c_1, d_1 < a_1$ and $c_2, d_2 < b_2$. It now follows from our previous claim, that the edges ab and cd do not cross.

Finally let us show that the edge xz does not cross any edge having y as an endpoint, say ay . Let us begin by proving that if $a \in \{x, z\}$ then the edges do not cross, in other words, the points x, y and z are not collinear. By analyzing the regions for x, y and z we conclude that $z_1 < y_1 < x_1$, $x_2 < z_2 = y_2$ and $x_3 < y_3 < z_3$. Therefore, if x, y and z are to be collinear, there must be $t \in [0, 1]$ such that

$$(y_1, y_2, y_3) = ((1 - t)x_1 + tz_1, (1 - t)x_2 + tz_2, (1 - t)x_3 + tz_3).$$

Since $x_2 < y_2$ and $z_2 = y_2$ we must have $t = 1$, but this contradicts the fact that $z_1 < y_1$. Therefore x, y and z are non collinear. Now suppose a is a neighbour of y that is different from x and z . Clearly any such neighbour satisfies $xz \in R_2(a)$, thus $x_2, z_2 < a_2$. From this it follows that there is no edge crossing in the projections to the planes $r = 0$ and $t = 0$. So, suppose there is an edge crossing in the projection to the plane $s = 0$. Note that xz defines a negative slope line segment. By our claim from above applied to xz and a we conclude that a cannot lie in the shaded region from Figure 5.9. This together with the facts that $a_1 < x_1$, $a_3 < z_3$, and x, y and z are not collinear implies that x must lie inside the shaded region from Figure 5.9. By using this assumptions we can formulate strict inequalities as (5.2) and (5.3) which would lead us to a contradiction by an analogous argument to that used in the proof of the claim. Therefore the drawing given by S and \mathbf{w} is planar, as desired.

2. Now let us suppose that g is a cyclically oriented face. In this case we will show that the positions given by \mathbf{w} and S as given in the statement of Theorem 2.4.3 define a barycentric embedding of T . It is clear that each vertex is assigned a point in the plane $r + s + t = 2n - 5$. Let $uw \in E$ and let $v \in V \setminus \{a, b\}$. If v is an exterior vertex, say a_i then we can see that $v_i > u_i, w_i$, as desired. Now suppose v is an interior vertex. We have that $uw \in R_i(v)$ for some $i \in \{1, 2, 3\}$. If u is an exterior vertex, then $u_i = 0$, since the exterior vertex a_i is not in $R_i(v)$. Therefore $v_i > u_i$. Now, if u is an interior vertex, then it follows from Lemma 2.4.2 that the set of faces $A := R_i(u) \subsetneq R_i(v)$ contains at least one face. If $|A| \geq 2$ then at least one of the faces in A has positive weight, therefore $v_i > u_i$. Finally, if $|A| = 1$ the the face in A cannot be g , as by Lemma 2.4.2 we must have that the face in A is not cyclically oriented. Thus the face in A has positive weight and therefore $v_i > u_i$. An analogous argument can be used to show that $v_i > w_i$. It now follows that \mathbf{w} and S define a barycentric embedding.

□

So far we have analyzed all possible configurations for contractible edges except two. The cases that remain to be considered are those where $\deg_T(u) = 5$, $(x, v), (x, z)$ are in the Schnyder wood of $T_{u,x}$ and

1. neither of vwx and xyz are cyclically oriented in the Schnyder wood of $T_{u,x}$,
2. at least one of vwx and xyz is cyclically oriented in the Schnyder wood of $T_{u,x}$.

Case 1 is treated in the next lemma, whereas case 2 can be handled by performing a flip or a flop operation on the cyclically oriented face, thus allowing us to apply Lemma 5.3.3. We do not state case 2 explicitly as a lemma, instead we will handle it directly when it arises in the next section.

Lemma 5.4.2. *Let $T = (V, E)$ be a planar triangulation and let $e = ux \in E$ be a contractible edge with $\deg(u) = 5$. Say v, w, x, y and z are the neighbours of u in T listed in clockwise order. Suppose S' is a Schnyder wood of $T_{u,x}$ such that (x, v) and (x, z) are in S' and none of vw and xy are cyclically oriented. Then*

- *if $(w, x) \in S'$ and \mathbf{w}' is a near weight distribution of $\mathcal{F}(T_{u,x}) \setminus \{vwx\}$ then there exists a Schnyder wood S and a near weight distribution \mathbf{w} of $\mathcal{F}(T) \setminus \{uwx\}$ such that the drawings induced by S' and \mathbf{w}' and by S and \mathbf{w} coincide at all vertices of $T_{u,x}$,*
- *if $(y, x) \in S'$ and \mathbf{w}' is a near weight distribution of $\mathcal{F}(T_{u,x}) \setminus \{xyz\}$ then there exists a Schnyder wood S and near weight distribution \mathbf{w} of $\mathcal{F}(T) \setminus \{uxy\}$ such that the drawings induced by S' and \mathbf{w}' and by S and \mathbf{w} coincide at all vertices of $T_{u,x}$.*

Proof. Let Γ' be the drawing of $T_{u,x}$ induced by \mathbf{w}' and S' . By Lemma 5.4.1 we have that Γ' is a planar drawing of $T_{u,x}$. We may assume without loss of generality that (x, z) has colour 2 in S' and by condition (D1) it follows that (x, v) has colour 3 in S' . We only prove the result for the case where $(w, x) \in S'$, since if $(x, w) \in S'$ then by property (D1) at x it follows that $(y, x) \in S'$ and this case can be handled by an analogous argument. Since $(w, x) \in S'$, it follows from (D1) that (w, x) has colour 2 in S' , see Figure 5.10. We consider an orientation and assignment of colours S for T where all the arcs in S' are preserved except for (w, x) , (x, z) and (x, v) . See Figure 5.10 right, for the definition of the remaining arcs in S . We claim that S is a Schnyder wood of T . Indeed, the vertices in $V \setminus \{w, x, y\}$ satisfy the required conditions. Since (x, y) has colour 1 or (y, x) has colour 3 then the arcs around x and y have the appropriate colours and order as required by (D1). Finally w also satisfies condition (D1), and this follows since (w, v) has colour 3, as by assumption $(v, w) \notin S'$, (w, u) has colour 2 and (v, w) has colour 3 in S . Thus S is a Schnyder wood of T , as claimed.

We now proceed to find define a near weight distribution \mathbf{w} of $\mathcal{F}(T) \setminus \{uwx\}$ such that together with S it induces a drawing that assigns the same position to vertices in $T_{u,x}$ as those from Γ' . Let $A = \mathcal{F}(T) \setminus \mathcal{F}(T_{u,x}) = \{uvw, uvz, uwx, uxy, uyz\}$ and $A' = \mathcal{F}(T_{u,x}) \setminus \mathcal{F}(T) = \{vwx, vxz, xyz\}$. Let a, b, c and p, q, r, s, t be the weights assigned by \mathbf{w}' and \mathbf{w} respectively to the faces in A' and A , see Figure 5.10. Note that $c = 0$. Let us

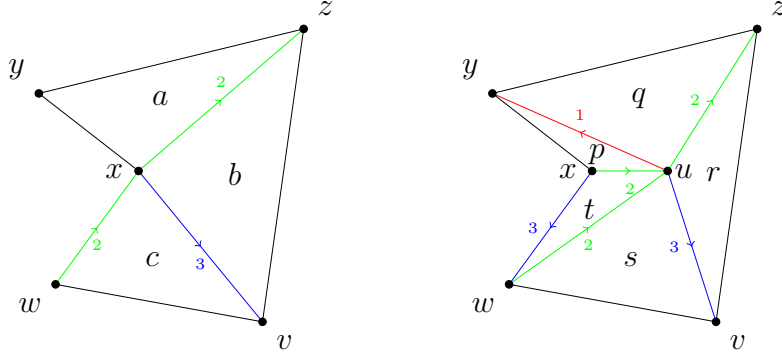


Figure 5.10: 5-gon case 3

define \mathbf{w} as follows, we let $\mathbf{w}(f) = \mathbf{w}'(f)$ for all $f \in \mathcal{F}(T) \cap \mathcal{F}(T_{u,x})$ and $p = q = a/2$, $r = s = b/2$ and $t = 0$. We can see that \mathbf{w} satisfies

$$\begin{aligned}
\sum_{f \in \mathcal{F}(T)} \mathbf{w}(f) &= p + q + r + s + t + \sum_{f \in \mathcal{F}(T) \setminus A} \mathbf{w}(f) \\
&= a + b + c + \sum_{f \in \mathcal{F}(T_{u,x}) \setminus A'} \mathbf{w}'(f) \\
&= \sum_{f \in \mathcal{F}(T_{u,x})} \mathbf{w}'(f) = 2n - 5.
\end{aligned}$$

Therefore the drawing Γ defined by S and \mathbf{w} is a planar drawing by Lemma 5.4.1. To conclude the proof we show that the positions of the vertices of $T_{u,x}$ in Γ and Γ' coincide.

Let α be a vertex of $T \setminus \{u\}$. Observe that if $\alpha \notin D_2(x) \cup D_3(x)$, then $A \subseteq R_i(\alpha)$ or $A \cap R_i(\alpha) = \emptyset$ for $i \in \{1, 2, 3\}$. In either case we have that $\sum_{f \in R'_i(\alpha)} \mathbf{w}'(f) = \sum_{f \in R_i(\alpha)} \mathbf{w}(f)$, thus the i -th coordinate of α remains unchanged from Γ' to Γ . Next we consider the three possible remaining cases, namely $\alpha = x$, $\alpha \in D_2(x) \setminus \{x\}$ and $\alpha \in D_3(x) \setminus \{x\}$.

1. Suppose $\alpha = x$. Here we consider three possibilities, depending on the value of i . If $i = 1$ then we have that

$$\begin{aligned}
\sum_{f \in R_1(x)} \mathbf{w}(f) &= r + s + t + \sum_{f \in R_1(x) \setminus A} \mathbf{w}(f) \\
&= b + \sum_{R'_1(x) \setminus A'} \mathbf{w}'(f) \\
&= \sum_{R'_1(x)} \mathbf{w}'(f).
\end{aligned}$$

Now, if $i = 2$ then

$$\begin{aligned}
\sum_{f \in R_2(x)} \mathbf{w}(f) &= \sum_{f \in R_2(x) \setminus A} \mathbf{w}(f) \\
&= c + \sum_{R'_2(x) \setminus A'} \mathbf{w}'(f) \\
&= \sum_{R'_2(x)} \mathbf{w}'(f).
\end{aligned}$$

Finally, we observe that for $i = 3$ we have that

$$\begin{aligned}
\sum_{f \in R_3(x)} \mathbf{w}(f) &= 2n - 5 - \left(\sum_{f \in R_1(x)} \mathbf{w}(f) + \sum_{f \in R_2(x)} \mathbf{w}(f) \right) \\
&= 2n - 5 - \left(\sum_{f \in R'_1(x)} \mathbf{w}'(f) + \sum_{f \in R'_2(x)} \mathbf{w}'(f) \right) \\
&= \sum_{f \in R'_3(x)} \mathbf{w}'(f)
\end{aligned}$$

In each case we observe that the coordinates of x remain unchanged.

2. Now assume $\alpha \in D_2(x) \setminus \{x\}$. Begin by noting that for $i = 2$ we have that $R'_2(\alpha) = R_2(\alpha)$ since $A' \cap R'_2(\alpha) = \emptyset$ and $A \cap R_2(\alpha) = \emptyset$. Also observe that (w, x) has colour 2 in S' and $(w, x) \notin S$. It follows from this observation that we will require to consider two possible subcases here, namely $\alpha \in D_2(w)$ and $\alpha \in D_2(x) \setminus (D_2(w) \cup \{x\})$.

- (a) Suppose $\alpha \in D_2(w)$. For $i = 1$ we have

$$\begin{aligned}
\sum_{f \in R_1(\alpha)} \mathbf{w}(f) &= r + s + \sum_{f \in R_1(\alpha) \setminus A} \mathbf{w}(f) \\
&= c + b + \sum_{R'_1(\alpha) \setminus A'} \mathbf{w}'(f) \\
&= \sum_{R'_1(\alpha)} \mathbf{w}'(f).
\end{aligned}$$

Therefore the first and second coordinate of α remain unchanged from Γ' to Γ . Since the total weight is $2n - 5$ it follows that the third coordinate of α is also preserved.

(b) Assume $\alpha \in D_2(x) \setminus (D_2(w) \cup \{x\})$ and let $i = 1$. We have the following.

$$\begin{aligned} \sum_{f \in R_1(\alpha)} \mathbf{w}(f) &= r + s + t + \sum_{f \in R_1(\alpha) \setminus A} \mathbf{w}(f) \\ &= c + b + \sum_{R'_1(\alpha) \setminus A'} \mathbf{w}'(f) \\ &= \sum_{R'_1(\alpha)} \mathbf{w}'(f). \end{aligned}$$

As above, since the first two coordinates of α coincide in Γ and Γ' , and since the total weight is $2n - 5$ we have that the position of α remains unchanged in this case.

3. Finally we consider the case where $\alpha \in D_3(x) \setminus \{x\}$. For this case we begin by noting that if $i = 3$ then we have that $R'_3(\alpha) = R_3(\alpha)$ since $A' \cap R'_3(\alpha) = \emptyset$ and $A \cap R_3(\alpha) = \emptyset$. Now, if $i = 1$ we have that

$$\begin{aligned} \sum_{f \in R_1(\alpha)} \mathbf{w}(f) &= p + q + r + s + t + \sum_{f \in R_1(\alpha) \setminus A} \mathbf{w}(f) \\ &= a + b + \sum_{f \in R'_1(\alpha) \setminus A'} \mathbf{w}'(f) \\ &= \sum_{f \in R'_1(\alpha)} \mathbf{w}'(f). \end{aligned}$$

We note that coordinates 1 and 3 of α are preserved from Γ' to Γ , and since the total weight is constant, we conclude that coordinate 2 of α is also preserved.

Therefore the coordinates of vertices in $T_{u,x}$ are preserved from Γ' to Γ , as required. \square

5.5 Towards a morph using unidirectional morphs

Recall that our aim for this chapter is to provide a morph consisting of unidirectional morphs from an arbitrary drawing of a planar triangulation T to a Schnyder drawing of T obtained from positive weights. We use an inductive approach on the number of vertices, by performing edge contractions at each step. After the contraction phase, our aim will be to uncontract the edges in reverse order while maintaining a weighted Schnyder drawing. If

we are given a contractible edge then it can be contracted by using a single unidirectional morph, this follows from the definition of contractible (see conditions (C1), (C2) and (C3)). The uncontraction phase must be examined carefully since we wish to maintain a Schnyder drawing during this phase. In this section we use the tools we developed in Sections 5.3 and 5.4 to show that the uncontraction phase can be performed by using only unidirectional morphs.

This section is structured as follows. We begin by showing that the Schnyder drawings resulting from shifting weight between adjacent faces define a unidirectional morph. This result will be useful when the weight distribution requires adjustments. One such case arises in the configuration given in Lemma 5.3.3. Then we show that the linear morph resulting from flipping a face, see Theorem 4.2.4, can be implemented by using 3 unidirectional morphs. We need this because one case arising in Lemma 5.4.2 requires a face flip. We conclude this section with a lemma that shows that a constant number of unidirectional morphs suffice to perform uncontractions, while maintaining a Schnyder drawing. The details pertaining to the uncontraction phase will be stated explicitly in the last section of this chapter.

As mentioned above, we begin by showing that if we are given a weight distribution and a Schnyder wood then transferring weight through an edge defines a planar unidirectional morph.

Lemma 5.5.1. *Let T be a planar triangulation and let S be a Schnyder wood of T . If \mathbf{w} and \mathbf{w}' are weight distributions whose values differ only at two adjacent faces, then morphing linearly between the drawing induced by S and \mathbf{w} and the drawing induced by S and \mathbf{w}' defines a planar unidirectional morph. Furthermore, if $xyz \in \mathcal{F}(T)$ is a face of type (i) or (ii) in S (see Lemma 2.3.1) and \mathbf{w}' is a near weight distribution of $\mathcal{F}(T) \setminus \{xyz\}$ then the resulting morph from the associated drawings is also planar unidirectional.*

Proof. Let Γ and Γ' be the weighted Schnyder drawings obtained from S and \mathbf{w} , and from S and \mathbf{w}' respectively, and let wxz and xyz be the faces at which \mathbf{w} and \mathbf{w}' differ. We may assume without loss of generality that (x, z) has colour $i = 1$ in S . By Lemma 4.1.2 it follows that $\langle \Gamma, \Gamma' \rangle$ is a planar linear morph. The result now follows from the observation that the only vertices whose positions change are those in $D_1(x)$, since they move in a direction parallel to the exterior edge a_3a_2 .

Let us now show the second statement of the lemma. Let $\mathbf{w}^t = t\mathbf{w}' + (1 - t)\mathbf{w}$ and let Γ^t be the drawing given by S and \mathbf{w}^t , $t \in [0, 1]$. From above we have that for any $\varepsilon > 0$ the morph $\{\Gamma^t\}_{t \in [0, 1 - \varepsilon]}$ is planar unidirectional. By Lemma 5.4.1 we have that Γ^1 is a planar drawing. Therefore, by continuity, $\{\Gamma^t\}_{t \in [0, 1]}$ defines a planar unidirectional morph. \square

Now we show that the linear morph resulting from a face flip can be implemented as a sequence of planar morphs consisting of 3 unidirectional morphs.

Lemma 5.5.2. *Let T be a planar triangulation and let S and S' be Schnyder woods of T that differ by a face flip. Then the linear morph resulting from flipping from S to S' , see Theorem 4.2.4, can be implemented using 3 unidirectional morphs.*

Proof. Let $f = xyz$ be the face of T such that flipping f in S yields S' , let \mathbf{w} be a weight distribution and let Γ and Γ' be the weighted Schnyder drawings given by \mathbf{w} and S and S' respectively. We may assume without loss of generality that (x, y) has colour 1. Note that in $\langle \Gamma, \Gamma' \rangle$ the vertices whose position change move in three directions, namely vertices in $D_1(x)$, $D_2(z)$ and $D_3(y)$ move in directions parallel to the exterior edge a_2a_3 , a_1a_3 and a_1a_2 respectively. Also recall that no edges between these sets cross and that the face xyz does not collapse during $\langle \Gamma, \Gamma' \rangle$ by Theorem 4.2.4. Since $(z, x), (x, y) \in S$ have colour 2 and 1 respectively, it follows that $x \in R_1(z)$ and $x \in R_1(y)$. Now, let $s \in D_2(z)$. Since $z \in P_2(s)$ it follows that $x \in P_2(s)$ and therefore $x \in R_1(s)$. Similarly, for any $t \in D_3(y)$ we have that $x \in R_1(t)$. Therefore we have that first coordinate of x in Γ is strictly smaller than the first coordinates of s and t for any $s \in D_2(z)$ and $t \in D_3(y)$, namely $x_1 < s_1, t_1$. By a similar analysis we can conclude that the first coordinate of x in Γ' is strictly smaller than the first coordinates of s and t for any $s \in D'_2(z)$ and $t \in D'_3(y)$, namely $x'_1 < s'_1, t'_1$. Since coordinate 1 of x is larger than the first coordinate of any vertex in $D_1(x) \setminus \{x\}$, we have that the vertices in $D_1(x)$ remain below the vertices in $D_2(z)$ and $D_3(y)$ during the morph $\langle \Gamma, \Gamma' \rangle$. By Lemma 4.2.3 we have that no face collapses in $R_1(x)$ during the morph $\langle \Gamma, \Gamma' \rangle$. It now follows from our previous two observations that moving all vertices in $D_1(x)$ from their positions in Γ to their positions in Γ' while maintaining all other vertices fixed defines a unidirectional planar morph. We can now use similar arguments, now applied to the second and third coordinates of vertices in $D_2(z)$ and $D_3(y)$ respectively. This proves that the morph $\langle \Gamma, \Gamma' \rangle$ can be simulated by 3 unidirectional planar morphs. During the first step, vertices in $D_1(x)$ move unidirectionally from their positions in Γ to their positions in Γ' . During the second step, vertices in $D_2(z)$ move unidirectionally from their positions in Γ to their positions in Γ' . Finally, during the third step, vertices in $D_3(y)$ move unidirectionally from their position in Γ to their position in Γ' . \square

We now state the main result of this section.

Lemma 5.5.3. *Let T be a planar triangulation with at least 5 vertices containing a contractible edge ux , with u being the low degree vertex. If Γ' is a Schnyder drawing of $T_{u,x}$, then we can arrive at a Schnyder drawing Γ of T by performing at most 5 planar unidirectional morphs and an uncontraction of u .*

Proof. Let us assume that Γ' is the Schnyder drawing of $T_{u,x}$ obtained from the weight distribution \mathbf{w}' and the Schnyder wood S' . We proceed by considering two cases, depending on the degree of u . The first case to consider is the one with $\deg(u) \leq 4$. As we will see this case can be handled in a straightforward fashion. Then we consider the case where $\deg(u) = 5$, here we further consider three possible subcases, depending on the local structure of the Schnyder wood S' around vertex x .

We begin by considering the case with $\deg(u) \leq 4$. By Lemma 5.3.1 there exists a Schnyder drawing Γ of T such that the position of each vertex of $T_{u,x}$ is preserved from Γ' to Γ . Note that in Γ' vertex x is in the kernel of the polygon defined by the neighbours of u in T . Similarly, u is in the kernel of this same polygon in Γ . Since the kernel is a convex set, as it is the intersection of half planes, it follows that simply uncontracting vertex u from x in Γ' to its position in Γ yields the desired result.

Now we consider the case where $\deg(u) = 5$. Let v, w, x, y and z be the neighbours of u in T listed in clockwise order, thus $T_{u,x}$ contains edges vx and xz . We consider three possible subcases depending on the orientation of the edges vx and xz in S' .

1. First let us consider the case where $(v, x), (z, x) \in S'$. This case can be handled as the case where $\deg(u) \leq 4$. It follows from Lemma 5.3.2 that there exists a Schnyder drawing Γ such that the positions of each vertex in $T_{u,x}$ are preserved from Γ' to Γ . We observe that x and u are in the kernel of the 5-gon $vwxyz$ in Γ' and Γ respectively. Since the kernel of $vwxyz$ is a convex set we can see the result follows for this case by uncontracting vertex u from x in Γ' to its position in Γ .
2. Now we consider the case where exactly one of (v, x) and (z, x) is in S' . We only consider the case where $(z, x) \in S'$, as the other case can be handled in a similar fashion. Let \mathbf{w}' be the weight distribution associated to Γ' . Our aim will be to use Lemma 5.3.3 for this case. Note that we may not be able to directly apply such result, unless $\mathbf{w}'(xyz) > \mathbf{w}'(vwx)/2 + \delta_1(wx)$. If required we shift enough weight, first from vwx to vxz and then from vxz to xyz , so that the resulting weight distribution \mathbf{w}'' satisfies $\mathbf{w}''(xyz) > \mathbf{w}''(vwx)/2 + \delta_1(wx)$, otherwise let $\mathbf{w}'' = \mathbf{w}'$. Now, let Γ be the Schnyder drawing resulting from Lemma 5.3.3 applied to T , S' and \mathbf{w}'' . Therefore, if Γ'' denotes the drawing obtained from S' and \mathbf{w}'' , then we can see that, by Lemma 5.5.1, we require at most two unidirectional morphs to go from Γ' to Γ'' exactly one per weight shift used. At this stage we can simply uncontract u from x in Γ'' to its position in Γ , here the uncontraction is possible since x and u are in the kernel of $vwxyz$ in Γ . This yields the desired result for this case.
3. Finally, we consider the case where neither of (v, x) and (z, x) are in S' . In particular

we have that $(x, v), (x, z) \in S'$. Here we consider two possible subcases. The first case we consider is that where at least one of vwx and xyz is cyclically oriented in S' . As mentioned before, this case will be handled by performing a face flip or flop, thus reducing the configuration to the one from case 2 above. The second case is that where none of vwx and xyz is cyclically oriented. For the second case, we will use Lemma 5.4.2.

- (a) Suppose that at least one of the faces vwx or xyz is cyclically oriented. Since the two cases can be handled in a similar way, we just consider the case where xyz is cyclically oriented in S' . If this is the case, then we can flop face xyz to obtain a Schnyder wood S'' in which there is exactly one edge incoming to x , namely $(z, x) \in S''$. At this point we could proceed as in case 2 above. In terms of morphs, this would require that we use 3 unidirectional morphs to flop face xyz in Γ' , then possibly use two more unidirectional morphs which represent the potential weight shifting and the final uncontraction step, these last two morphs arising from the reduction to case 2. Thus the result holds in this case.
- (b) Finally, suppose that none of vwx and xyz is cyclically oriented. We only consider the case where $(w, x) \in S'$, as the case where $(y, x) \in S'$ can be handled similarly. Since Γ' is a Schnyder drawing we must have that $\mathbf{w}'(vwx) > 0$. Our aim will be to apply Lemma 5.4.2, and for this we require a near weight distribution $\mathbf{w}^{(2)}$ of $\mathcal{F}(T_{u,x}) \setminus \{vwx\}$. Let $\mathbf{w}^{(2)}$ be defined as follows. Take $\mathbf{w}^{(2)}(f) = \mathbf{w}'(f)$ for all $f \in \mathcal{F}(T_{u,x}) \setminus \{vwx, vxz\}$, $\mathbf{w}^{(2)}(vxz) = \mathbf{w}'(vxz) + \mathbf{w}'(vwx)$ and $\mathbf{w}^{(2)}(vwx) = 0$. Morphing from Γ' to the drawing associated to $\mathbf{w}^{(2)}$, $\Gamma^{(2)}$, can be achieved by using one planar unidirectional morph by Lemma 5.5.1. We achieve this by depleting the weight of vwx towards the adjacent face vxz . By applying Lemma 5.4.2 to S' and $\mathbf{w}^{(2)}$ we obtain a drawing $\Gamma^{(3)}$ of T in which the positions of vertices of $T_{u,x}$ from $\Gamma^{(2)}$ are preserved. Note that $\Gamma^{(3)}$ is a drawing that is obtained from a near weight distribution $\mathbf{w}^{(3)}$ of $\mathcal{F}(T) \setminus \{uwx\}$ and from a Schnyder wood S of T . We define Γ to be the drawing induced by a weight distribution \mathbf{w} and S , where \mathbf{w} is a weight distribution obtained from adding some weight to face uwx in $\mathbf{w}^{(3)}$ from, say, faces uvw and uvz . This last step requires 2 unidirectional morphs and they are planar by Lemma 5.5.1. Therefore this case can be handled by using 1 planar unidirectional morph from Γ' to $\Gamma^{(2)}$, an uncontraction from $\Gamma^{(2)}$ to $\Gamma^{(3)}$, and 2 planar unidirectional morphs from $\Gamma^{(3)}$ to Γ . The result now follows.

□

5.6 Morphing to a Schnyder drawing using unidirectional morphs

In this section we present the main result of this chapter. We prove that given an arbitrary drawing Γ of a planar triangulation T , there exists a planar morph consisting of $O(n)$ unidirectional morphs from Γ to a Schnyder drawing of T . The proof we provide of this result is by induction—at each step we reduce the number of vertices by performing an edge contraction. The main result from Section 5.5 is of central importance to our proof, since we use it for the uncontraction step of our proof.

Let us prove the central result of this chapter.

Theorem 5.6.1. *Let T be a planar triangulation and let Γ be any planar drawing of T . Then there exists a weighted Schnyder drawing Γ' of T , and a morph from Γ to Γ' that requires $O(n)$ unidirectional morphs.*

Proof. We proceed by induction on the number of vertices. It is clear that the result holds for K_4 , as any planar drawing of it is a weighted Schnyder drawing.

Now, assume the result holds for all drawings of all planar triangulations with fewer than n vertices. Let $T = (V, E)$ be a planar triangulation on n vertices and let Γ be an arbitrary planar drawing of T . Let $ux \in E$ be a contractible edge of T with u being the low-degree vertex, this edge exists by Theorem 5.1.1. Clearly there is a unidirectional pseudo morph from Γ to a drawing Γ_1 of $T_{u,x}$. By the induction hypothesis, we obtain a unidirectional pseudo morph \mathcal{M} from Γ_1 to Γ_2 , where Γ_2 is a weighted Schnyder drawing of $T_{u,x}$. Finally, by Lemma 5.5.3 it follows that there exists a weighted Schnyder drawing Γ' of T , which can be reached from Γ_2 by performing at most 5 planar unidirectional morphs and an uncontraction of vertex u . Here Γ' denotes a weighted Schnyder drawing of T . Putting it all together, going from Γ to Γ_1 by contracting ux , from Γ_1 to Γ_2 by using \mathcal{M} , and from Γ_2 to Γ' by using the planar unidirectional morphs and the uncontraction, we obtain a pseudo morph \mathcal{M}' from Γ to Γ' . Note that \mathcal{M}' consists of $O(n)$ steps, since it consists of the $O(n)$ steps from \mathcal{M} , a contraction, an uncontraction and a constant number of unidirectional morphs. Now, by our results from Section 3.4, Lemmas 3.4.2 and 3.4.3, it follows that from the pseudo morph \mathcal{M}' we can obtain a true morph from Γ to Γ' , a weighted Schnyder drawing, in $O(n)$ unidirectional morphs. \square

5.7 Morphing planar triangulations using Schnyder drawings

In this section we present two algorithms that are a consequence of Theorem 5.6.1. The first algorithm yields a morph consisting of $O(n)$ unidirectional morphs from an arbitrary drawing of a planar triangulation to a Schnyder drawing. Then we use this algorithm to provide an alternate solution to the morphing problem as described in Chapter 1. The planar morph we obtain consists of $O(n^2)$ linear morphs and can be thought of as consisting of two components. The first and last part of the morph transform each of the input drawings into Schnyder drawings in $O(n)$ unidirectional morphs. The second component of the algorithm morphs between the two resulting Schnyder drawings by using Algorithm 3, the morphing algorithm from Chapter 4. The second component has the advantage that each of the drawings is realized in an $O(n) \times O(n)$ grid.

Now we present the algorithm that is directly obtained from Theorem 5.6.1. The proof of correctness and running time is an immediate consequence of the proof of Theorem 5.6.1.

Algorithm 4 Morphing from an arbitrary drawing to a Schnyder drawing

```

1: procedure MORPH TO SCHNYDER DRAWING( $T, \Gamma$ )
Require:  $T$  a planar triangulation and  $\Gamma$  a planar drawing of  $T$ .
2:   if  $T$  has 4 vertices then
       return  $\Gamma$ . ▷  $\Gamma$  is already a Schnyder drawing.
3:   end if
4:   Let  $ux$  be a contractible edge.
5:   Let  $M_1 := \{\Gamma_t^{(1)}\}_{t \in [0,1]}$  be the contraction of  $ux$ .
6:   Let  $M_2$  be the morph resulting from the recursive call MORPH TO SCHNYDER
   DRAWING( $T_{u,x}, \Gamma_1^{(1)}$ ).
▷ Suppose  $M_2 = \{\Gamma_t^{(2)}\}_{t \in [0,1]}$ 
7:   Let  $M_3$  be the pseudo morph resulting from Lemma 5.5.3 applied to  $\Gamma_1^{(2)}$ .
8:   Let  $\mathcal{M}$  be the pseudo morph obtained by concatenating  $M_1, M_2$  and  $M_3$ .
▷ Note that  $\mathcal{M}$  is a pseudo morph from  $\Gamma$  to a Schnyder drawing  $\Gamma_1^{(2)}$ .
9:    $M = \text{CONVERT PSEUDO MORPH TO UNIDIRECTIONAL MORPH}(\mathcal{M})$  ▷ Here we use
   Algorithm 1 to convert the pseudo morph to a true morph.
       return  $M$ 
10: end procedure

```

We conclude this chapter by presenting the algorithm which provides an alternate solution to the morphing problem. It should be noted that if we desire that the resulting morph consists exclusively of unidirectional morphs, then the only thing that needs to be checked is that the morphs resulting from flipping separating triangles can be simulated using unidirectional morphs. Unlike the case of flipping facial triangles, Lemma 5.5.2, this is not essential to the proof of Theorem 5.6.1.

Algorithm 5 Morph between any two drawings of a planar triangulation

- 1: **procedure** FIND MORPH(T, Γ_1, Γ_2)
 - Require:** T a planar triangulation and Γ_1, Γ_2 are planar drawings of T having the same exterior face.
 - 2: Let M_1 be the morph resulting from MORPH TO SCHNYDER DRAWING(T, Γ_1) ▷
 We use Algorithm 4, suppose Γ'_1 is the resulting Schnyder drawing.
 - 3: Let M_2 be the morph resulting from MORPH TO SCHNYDER DRAWING(T, Γ_1) ▷
 We use Algorithm 4, suppose Γ'_2 is the resulting Schnyder drawing.
 - 4: Let M_3 be the morph resulting from SCHNYDER MORPH(Γ'_1, Γ'_2) ▷ Here we use
 Algorithm 3, M_3 is the morph between Schnyder drawings.
 - 5: Let M'_2 be the morph resulting from reversing M_2
 - 6: Let M be the morph resulting from concatenating M_1, M_3, M'_2
 - return** M
 - 7: **end procedure**
-

Chapter 6

Simulating morphing steps via weight shifts

In this brief chapter we present a theorem that shows that it is possible to simulate the morph resulting from flipping a facial triangle, as seen in Chapter 4, by shifting weights. This could be useful, for example, in the implementation of the algorithms given in the previous chapters, if we develop a general-purpose subroutine for shifting weights. As we will see this will require that we consider drawings given by assignment of weights to interior faces that are negative.

6.1 Simulating flips by weight shifts

Let T be a planar triangulation and let S be a Schnyder wood of T . Recall that the morph resulting from shifting weight across an interior edge of T results in a unidirectional morph, see Lemma 5.5.1. If the weight is shifted through arc $(x, y) \in S$ of colour 1, then the vertices in $D_1(x)$ move unidirectionally in a direction parallel to a_2a_3 . We note that this unidirectional movement also arises in the morph resulting from flipping a face. See Theorem 4.2.4, here three sets of descendants move in a direction parallel to each of the exterior edges. The aim of this section is to show that the morph arising from flipping a cyclically oriented face f in S can be simulated by shifting weight away from f towards its three neighbours. Here we allow the weight of f to become negative.

Theorem 6.1.1. *Let T be a planar triangulation and let S and S' be Schnyder woods of T that differ by a face flip, say at face f . Suppose Γ and Γ' are the Schnyder drawings*

induced by S and S' and an arbitrary weight distribution \mathbf{w} . Then there exists an assignment of weights $\mathbf{w}' : \mathcal{F}(T) \rightarrow \mathbb{R}$ such that $\mathbf{w}'(f) < 0$, $\mathbf{w}'(g) > 0$ for $g \in \mathcal{F}(T) \setminus \{f\}$, $\sum_{g \in \mathcal{F}(T)} \mathbf{w}'(g) = 2n - 5$ and the drawing given by S and \mathbf{w}' is Γ' .

Proof. Let us begin by finding an assignment of weights \mathbf{w}' of $\mathcal{F}(T)$ such that the drawing resulting from \mathbf{w}' and S is Γ' .

Let us assume without loss of generality that the face $f = xyz$ at which S and S' differ is oriented counterclockwise in S . We may assume further that $(x, y) \in S$ has colour 1. Denote by f_i , $1 \leq i \leq 3$, the face adjacent to f through the arc in colour i , see Figure 6.1, and let $A := \{f_1, f_2, f_3, f\}$.

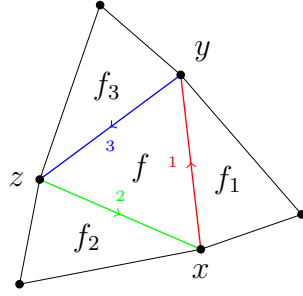


Figure 6.1: The face f and its three neighbours.

We define $\mathbf{w}' : \mathcal{F}(T) \rightarrow \mathbb{R}$ as follows. Let $\mathbf{w}'(g) := \mathbf{w}(g)$ for all $g \in \mathcal{F}(T) \setminus A$, $\mathbf{w}'(f_i) := \mathbf{w}(f_i) + \delta_i + \mathbf{w}(f)$, $1 \leq i \leq 3$, and $\mathbf{w}'(f) := -2\mathbf{w}(f) - \delta_1 - \delta_2 - \delta_3$.

Observe that

$$\begin{aligned}
 \sum_{g \in \mathcal{F}(T)} \mathbf{w}'(g) &= \sum_{g \in \mathcal{F}(T) \setminus A} \mathbf{w}'(g) + \sum_{i \in \{1,2,3\}} \mathbf{w}'(f_i) + \mathbf{w}'(f) \\
 &= \sum_{g \in \mathcal{F}(T) \setminus A} \mathbf{w}(g) + \sum_{i \in \{1,2,3\}} (\mathbf{w}(f_i) + \delta_i + \mathbf{w}(f)) - 2\mathbf{w}(f) - \delta_1 - \delta_2 - \delta_3 \\
 &= \sum_{g \in \mathcal{F}(T) \setminus A} \mathbf{w}(g) + \sum_{i \in \{1,2,3\}} \mathbf{w}(f_i) + \mathbf{w}(f) \\
 &= \sum_{g \in \mathcal{F}(T)} \mathbf{w}(g) = 2n - 5.
 \end{aligned}$$

Therefore, we may think of \mathbf{w}' as obtained from \mathbf{w} by extracting weight from f and distributing it among the three faces adjacent to it. Let us now show that the drawing given by S and \mathbf{w}' is Γ' .

Let $v \in V$. Suppose $v \notin D_1(x) \cup D_2(z) \cup D_3(y)$. If this is the case, then none $P_1(v)$, $P_2(v)$ and $P_3(v)$ use the edges incident to f . Observe that $A \subseteq R_i(v)$ or $A \cap R_i(v) = \emptyset$ for any $i \in \{1, 2, 3\}$. Therefore, since the weight assigned by \mathbf{w} was just redistributed among elements of A , the coordinates of v remain the same as those in Γ . Thus by Lemma 4.2.2 this corresponds to the position of v in Γ' .

Now let us consider the case where $v \in D_1(x) \cup D_2(z) \cup D_3(y)$. By Lemma 4.2.1 the sets $D_1(x)$, $D_2(z)$ and $D_3(y)$ are pairwise disjoint and by symmetry we may just consider the case where $v \in D_1(x)$. Note that since $P_2(v)$ and $P_3(v)$ do not use any edge of f then the weight assigned by \mathbf{w}' to $R_1(v)$ remains unchanged, therefore the first coordinate of v remains unchanged. Now let us analyze the second coordinate of v . The only face in $R_2(v)$ whose weight changed from \mathbf{w} to \mathbf{w}' is f_1 . Note that the increase in the weight of f_1 is $\delta_1 + \mathbf{w}(f)$, therefore the second coordinate of v , v'_2 , satisfied $v'_2 = v_2 + \delta_1 + \mathbf{w}(f)$. Finally, since the total weight is $2n - 5$, it follows that the third coordinate decreased weight by the same amount that f_1 increased, namely $\delta_1 + \mathbf{w}(f)$, that is $v'_3 = v_3 - \delta_1 - \mathbf{w}(f)$. Therefore $(v'_1, v'_2, v'_3) = (v_1, v_2 + \delta_1 + \mathbf{w}(f), v_3 - \delta_1 - \mathbf{w}(f))$. Thus, by Lemma 4.2.2 this corresponds to the position of v in Γ' . \square

We now outline how to implement the morph resulting from the previous theorem. Consider a planar triangulation T and a Schnyder wood S of T with a flippable face $f = xyz$, say with $(x, y) \in S$ of colour 1. Let Γ denote the drawing induced by S and an arbitrary weight distribution \mathbf{w} , let S' be the Schnyder wood resulting from flipping f in S and let \mathbf{w}' be the weight distribution obtained from Theorem 6.1.1 applied to S , S' and \mathbf{w} . Note that we can think of \mathbf{w}' as reassigning coordinates to the sets $D_1(x)$, $D_2(z)$ and $D_3(y)$. The weight assignments \mathbf{w}' and \mathbf{w} coincide at all faces except at f and its three neighbours and the changes in weights are closely related to the change of coordinates from Lemma 4.2.2. Theorem 6.1.1 guarantees that redistributing weights as prescribed by \mathbf{w}' yields the linear morph corresponding to flipping face f . Therefore to simulate the morph from Theorem 4.2.4 one just needs to redistribute weights as prescribed by \mathbf{w}' and then reverse and recolour the three arcs (x, y) , (y, z) and (z, x) .

It should be mentioned that the planar morph resulting from moving linearly a single vertex can also be implemented using weight shifting. This weight redistribution can also be implemented for the case where the drawings do not necessarily arise from positive weight assignments. This together with the simulation of facial flips by weight shifting would provide the necessary steps for implementing our morphs from Chapter 4 and 5 by using only weight shifts.

Chapter 7

Future work

The work developed in this thesis points towards proving that it is possible to morph between any two drawings of a planar triangulation in polynomially many steps, where each step is a linear morph and where each intermediate drawing can be realized in a grid of polynomial size. One possible direction to follow is to improve our result from Chapter 5 so that we can arrive from an arbitrary drawing of a planar triangulation to a Schnyder drawing while remaining on a polynomially size grid, say $O(n^k) \times O(n^k)$. Then this together with our algorithm from Chapter 4, in which we can morph between any two drawings in the Schnyder lattice while staying on a linear-sized grid, would give a complete solution to the morphing problem on a polynomial-sized grid.

If true, the previous result would imply, together with the aid of *compatible triangulations* [6], the existence of a morph between any two planar graphs with polynomially many steps, where each intermediate drawing can be realized in an $O(n^{2k}) \times O(n^{2k})$ grid. In order to try to avoid this increase in the grid size, one may try to generalize our results from Chapters 4 and 5 to another class of graphs, namely 3-connected planar graphs. The concept of Schnyder wood has been generalized to the class of 3-connected planar graphs [28], and it is known that drawings in an $O(n) \times O(n)$ grid can be obtained in linear time. It would therefore be interesting to investigate if it is possible to traverse the “lattice of Schnyder drawings” of a 3-connected planar graph by using the morphs resulting from performing flip operations.

In Schnyder’s publication [50] he introduced weak barycentric embeddings of graphs. These embeddings also induce planar graph drawings. Weak barycentric embeddings can be obtained from Schnyder woods by counting the vertices in a specific way (closely related to the regions of an interior vertex). We have experimental evidence that the morphs resulting

from flipping facial triangles in Schnyder woods using the weak barycentric embeddings yield planar morphs. It would therefore be of interest to try to explore assignment of weights on vertices as well as to try to study the flip operations under this framework.

References

- [1] G. AGNARSSON, S. FELSNER, and W. T. TROTTER. The maximum number of edges in a graph of bounded dimension, with applications to ring theory. *Discrete Mathematics* 201, 1-3 (1999), 5–19.
- [2] S. ALAMDARI, P. ANGELINI, T. M. CHAN, G. DI BATTISTA, F. FRATI, A. LUBIW, M. PATRIGNANI, V. ROSELLI, S. SINGLA, and B. T. WILKINSON. Morphing planar graph drawings with a polynomial number of steps. *Symposium on Discrete Algorithms*. 2013, 1656–1667.
- [3] L. C. ALEARDI, É. FUSY, and T. LEWINER. Schnyder woods for higher genus triangulated surfaces, with applications to encoding. *Discrete & Computational Geometry* 42, 3 (2009), 489–516.
- [4] B. ANDERSEN and K. NOONE. Controlled texture pushing and crossing seams in UV space using Maya and Photorealistic Renderman. *J. Graphics, GPU, & Game Tools* 9, 4 (2004), 57–67.
- [5] P. ANGELINI, G. DA LOZZO, G. DI BATTISTA, F. FRATI, M. PATRIGNANI, and V. ROSELLI. *Morphing planar graph drawings optimally*. Version 2. Feb. 19, 2014. arXiv: 1402.4364v2 [cs.DS, cs.CG].
- [6] B. ARONOV, R. SEIDEL, and D. L. SOUVAINE. On compatible triangulations of simple polygons. *Comput. Geom.* 3 (1993), 27–35.
- [7] G. BAREQUET, M. T. GOODRICH, A. LEVI-STEINER, and D. STEINER. Contour interpolation by straight skeletons. *Graphical Models* 66, 4 (2004), 245–260.
- [8] G. BAREQUET and M. SHARIR. Piecewise-linear interpolation between polygonal slices. *Computer Vision and Image Understanding* 63, 2 (1996), 251–272.
- [9] F. BARRERA-CRUZ and P. HAXELL. A note on Schnyder’s theorem. *Order* 28, 2 (2011), 221–226.

- [10] F. BARRERA-CRUZ, P. HAXELL, and A. LUBIW. Morphing planar graphs with uni-directional moves. *Mexican Conference on Discrete Mathematics and Computational Geometry*. 2013.
- [11] G. D. BATTISTA, P. EADES, R. TAMASSIA, and I. G. TOLLIS. *Graph Drawing: Algorithms for the Visualization of Graphs*. Prentice-Hall, 1999.
- [12] O. BERNARDI and N. BONICHON. Intervals in Catalan lattices and realizers of triangulations. *J. Comb. Theory, Ser. A* 116, 1 (2009), 55–75.
- [13] O. BERNARDI and É. FUSY. Schnyder decompositions for regular plane graphs and application to drawing. *Algorithmica* 62, 3-4 (2012), 1159–1197.
- [14] T. C. BIEDL, A. LUBIW, M. PETRICK, and M. J. SPRIGGS. Morphing orthogonal planar graph drawings. *ACM Transactions on Algorithms* 9, 4 (2013), 29.
- [15] N. BONICHON. A bijection between realizers of maximal plane graphs and pairs of non-crossing Dyck paths. *Discrete Mathematics* 298, 1-3 (2005), 104–114.
- [16] N. BONICHON, S. FELSNER, and M. MOSBAH. Convex drawings of 3-connected plane graphs. *Algorithmica* 47, 4 (2007), 399–420.
- [17] N. BONICHON, C. GAVOILLE, N. HANUSSE, and D. ILCINKAS. Connections between theta-graphs, delaunay triangulations, and orthogonal surfaces. *WG*. 2010, 266–278.
- [18] N. BONICHON, B. LE SAËC, and M. MOSBAH. Wagner’s theorem on realizers. *International Colloquium on Automata, Languages, and Programming*. 2002, 1043–1053.
- [19] E. BREHM. 3-orientations and Schnyder 3-tree-decompositions. *Master’s thesis, FB Mathematik und Informatik, Freie Universität Berlin* (2000).
- [20] G. BRIGHTWELL and W. T. TROTTER. The order dimension of convex polytopes. *SIAM J. Discrete Math.* 6, 2 (1993), 230–245.
- [21] G. BRIGHTWELL and W. T. TROTTER. The order dimension of planar maps. *SIAM J. Discrete Math.* 10, 4 (1997), 515–528.
- [22] S. S. CAIRNS. Deformations of plane rectilinear complexes. *The American Mathematical Monthly* 51, 5 (1944), 247–252.
- [23] Y.-T. CHIANG, C.-C. LIN, and H.-I. LU. Orderly spanning trees with applications. *SIAM J. Comput.* 34, 4 (2005), 924–945.
- [24] H. DE FRAYSSEIX, J. PACH, and R. POLLACK. How to draw a planar graph on a grid. *Combinatorica* 10, 1 (1990), 41–51.
- [25] R. DHANDAPANI. Greedy drawings of triangulations. *Discrete & Computational Geometry* 43, 2 (2010), 375–392.

- [26] P. EADES and P. GARVAN. Drawing stressed planar graphs in three dimensions. *Graph Drawing*. 1995, 212–223.
- [27] I. FÁRY. On straight line representation of planar graphs. *Acta. Sci. Math. Szeged* 11 (1948), 229–233.
- [28] S. FELSNER. Convex drawings of planar graphs and the order dimension of 3-polytopes. *Order* 18, 1 (2001), 19–37.
- [29] S. FELSNER. Geodesic embeddings and planar graphs. *Order* 20, 2 (2003), 135–150.
- [30] S. FELSNER. Lattice structures from planar graphs. *Journal of Combinatorics* 11, 1 (2004), 15.
- [31] S. FELSNER and W. T. TROTTER. Posets and planar graphs. *Journal of Graph Theory* 49, 4 (2005), 273–284.
- [32] S. FELSNER and F. ZICKFELD. On the number of α -orientations. *International Workshop on Graph-Theoretic Concepts in Computer Science*. 2007, 190–201.
- [33] S. FELSNER and F. ZICKFELD. Schnyder woods and orthogonal surfaces. *Discrete & Computational Geometry* 40, 1 (2008), 103–126.
- [34] M. S. FLOATER. Parametric tilings and scattered data approximation. *International Journal of Shape Modeling* 4 (1998), 165–182.
- [35] M. S. FLOATER. Parametrization and smooth approximation of surface triangulations. *Computer Aided Geometric Design* 14, 3 (1997), 231–250.
- [36] M. S. FLOATER and C. GOTSMAN. How to morph tilings injectively. *Journal of Computational and Applied Mathematics* 101, 1 (1999), 117–129.
- [37] J. GEELLEN. On how to draw a graph. Unpublished. 2012.
- [38] J. GOMES. *Warping and morphing of graphical objects*. Vol. 1. Morgan Kaufmann, 1999.
- [39] X. HE and H. ZHANG. A simple routing algorithm based on Schnyder coordinates. *Theor. Comput. Sci.* 494 (2013), 112–121.
- [40] X. HE and H. ZHANG. On succinct convex greedy drawing of 3-connected plane graphs. *Symposium on Discrete Algorithms*. 2011, 1477–1486.
- [41] X. HE and H. ZHANG. Schnyder greedy routing algorithm. *Theory and Applications of Models of Computation*. 2010, 271–283.
- [42] C.-C. LIN, H.-I. LU, and I.-F. SUN. Improved compact visibility representation of planar graph via Schnyder’s realizer. *SIAM J. Discrete Math.* 18, 1 (2004), 19–29.

- [43] A. LUBIW. Morphing planar graph drawings. *Canadian Conference on Computational Geometry*. 2007, 1.
- [44] A. LUBIW and M. PETRICK. Morphing planar graph drawings with bent edges. *J. Graph Algorithms Appl.* 15, 2 (2011), 205–227.
- [45] A. LUBIW, M. PETRICK, and M. J. SPRIGGS. Morphing orthogonal planar graph drawings. *Symposium on Discrete Algorithms*. 2006, 222–230.
- [46] S. MIRACLE, D. RANDALL, A. P. STREIB, and P. TETALI. *Algorithms for sampling 3-orientations of planar triangulations*. Version 1. Feb. 22, 2012. arXiv: 1202.4945 [cs.DS].
- [47] P. OSSONA DE MENDEZ. Geometric realization of simplicial complexes. *Graph Drawing*. 1999, 323–332.
- [48] P. OSSONA DE MENDEZ. Orientations bipolaires. PhD thesis. Ecole des Hautes Etudes en Sciences Sociales, Paris, 1994.
- [49] P. OSSONA DE MENDEZ. Realization of posets. *J. Graph Algorithms Appl.* 6, 1 (2002), 149–153.
- [50] W. SCHNYDER. Embedding planar graphs on the grid. *Symposium on Discrete Algorithms*. 1990, 138–148.
- [51] W. SCHNYDER. Planar graphs and poset dimension. *Order* 5, 4 (1989), 323–343.
- [52] V. SURAZHISKY and C. GOTSMAN. Controllable morphing of compatible planar triangulations. *ACM Trans. Graph.* 20, 4 (2001), 203–231.
- [53] R. TAMASSIA, ed. *Handbook of Graph Drawing and Visualization*. CRC Press, 2013.
- [54] C. THOMASSEN. Deformations of plane graphs. *J. Comb. Theory, Ser. B* 34, 3 (1983), 244–257.
- [55] W. T. TUTTE. How to draw a graph. *Proc. London Math. Soc* 13, 3 (1963), 743–768.
- [56] H. ZHANG and X. HE. Compact visibility representation and straight-line grid embedding of plane graphs. *Workshop on Algorithms and Data Structures*. 2003, 493–504.
- [57] H. ZHANG and X. HE. Improved visibility representation of plane graphs. *Comput. Geom.* 30, 1 (2005), 29–39.